7-31-2015

Color Tuning Neutrality and Gel Polymer Electrolyte Materials for Optoelectronic Application

Yumin Zhu
University of Connecticut - Storrs, yumin.zhu@uconn.edu

Color Tuning Neutrality and Gel Polymer Electrolyte Materials for Optoelectronic Application

Yumin Zhu, Ph.D.

University of Connecticut, 2015

Conjugated polymers (CPs), also known as conducting polymers are polymers consisting of alternating single/double bonds along the polymer backbone. They are known to be conductive upon doping. One important property of CPs is their ability to undergo reversible redox switch from a neutral (insulting) state to an oxidized (conducting) state upon potential application. Induced by electrical stimuli, accompanied with the change in electronic state of the material is usually a distinguishable change in the materials absorption characteristics within the visible region (400–800 nm) or near IR region, resulting in the material's color change, known as "electrochromism".

In order to have useful Electrochromic applications, conducting polymers should be built into **electrochomic devices (ECDs)**. We have developed a novel processing technique of conjugated polymers for large area electrochromic device manufacturing. Compared with conventional device fabrication process, this novel approach, termed **"*in situ* assembly"**, eliminates the solution step, has resulted in less waste, versatility in device manufacturing, the ability for open atmosphere fabrication, and shorter device assembly time by direct conversion of monomers in a cross-linked solid polyelectrolyte matrix after device construction.

This dissertation is focused on conducting polymers and electrochromic devices (ECDs) assembled from *"in situ"* method and divided into two corresponding main parts. **PART I** (**Chapter 3** and **Chapter 5**) is focused on the development of gel polymer electrolyte materials for supporting the maximum functioning of electrochromic devices prepared from the "*in situ"* approach. **Chapter 3**: a study on varying salts and their composition used in the gel polymer electrolyte for "*in situ"* assembly for electrochromic devices was carried out to explore their effects on various electrochromic performance parameters, such as color uniformity, photopic contrast, switching speed, and optical memory. It was found that the lithium salts yielded devices with the best color uniformity, photopic contrast as high as 48%, and switching response speeds as low as 1 s. Hermetically sealed electrochromic devices exhibited optical memory of 27 h for a 2% photopic transmittance loss under normal laboratory conditions. In **Chapter 5**, novel flexible gel polymeric electrolyte (GPE) materials were formulated and optimized. Electrolyte composition parameters were fully investigated and studied to maximize the performance of ECDs fabricated via the *in situ* method. An optimal polyelectrolyte demonstrated a high ionic conductivity of 1.36×10^{-3} S/cm and yielded ECDs with a photopic contrast as high as 53% with less than 6% photopic contrast loss after 2000 switching cycles. More importantly, a systematic study was carried out on the mechanical flexibility properties of the gel electrolytes side by side with an evaluation of commercially available indium doped tin oxide (ITO) coated polyethylene terephthalate (PET) substrates. Optimized GPEs were found to withstand a much larger bending extent, exceeding that of ITO coated PET, ensuring that ECDs will function still under extreme stresses even if the substrate becomes damaged. **PART II** (**Chapter 4** and **Chapter 6**) is

the discovery of optimal color tuning methods to achieve a desired electrochromic device color. In **Chapter 4**, demonstrates the ability to achieve neutral color ECDs by adding a commercially available yellow dye into the gel polymer electrolyte utilizing the *"in situ"* device fabrication approach. The conjugated dye was shown to not interfere with the electropolymerization of our chosen monomer 3,4-ethylenedioxythiophene (EDOT), allowing a combinatorial effect in the subtractive color spectrum. Optimized polymer and yellow dye absorption intensities yielded neutral grey color ECDs with 30% photopic contrast and switch speeds as low as 1 second on flexible PET substrates. In addition, this study opens up new directions to tune optical and colorimetric properties of other EC polymers in combination with the use of commercially available dyes for increased contrast. **Chapter 6** introduces a method to neutral color-tune flexible electrochromic devices using the "*in situ"* approach, where three monomers (1,3-di-tert-butyl-3,4-propylenedioxythiophene, 2,2-dimethyl-3,4 propylenedioxythiophene, and thieno[3,4- b]thio-phene) were used to form two distinct copolymers. The monomer ratios for the conjugated random copolymers were predetermined and optimized via theoretical calculations to provide the most desirable optical properties when combined within an electrochromic device. The demonstration of color tuning based on determining feed ratios using two distinct complimentary copolymer systems consisting of only 3 monomers in a single electrochromic layer solid state device achieved excellent neutrality (2%) to date. And of note, this most neutral colored electrochromic device in the literature also demonstrated a highest reported photopic contrast of a neutral colored electrochromic device ca. 38%.

Color Tuning Neutrality and Gel Polymer Electrolyte Materials for Optoelectronic Application

Yumin Zhu

B. S., University of Electronic Science and Technology of China, 2011

A Dissertation

Submitted in Partial Fulfillment of the

Requirements for the Degree of

Doctor of Philosophy

at the

University of Connecticut

2015

APPROVAL PAGE

Doctor of Philosophy Dissertation

Color Tuning Neutrality and Gel Polymer Materials for Optoelectronic Application

Presented by

Yumin Zhu, B.S.

Major Advisor: _____

Gregory A. Sotzing, Ph.D.

Associate Advisor: _____

Douglas H. Adamson , Ph.D.

Associate Advisor: _____

Jing Zhao, Ph.D.

Associate Advisor: _____

Alfredo Angeles-Boza, Ph.D.

Associate Advisor: _____

Jie He, Ph.D.

University of Connecticut

2015

I dedicate this doctoral thesis to my Maker and Lord. For always giving me the Power and Strengths to go through the dark days and bringing me Hope and Peacefulness.

July 30th, 2015

Acknowledgements

"Yumin, when you are not experienced, you are less confident than you really desire. Nevertheless, you are very willing to take risks because you always believe the benefits are far greater than the risks you go through." This is what my career advisor spoke of me during our last meeting.

He is true. But I didn't realize this until the end of my graduate journey by looking back through my past 25 years in life. Grown and raised up in a small town in China, when I was young, there was rarely people who had the desire to study in the United States due to language, culture barriers as well as financial issues. But I am so grateful that I took on the challenge and made it through with the tremendous support and help from a lot of people I have met during the past four years.

First of all, I most acknowledge the guidance of my academic advisor, Gregory Sotzing. He is very humorous and laidback but has a keen eye for details and a very thoughtful mind. He really cares for you but in his unique way. A professor in need is a professor indeed. This is how I can best describe him. I have had a great pleasure working for him over the years. I am truly grateful for all what I have learnt from him. And of note, he is the Coolest Professor in Chemistry.

Secondly, I would like to thank my associate advisors, Prof. Jing Zhao, for always being soooo supportive and helpful to me, giving a lot of useful suggestions both in my academic and career developments. She is the most Elegant Professor in Chemistry. And Prof. Douglas Adamson, for always being soooo approachable and considerate. He is the most Gentle Professor in Chemistry. I also thank Prof. Angeles-Boza and Prof. Jie He for their time and compliments being in my committee. Another special thanks to my

teaching supervisor also a good friend, Dr. Fatma Selampinar, for always caring for me. Without your guidance, I probably wouldn't get a chance to figure out what I really wanna do in the future upon graduation.

Next, I would love to give my sincere thanks to people who have mentored and worked with me, Dr. Michael Invernale, Dr. Yujie Ding, Dr. Donna Mammangun, Dr. Chris Asemota, Dr. Fahad Alhashmi Alamer, Dr. Amrita Kumar, Dr. Michael Otley and Dr. Aaron Baldwin. Without your help and support, I wouldn't be able to adapt to the laboratory environment and learnt and mastered research skills within a short period of time. My working experience with you guys have gained me a better insight into not only scientific research work but also life. It has been an invaluable part of my growth. I also have to thank my groupmates for making my graduate life so unforgettable and beautiful: Xiaozheng Zhang, Mengfang Li, Rui Ma, Geng Li, Omer Yassin, Shadidul Islam, Gregory Treich, Shamima Nasreen. Especially, Ms. Xiaozheng Zhang and Mr. Mengfang Li, thank you two for always being supportive. We three have encountered a lot hardships together but we finally made it through with unexpected rewards.

My graduate life was also made memorable because of good friends, especially Mr. Christian Malapit, Mr. Di Shu, Mr. Zhiwei Zhang, Mr. Hongyu Hong, Mr. Wenbo Li and Mr. Kan Fu. Thank you all for being part of my life. I also thank my families for their endless love and support, for always being my anchor when I felt down.

Last but not least, I give my deepest and sincerest gratitude to my Maker. My Lord, thanks for choosing me, I am truly blessed to be your Son. All my glory on earth goes back to you. Amen!

List of Figures

surface (1) before bending; and after 100 bending cycles under (2) 7.5 mm; (3) 6.25 mm; (4) 5.5 mm; (5) 3.0 mm.

Fig. 5.5 Sheet resistance of Sample B ITO/PET as a function of bending radius of curvature under tensile (solid black square) and compressive (open red triangle) stress after 100 bending cycles.

Fig. 5.6 (a) Optical microscopy images (×5 and ×100 magnification) of GPE consisting of 10wt% PegDMA in PEG before and after bending under 3 mm radius of curvature for 500 cycles; (b) (1) GPE consisting of 10wt% PegDMA in PEG and (2) corresponding PProDOT-Me2/gel electrolyte composite conformally bended to cylinder with 3 mm radius; (c) A 3 cm × 3 cm flexible *in situ* ProDOT-Me_2 ECD bended diagonally and from the middle line its colored (1) (2) and bleached (3) (4) states.

Fig. 5.7 Images of 110 cm^2 *in situ* flexible ECDs patterned with (a) UCONN logo employing PEDOT and (b) HUSKY logo employing a copolymer *in situ* copolymerized from Pyrrole and EDOT (monomer feed ratio 99 wt%:1 wt%) in their neutral and oxidized states under (1) unbent and (2) bended states, respectively.

Fig. 6.1 (a) Normalized Absorbance of Homopolymers or Copolymers by *in situ* polymerization of monomers at different feed ratios: 1. 100 wt% ProDOT-tBu_2, Abs max= 392 nm; 2. 80 wt% ProDOT-tBu_2 : 20 wt% ProDOT-Me_2 ,Abs max=446 nm; 3. 75% wt% ProDOT-tBu_2: 25% ProDOT-Me_2, Abs max= 460 nm 4. 65% ProDOT-tBu_2 : 35% ProDOT-Me_2, Abs max= 485 nm 5. 60% ProDOT-tBu_2 :40% ProDOT-Me_2, Abs max = 500 nm 6. 40% ProDOT-tBu_2: 60% ProDOT-Me_2, Abs max= 537 nm 7. 25% ProDOT-tBu_2: 75% ProDOT-Me_2 , abs max= 565 nm 8. 100% ProDOT-Me_2, Abs max= 575 nm.

Fig. 6.2 (a). Color coordinates and images of (1). ProDOT-Me_2/ ProDOT-tBu_2 copolymer device: dark state (solid green square on color space) and bleach state (open green square on color space); (2). ProDOT-Me_2/T34bT copolymer device: dark state (solid blue triangle on color space) and bleach state (open blue triangle on color space); (3). Dual layer Copolymer Device: dark state (solid red triangle on color space), theoretical modeled dark state (solid red diamond), and bleach state (open red triangle on color space), Reference white point (solid black circle on color space); Grey circle in color space represents the neutral color region.

(b). UV-Vis absorption spectra of the dual copolymer single electrochromic layer device. (c). Percent transmittance change at 555 nm for dual copolymer layer device during constant potential stepping between -2 V to +2 V.

Fig. 6.3 (a). Absorbance spectra and (b). Images of dark and bleached states for an *in situ* PT34bT device. The absorbance max is at 850 nm in its dark state.

Fig. 6.4 Absorbance spectra of dark and bleach states for the *in situ* ProDOT-Me_2/ProDOT-tBu_2 device (monomer feed ratio: 75 wt% ProDOT-Me_2 : 25 wt% ProDOT-tBu_2) shown in Figure 2 (a). The absorbance max is at 460 nm in its dark state. The device has the same peak intensity at 460 nm as the control dual copolymer layer device in the main article.

Fig. 6.5 Absorbance spectra of dark and bleached states for the *in situ* PProDOT-Me_2/PT34bT device (monomer feed ratio: 98.5 wt% ProDOT-Me_2 : 1.5 wt% T34bT) shown in Figure 2 (a). The absorbance max is at 618 nm in its dark state.

Fig. 6.6 Images of Dark and Bleach states for the small area (2×4 cm^2) devices shown in Figure 2(a): (a) ProDOT-Me_2/ProDOT-tBu_2 device (absorbance spectra corresponds to Figure S2), (b). *in situ* PProDOT-Me_2/PT34bT device (absorbance spectra corresponds to Figure S3) and (c). dual layer copolymer device (absorbance spectra corresponds to Figure 2(b)).

Fig. 6.7 (a). Absorbance spectrum and (b). Images of dark and bleached states for the *in situ* neutral color device utilizing Copolymer 2 and Copolymer 12.

Fig 6.8 Color coordinates for the supporting neutral system (solid red triangle represents dark state and open red triangle represents bleach state); Theoretical modeled dark state (solid red diamond); Reference white point (solid black circle on color space); Grey circle in color space represents the neutral color region.

Fig. 6.9 (a). Neutral and oxidized state images of a 75 cm^2 flexible dual copolymer layer device in its (1). non-bent and (2). bent states.

(b). Percent Transmittance of the 75 cm^2 flexible dual copolymer layer device in its neutral and oxidized states

List of Tables

TABLE OF CONTENTS

Chapter 1: Introduction

1.1 Conjugated Polymers

Polymers have been playing a significant role in the advancement of human society. For a long period of time, polymers have found extensive applications in primary areas such as coatings, containers, textiles, and such. While traditional polymers that are widely used in our daily lives (e.g. polyethylene, polystyrene and polyamide), are usually insulating materials, it was not until the last decade that polymers were found to have useful applications in optics, electronics, energy storage, etc. Conducting polymers were the trigger for this development. In the late 1970's, when the first discovery of conducting polymers came, the synthesis of polyacetylene and its subsequent doping with iodine established the field of synthetic metals: polymers with conductivities approaching those of metals. The Nobel Prize in Chemistry 2000 was awarded jointly to pioneers Alan J. Heeger, Alan G. MacDiarmid and Hideki Shirakawa for their discovery and development of conductive polymers. They recognized the potential to replace metals or inorganic materials with these conducting polymers.

Conducting polymers are typically conjugated polymers, are polymers consisting of alternating single/double bonds along the polymer backbone.[1] The π-conjugated system allows the delocalization or mobility of charge carriers along the polymer backbone.[2] A few examples are listed below in **Fig. 1.1**.

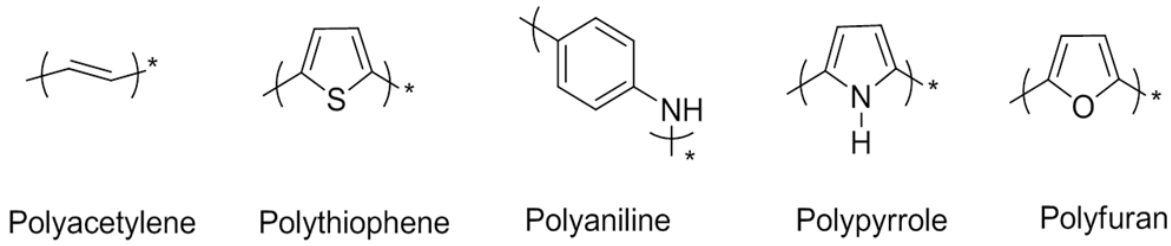

Fig. 1.1 Chemical structures of the most widely studied CPs

Polyacetylene and polypyrrole afterwards were the focus of scientific research community during the early stage development of conducting polymer. Much effort was placed onto developing synthetic routes that yileds polyacetylene with considerably crystallinity. In the meantime, although polypyrrole was found to be highly disordered and hard to characterize, it showed very attractive conduction properties. By 1995, there was a research interest shift into the semiconductor properties of conducting polymers. Polythiophene stood out and became the top candidate.[3] As an important class of CPs , polythiophenes have been extensively studied on the relationship between its chemical & geometrical structure and the corresponding optical and electronic properties. While unsubstituted polythiophenes are not easily processible, there have been a number of reports in the literature on its substituted derivatives as a result of the advantages that substituted derivatives of polythiophenes are soluble and fusible.

The design and synthesis of fused heterocyclic rings on the thiophene is a common modification resulting in polythiophenes with lower band gaps. Reynolds, et. al. reported on using donor-acceptor approach where electron-rich and -poor moieties were incorporated in the thiophene and benzothiodiazole repeating units. The resulting polymer absorbs the wavelength across the visible spectrum producing a polymer that appears black in its neutral state. In his earlier reports, Reynolds published on various

2,2-disubstitution on 3,4-propylenedioxythiophene (ProDOT) and using it as a platform to exhibit a full spectra tuning for the neutral state of electrochromic polymers.[4] On the other hand, Sotzing, et. al. studied substitution on the site with respect to oxygen. They found that depending on the substituent size the planarity of the consequential polymer was disrupted. The most notable of which is the 1,3-ditertbutylpropylenedioxythiophene (PProDOT-tB_2) having a 200nm shift in absorption max with respect to PProDOT-Me_2.[5] PProDOT-Me_2 has a deep purple color in its neutral state while substitution at 1,3-positions with tert-butyl, hexyl and isopropyl groups gave yellow, orange and red colored polymers, respectively. A few examples are listed below in **Fig. 1.2**.

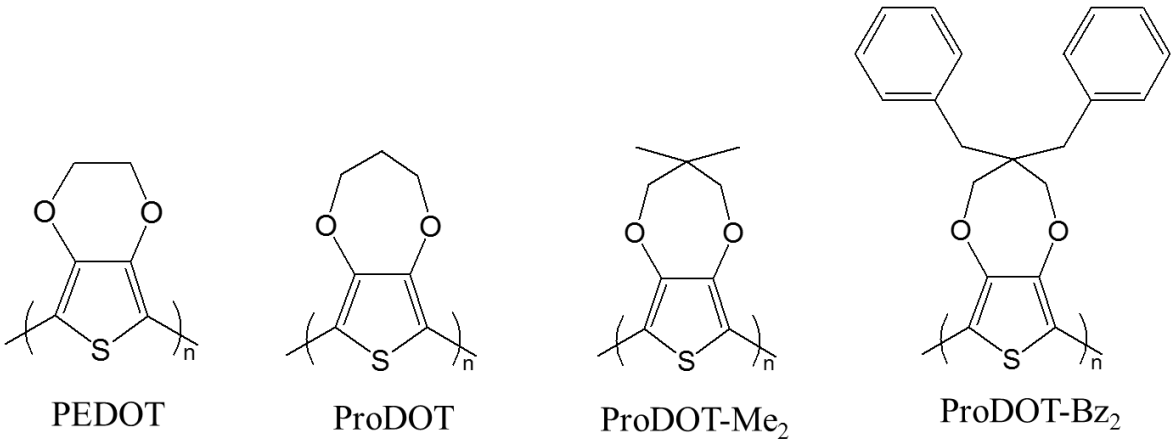

Fig. 1.2 Chemical structures of the most widely studied substituted Polythiophenes

1.2 Electrochromism

As implied by the name itself, ***Electrochromism*** is the phenomenon that color of a material changes in response to an applied electrical potential.[6] It is fundamentally based on the change of a material's electronic properties through oxidation or reduction, modulated by the material's band gap energy (Eg). Absorption characteristics of the material changes in the visible region are generated when an electrochromic material is switched between redox states. Typically, the color changes between a bleached state and a colored state.

A band gap is the energy difference between the Valence Band (VE) at the Highest Occupied Molecular Orbital (HOMO), and the Conduction Band (CE) at the Lowest Unoccupied Molecular Orbital (LUMO) and it is directly related to the absorption characteristics of a material and in turn its color properties

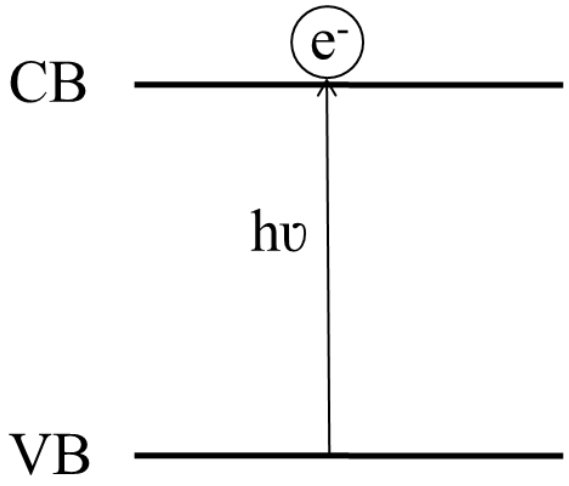

Fig. 1.3 π- π* transition upon the excitation across band gap

The π- π* transition that occurs upon the excitation across this gap is the source of the electrochromic behavior in CPs. In the neutral state, material absorbs light based upon

its band gap energy. These wavelengths or energies of absorption are typically within the visible region (350 to 800 nm). Once doped, the bands split and rearrange into a more complex pattern, resulting in lower energy absorption states (IR and microwave region).

The most successful commercial electrochromic polymer (ECP) is 3,4-ethylenedioxythiophene (PEDOT). PEDOT, in its neutral state demonstrates a deep blue and switches to a sky blue in oxidized state. Images are shown in **Fig. 1.4**.

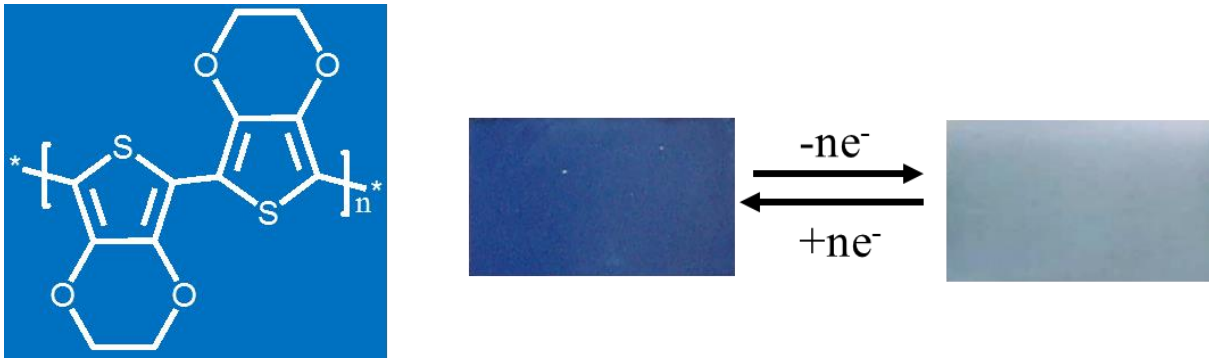

Fig. 1.4 Chemical structure of PEDOT and its color change between neutral and oxidized states

Advantages such as ease of processability, high contrast, and the ability to modify their structure to create multicolor electrochromes have made CPs a very important class of Electrochromic (EC) materials. To evaluate an EC material, there are a few important parameters we need to look at:

1. ***Electrochromic contrast*** is probably the most important factor in evaluating an electrochromic material. It is often reported as a percent transmittance change (%T) at a specified wavelength where the electrochromic material has the highest optical contrast. For some applications, it is more useful to report a contrast over a specified range rather than a single wavelength, e.g. photopic contrast (**Eq.1.1**),

where T(λ) is the spectral transmittance of the device, S(λ) the normalized spectral emittance of a 6000K blackbody and P(λ) is the normalized spectral response of the eye.[7]

$$T_{\text{photopic}} = \frac{\int_{\lambda_{\min}}^{\lambda_{\max}} T(\lambda)\, S(\lambda)\, P(\lambda)\, \mathrm{d}\lambda}{\int_{\lambda_{\min}}^{\lambda_{\max}} S(\lambda)\, P(\lambda)\, \mathrm{d}\lambda}$$

(Eq.1.1)

Just to give a visualized example, below are the pictures showing two different states of two different ECPs. One is for conducting polymer PEDOT and the other one is for PProDOT-Me_2. As can be seen by eye, the lower one has higher contrast.

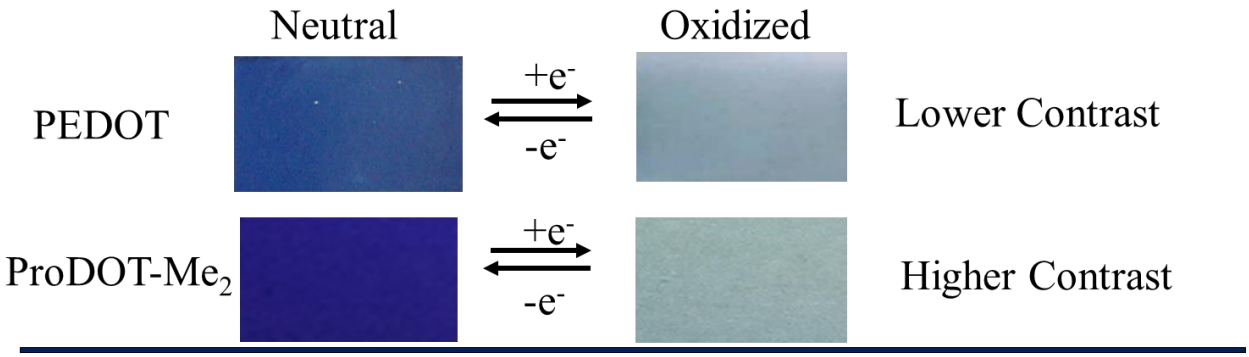

Fig. 1.5 Contrast Comparison between PEDOT and PProDOT-Me_2

2. ***Coloration Efficiency*** CE ($cm^2\ C^{-1}$) values measure the power requirements of an electrochromic material. It's determined as the optical absorbance change of an electrochrome at a given wavelength (ΔA) to the density of injected/ejected electrochemical charge necessary to induce a full switch (Qd). [8]The equation is shown below. If A larger Abs change is caused by a fewer charge requirement, a higher CE could be expected for this material.

$$\mathrm{CE} = \frac{\Delta A}{Qd} \quad \textbf{(Eq.1.2)}$$

3. **Switching speed.** Switching speed is often reported as the time required for the coloring/bleaching process of an EC material. For cathodically coloring polymer, the bleaching process is defined as the process for polymers going from neutral state (the colored state) to the oxidized state(the bleached state),and vice versa for the coloring process. Ions diffuse in and out. Generally speaking, the switching is dependent on several factors such as the ionic conductivity of the electrolyte, ion diffusion in polymer, polymer film thickness, and morphology of the polymer film. Other factors also include the potential applied, the substrate resistance and film area, etc. [9]

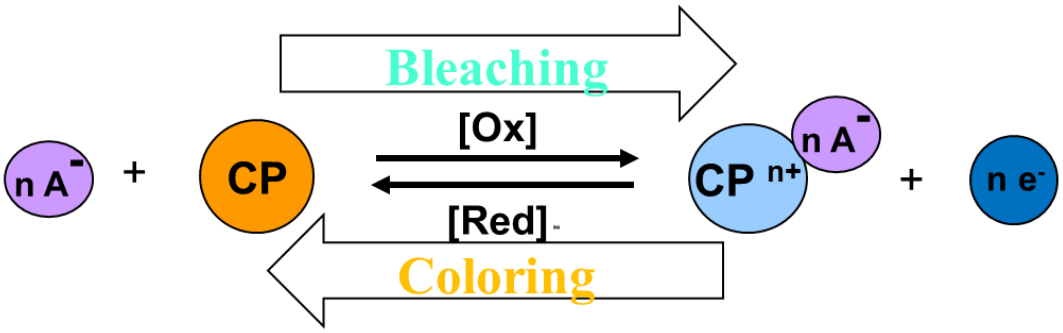

Fig. 1.6 Illustration for an cathodically coloring polymer switching between its neutral and oxidized states

4. **Stability**

EC material must undergo stable redox processes for its electrochromic properties to be reproducible upon repeated switching. Typical degradation processes encompass irreversible redox behavior under high potentials, water and oxygen redox interferences with the EC components, degradation of electrode materials or evaporation of the electrolyte, and resistive heating on repeated switching. The frequent shrinking and expanding of polymer chains during the redox switching (see **Fig. 1.7**) is also a reason for decreased stability of CP films.[10]

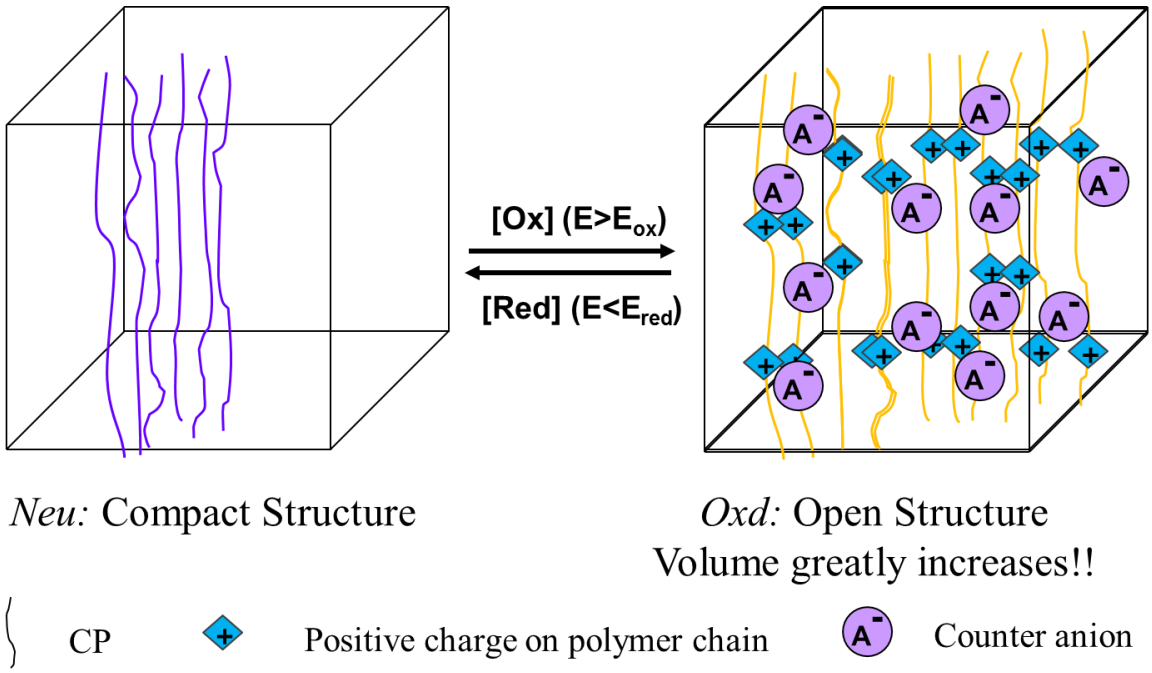

Fig. 1.7 Illustration for electrochemical switching of CPs between its neutral and oxidized states: polymer chains frequent shrinks and expands

5. **Optical Memory:**

It is defined as the time that an electrochromic device maintains its **colored** or bleached state when the applied potential is removed.[10] The optical memory effect originates from the stable electrochemical doping/dedoping process and is an important property of ECDs in eyewear and window applications. Devices that exhibit a higher optical memory will consume less energy for a given application or simplify the electronics.[20]

6. Color Analysis

Human eye perception of colors vary from one person to another, therefore, a system of ***colorimetry*** developed by the CIE has been applied to the quantitatively describe a color. Three main advantages can be expected from this colorimetric analysis: **1.** A quantitative measurements of color allows for accurate report of the colors of the materials; **2.** The electrochrome's color can be represented graphically and mapped onto color coordinate (see **Fig. 1.8**); **3.** The method is a valuable tool to build electrochromic devices with desired colors and can provide useful information for analysis.[21]

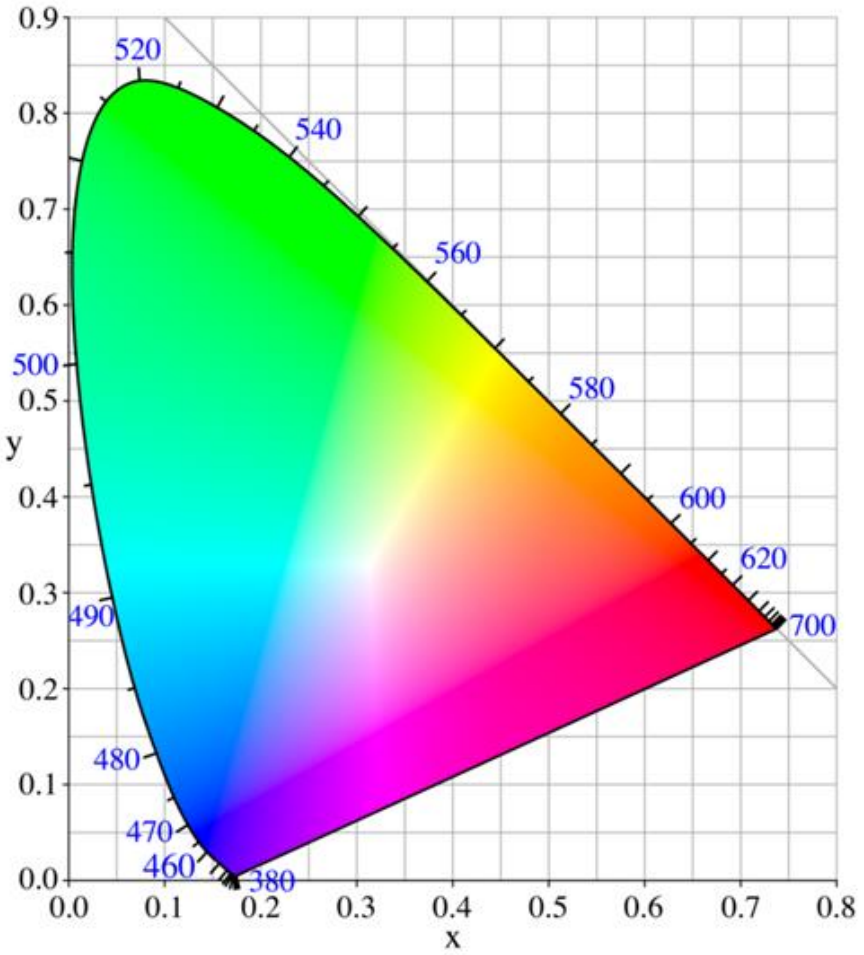

Fig. 1.8 The CIE xyY Chromaticity Diagram.

1.3 Electrochromic Device

For real applications, EC material is usually built into ECD. A typical ECD structure made of ECP is shown in **Fig. 1.9**. The basic components are two electrodes, typically ITO coated glass or ITO coated PET respectively serving as working electrode and counter electrode. Two electrochromic polymer layer are deposited onto the two electrodes. Each of the polymer layer acts as the ion storage layer for the other. Between the two EC polymer layers is sandwiched a gel electrolyte layer for ionic conduction.

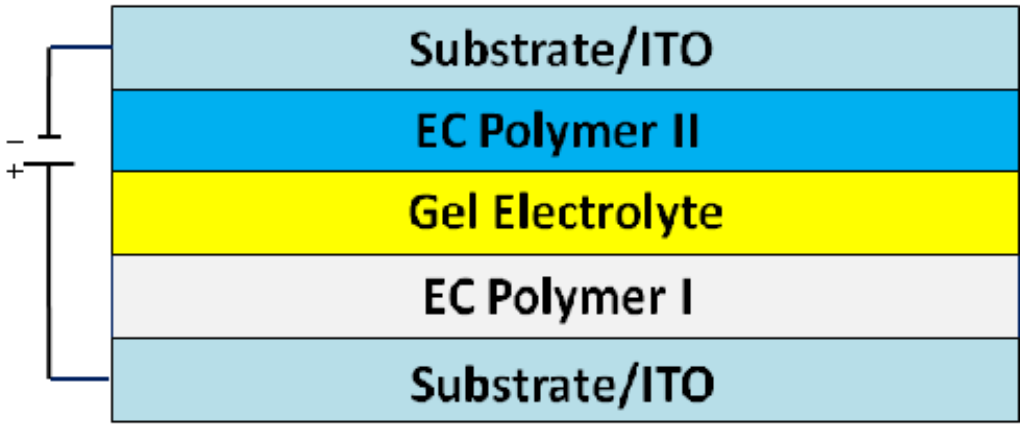

Fig. 1.9 Electrochromic Device sandwich configuration.

The most common applications of ECDs include a variety of displays and eyewear shown in **Fig. 1.10**. For example, electrochromic googles shift from one color to a different, smart windows used at household to control the amount of light allowed to pass through, and EC fabric devices which allow color changes on textile, to name a few.

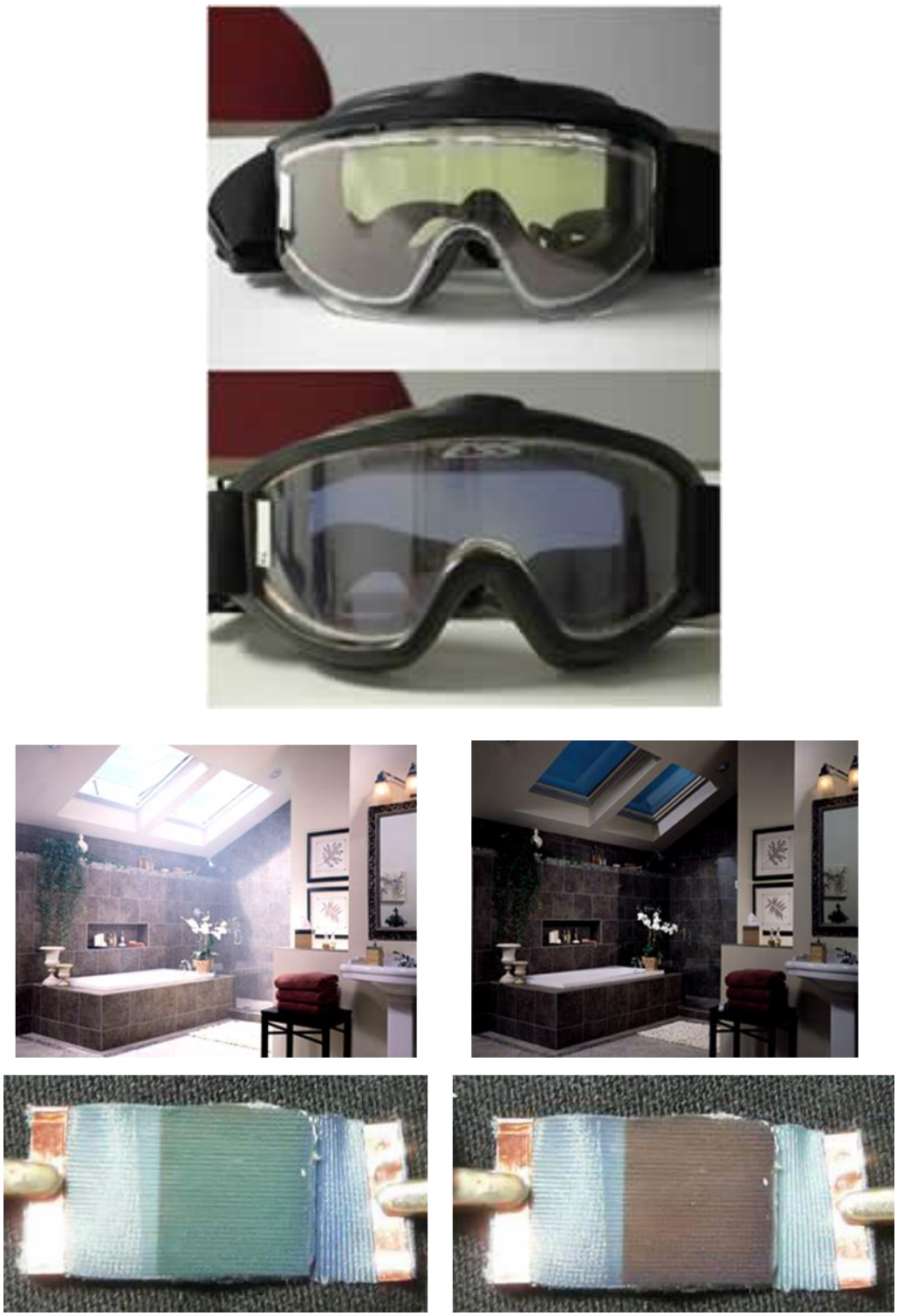

Fig. 1.10 Common applications of ECDs including color changing goggle, smart windows and color changing textile

1.4 Gel Polymer Electrolyte (GPE)

As an important component of ECDs, one role the gel polymer electrolyte serves is the ionic conduction medium enabling ions to move in and out of the electrochromic polymer. The gel polymer electrolyte is generally a salt-solvent-polymer hybrid system in which the salt is first dissolved in solvent and then immobilized in a polymer matrix. [11] The salt provides free mobile ions for conduction, and the solvent takes part in dissolving the salt as well as acting as the conducting medium for ion movement, while the polymer imparts mechanical stability.

Lithium salts are the most widely used salt in Gel Polymer Electrolyte since it is easy to dissolve and able to travel in the medium with high mobility which increases the ionic conductivity.[12]

Poly(ethylene glycol)s (PEG) are one of the most widely studied classes of polymers used for gel polymer electrolytes.[13] PEG has a wide potential window for operation and due to its polar ether groups and significant segmental mobility, PEG has excellent compatibility for a variety of salts in that the ether oxygens help coordinate to metal cations, which is favorable for compatibility of the salt with the polymer allowing for high ion concentration. In applications, liquid electrolytes are often not desired as they may cause safety issues when used in eyewear if a lens is broken due to proximity. Therefore an acrylate functionalized PEG, PEG-DA, was used for its ability to undergo UV crosslinking in the presence of a photoinitiator to form the solid gel matrix.

The solvent used in the solid gel matrix must possess a high dielectric constant, a wide operating temperature range, a low vapor pressure as well as good electrochemical stability. Propylene carbonate (PC) was chosen as the solvent as it meets all aforesaid

requirements: a dielectric constant of 64.42 at 25 ℃, a freezing point of -49 ℃ and a boiling point of 242 ℃ at normal pressure. [14] The solvent plays an important role in increasing the degree of dissociation of the salt; that is, solvating the ions thereby reducing ion-ion interactions. The flexibility and segmental motion of the host polymer chains are improved due to the plasticization effect of PC, which in turn enhances the conductivity of the gel electrolyte. In addition to the above properties, PC was chosen because it has been reported to yield films for electrochromic devices of high optical contrst and color efficiency as reported by Poverenov *et al.* [15]

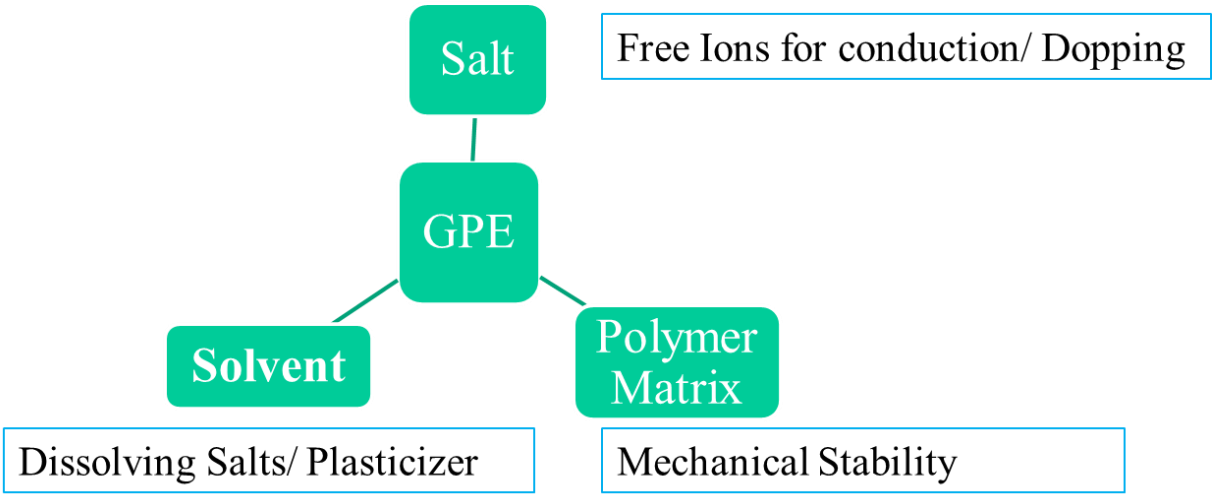

Fig. 1.11 Illustration for the composition of Gel Polymer Electrolyte and their functions

1.5 Diffusion Fundamentals

Mass transportation of the uncharged small molecules (e.g. monomers) in the polymer matrix is one of the most important factors to be considered for solid-state electrolytes. Mass transportation in an electrolyte medium takes place in three modes: **convection**, **migration** and **diffusion**. Convection is the physical movement of ions in the electrolyte. For unstirred, undisturbed electrolyte system (the case for ECD), convection is usually negligible. Migration represents the motion of charged ions caused by an external electric field. To minimize the effect of migration, the electrolyte is typically prepared with an excess amount of supporting ionic salt. These ions accumulate at the polarized electrodes and balance the charges and hence inhibiting continuous migration. However, it is believed that the migration effect is appreciable and plays a relatively more significant role in solid/polymer electrolytes and sometimes becomes a material property due to the interactions between the ions and the polymer network.[16]

The third mode, **diffusion**, is defined as the movement of neutral molecules from an area of high concentration to one of low concentration and it is the most important approach of mass transportation in solid gel electrolytes. The diffusion coefficient (D), represents the speed molecules travel through the solution under concentration gradients and its value does not change for a specified system.[17] When talking about diffusion, there are usually two cases to be considered, shown in **Fig. 1.12**

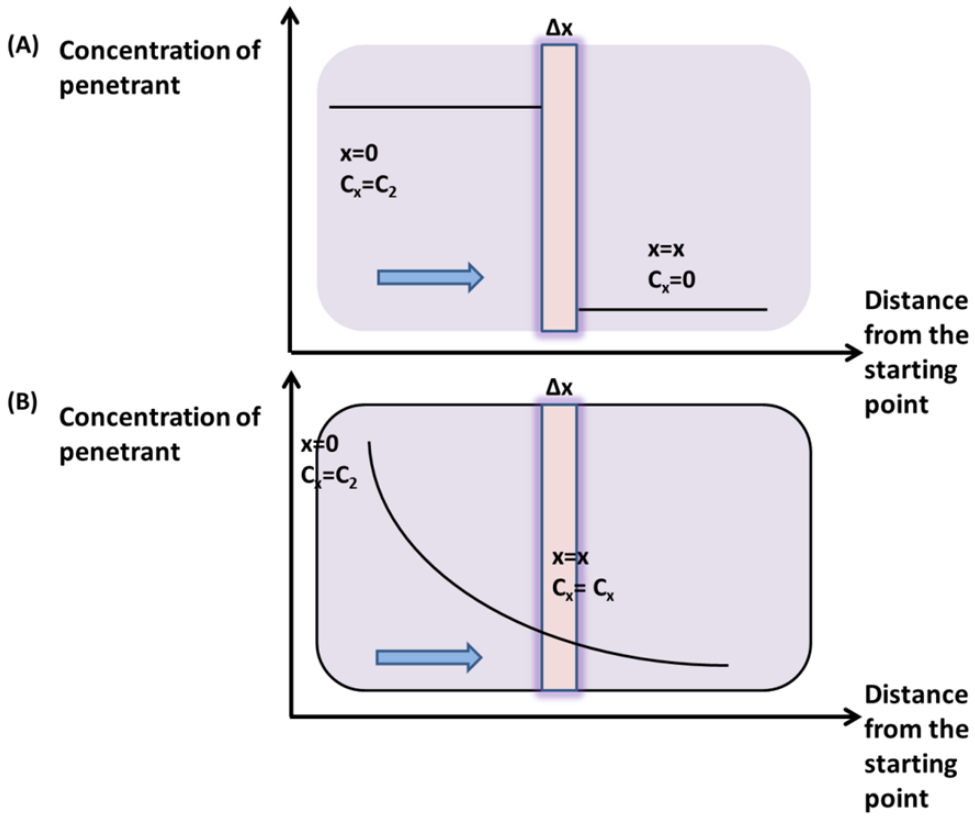

Fig. 1.12 Illustration for (A) steady-state diffusion and (B) non-steady-state diffusion

A. Steady State Diffusion: Concentration of Diffusion does not change with time and diffusion takes place at a constant rate. It follows **Fick's first Law**. [18]

$$J = -D \nabla C$$

where ***J*** is the net flow of the molecules, ∇C is the concentration gradient, D is the diffusivity.

B. Non-Steading State Diffusion: represents the diffusion process from a finite space into a finite volume. The rate of diffusion gradually slows down over time and distance as the concentration gradient decreases. This is the case which happens the monomer diffusion in solid-state electrolyte process inside assembled ECDs. It is described by **Fick's Second Law**.[19]

$$\frac{dC}{dt} = D\frac{\partial^2 C}{\partial x^2}$$

The rate of concentration change with time is equal to the diffusion times the rate of change in the concentration gradient.

1.6 Color Science

Colors are perceived by human eyes and the perception of color can vary from individual to individual. Many factors can affect people's perception of colors, including illumination, the angle at which a color is observed (iridescence), comparison of neighboring colors, to name a few. Apart from the individual differences, human eyes also have different sensitivity towards different colors. In the visible light region (350 nm to 800 nm), the light will be perceived from violet, blue to orange, and finally red. Human eye are most sensitive at 555 nm which corresponds to a green color, and the sensitivity decreases towards the two ends of the color spectrum (350 nm to 800 nm). Light with wavelengths below 350 nm or above 800 nm will become colorless to the eye. (see **Fig. 1.13**).

Fig. 1.13 Visible Color Spectrum

There are two ways how light reaches human eyes: ***Emission*** or ***Reflection***. Giving a simple definition: Emission means that light goes straight into human eye without hitting other objects; Reflection means light hits one object and the object absorbs certain wavelengths and the color we see from the object is the light is reflected off. ***Color mixing theory*** is another concept people frequently talk about when referring to color science. There are two types of color mixing: ***Subtractive*** and ***Additive*** color mixing. Giving an analogy, subtractive color mixing can be seen as adding two dyes together. The two dyes absorb different wavelengths to produce their individual colors. When they are mixed together, they would absorb both wavelengths simultaneously, the remaining unabsorbed light is what we will see. Black is produced when the entire visible wavelengths are absorbed, following the subtractive color mixing theory. Additive color mixing, on the other hand, can be viewed as when light of different colors shines onto the same spot. When all emitted colors are added together, it appears to be colorless (white light). The most common example is sunlight, which is a mixture of light with all wavelengths.

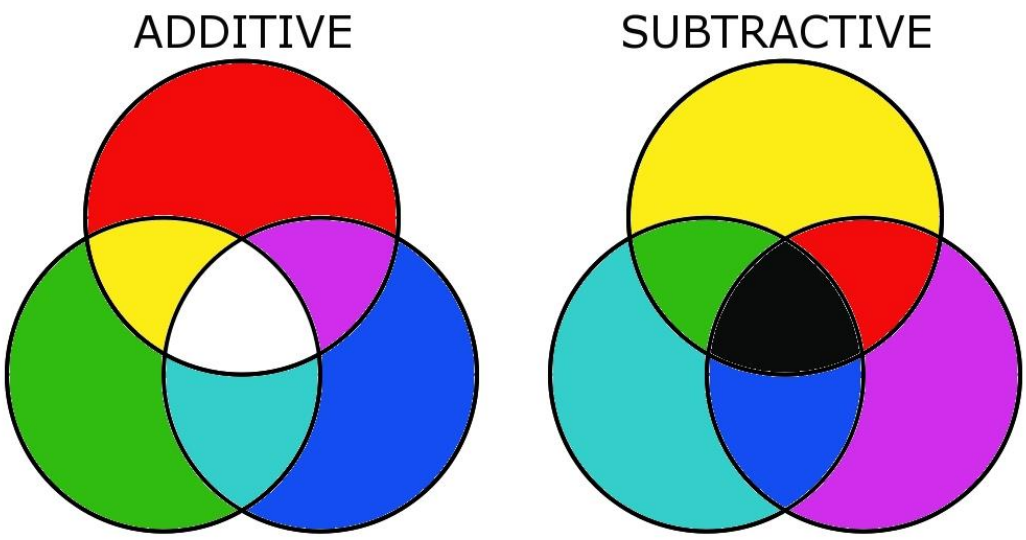

Fig. 1.14 Illustration for Subtractive and Additive Color Mixing

Regardless, we need a method to give an accurate definition of colors. The 1931 XYZ Color space is the most recognized color characterization system. The CIE 1931 color space system put together all the physics aspect of colors along with standard observer response to give a mathematical representation to the human perception of color. The eyes perceive color as a mixture of three primary colors, red, green and blue, which are expressed using the "tristimulus" values X, Y and Z, respectively. These tristimulus values were used to derive a color diagram, the xy chromaticity diagram, similar to a Cartesian coordinate system to represent a specific color. Here, the (x, y) values are calculated from the XYZ values. The luminance of the color is represented by Y and is kept in the system although not represented in the two-dimensional graph. Three dimensional set up makes it difficult to visualize the data on paper, so resulting values are "XYZ" and are transformed into Yxy by linear algebra. But this color space suffers from a drawback in that it is not uniform.[22]

Beyond that, the CIELu'v' coordinate system is another one of the most widely used chromaticity diagrams. It is a more uniform color space wherein the difference between two colors are related to their distance on the graph. In comparison with CIE xyY, it has improved color resolutions, it has spread out the colors on the graph so that it will be more clearly to assign a given color. This color space is widely used in television and video displays.

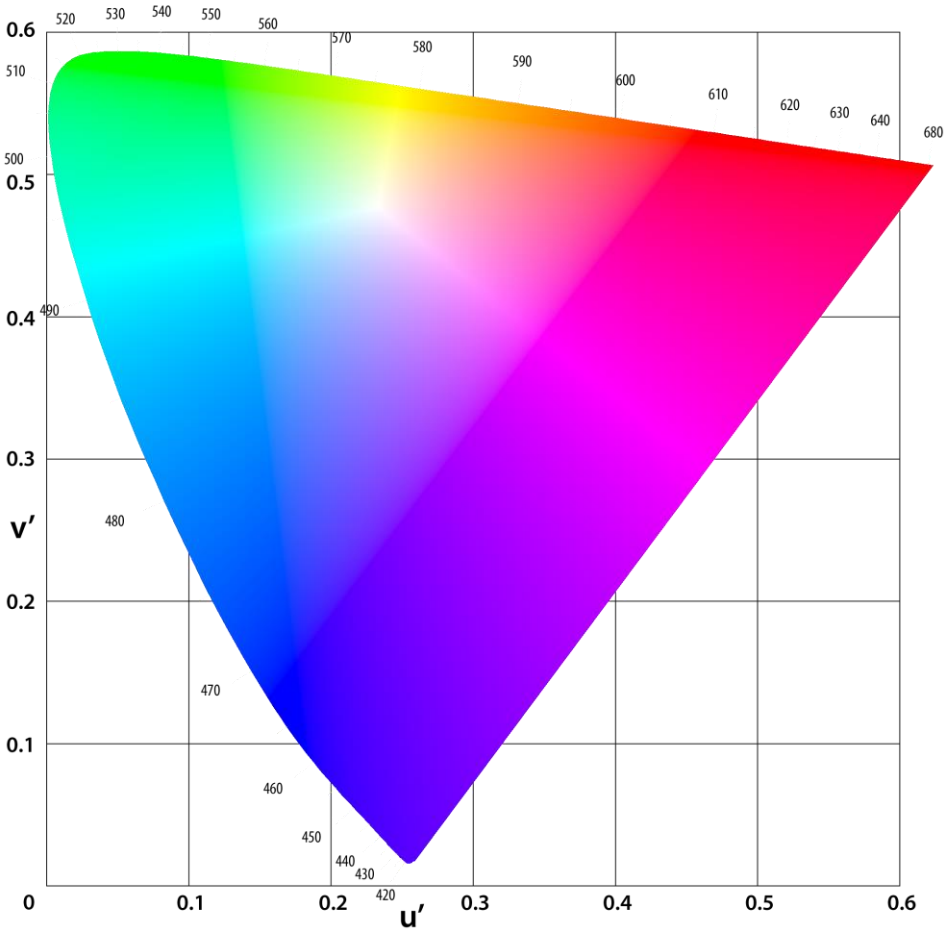

Fig. 1.15 The CIE 1976 LUV diagram

1.7 References

1. Chiang, C. K.; Druy, M. A.; Gau, S. C.; Heeger, A. J.; Louis, E. J.; MacDiarmid, A. G.; Park, Y. W.; Shirakawa, H. J. Am. Chem. Soc., 1978, 100(3), 1013-15.

2. A.A. Argun, P.H. Aubert, B.C. Thompson, I. Schwendeman, C.L. Gaupp, J. Hwang, N.J. Pinto, D.B. Tanner, A.G. MacDiarmid, J.R. Reynolds, Chem. Mater. 16 (2004) 4401-4412.

3. Nalwa, H. S. e. Handbook of Organic Conductive Molecules and Polymers; West Sussex, England: John Wiley & Sons, Ltd, 1997; Vol. 3.

4. A. A. Argun, P. H. Aubert, B. C. Thompson, I. Schwendeman, C. L. Gaupp, J. Hwang, N. J. Pinto, D. B. Tanner, A. G. MacDiarmid and J. R. Reynolds, Chem. Mater., 2004, 16, 440–4412

5. T. Dey, M. A. Invernale, Y. Ding, Z. Buyukmumcu, G. A. Sotzing, Macromolecules 2011, 44, 2415.

6. Wang, S.; Li, X.; Xun, S.; Wan, X.; Wang, Z.Y Macromolecules, 2006, 39 (22),7502–7507

7. M. A. Invernale, Y Ding, D. Mamangun, M. S. Yavuz, and Gregory A. Sotzing, Adv. Mater.2010, 22, 1379–1382

8. Padilla, J.; Seshadri, V.; Filloramo, J.; Mino, W. K.; Mishra, S. P.; Radmard, B.; Kumar, A.; Sotzing, G. A.; Otero, T. F. Synth. Met.2007, 157, 261.

9. Mortimer, R.J. Electrochim. Acta.1999, 44, 2971.

10. P. M. Beaujuge and J. R. Reynolds. Chem. Rev. 2010, 110, 268–320.

11. V.K. Thakur, G. Ding, J. Ma, P.S. Lee, X. Lu, Adv. Mater. 24 (2012) 4071-4096

12. S. Ahmad, Ionics. 15 (2009) 309-321.

13. S.A. Agnihotry, P. Pradeep, S.S. Sekhon, Electrochim. Acta. 44 (1999) 3121-3126

14. C. Ma, J. Zheng, S. Yang, D. Zhu, Y. Bin, C. Xu, Org. Electron. 12 (2011) 980-987

15. E. Poverenov, M. Li, A. Bitler, M. Bendikov, Chem. Mater. 22 (2010), 4019-4025

16. Monk, P. M. S. Mortimer, R. J.; Rosseinsky, D. R. Electrochromism and electrochromic devices; Cambridge University Press, 2007; p. 483.

17. R.J. Mortimer, Chem. Soc. Rev. 26, 1997, 147–156.

18. R.J. Mortimer, Electrochromic. Acta 44, 1999, 2971–2981.

19. D.R. Rosseinsky, R.J. Mortimer, Adv. Mater. 13, 2001, 783–793.

20. H. Shin, Y. Kim, T. Bhuvana, J. Lee, X. Yang, C. Park, E. Kim, ACS Appl. Mater. Interfaces. 4 (2012) 185-191.

21. Ohta, N. and Robertson, A. Colorimetry: Fundamentals and Applications. Wiley. 2006.

22. Nassau, K. The Physics and Chemistry of Color: The Fifteen Causes of Color. 2nd edition. Wiley Interscience. New York **2001**.

23. Nassau, K. The Physics and Chemistry of Color: The Fifteen Causes of Color; 2nd ed.; New York: John Wiley & Sons, Inc., 2001.

Chapter 2: Instrumental and Experimental Methods

In this chapter, the general instrumentation and experimental methods are introduced.

2.1 Basic Electrochemical Methods

All electrochemical characterizations were performed by CHI potentiostat model 400a or 720c. The image for a typical potentiastat is shown in **Fig. 2.1**.

Fig. 2.1 CHI Potentiostat 720c used for electrochemical experiments.

Two major electrochemical techniques are usually used in major work of the thesis.

(a) Cyclic Voltammetry (CV)

Cyclic Voltammetry is typically used to study redox potential and electrochemical activities of an electroactive species. By applying a linear sweep of potentials on the sample, the corresponding current flow is measured. The linear potential sweep is shown

in **Fig. 2.2**. The current increases when redox reaction takes places and decreases when the concentration is decreased. A lot of useful information can be obtained from a resulting CV diagram. It can show the onset point of monomer polymerization or the CP redox process, which can be used to determine the polymerization potential of monomers and oxidation or reduction potential of formed CPs. Other information including the oxidation and reduction peak potentials (Epc and Epa), the oxidation and reduction (Ipc and Ipa) peak currents can also be observed from a CV diagram. Usually, the peak current of a reversible reaction (ip) is described by the Randles and Sevick equation:

$$i_p = 2 \times 10^5 n^{3/2} A D^{1/2} v^{1/2} C_0$$

(**Eq.2.1**)

Where n is the number of electrons, A is the surface area of the working electrode (cm^2), D is the diffusion constant (cm^2/s), Co is the bulk concentration of the electroactive species (mol/cm^3), and *v* is the scan rate (V/s). [1]

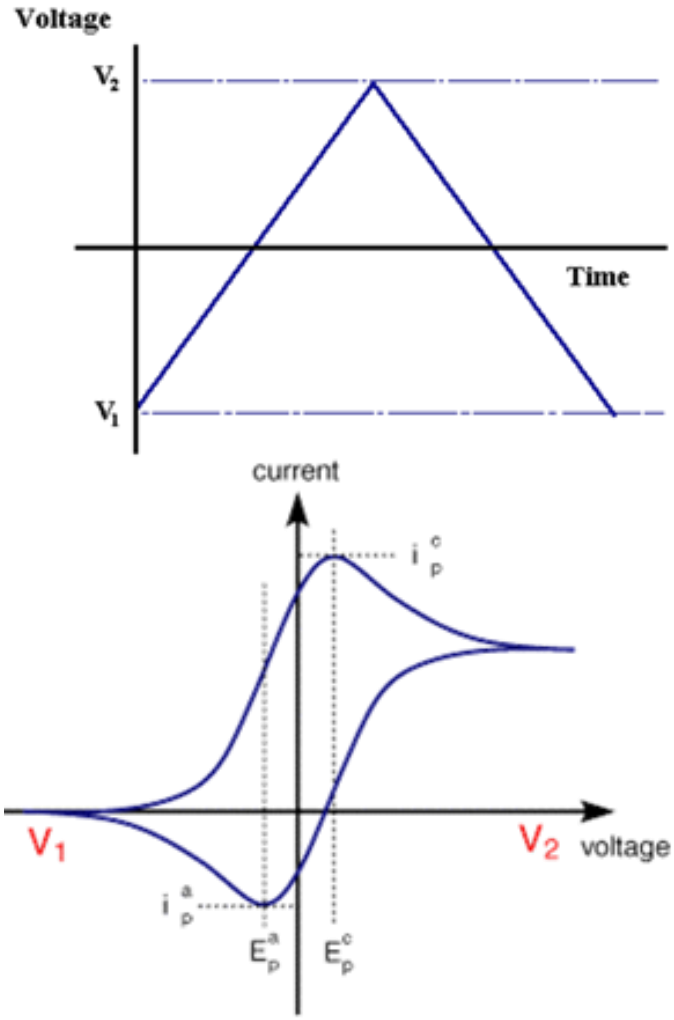

Fig. 2.2. Typical CV graphs: linear sweep of potentials and resulting CV diagram showing oxidation and reduction peak potentials (Epc and Epa), the oxidation and reduction (Ipc and Ipa) peak currents

(b) Chronocoulometry (CC)

Chronocoulometry (CC) technique, on the other hand, is typically used after obtaining information from the CV diagram. In CC, voltages are kept between two constant values and charges passed the sample were measured. In practical application,

the two potential values are very close to each other (11 mV difference), therefore the potential applied can be viewed as constant over the whole course. [2]

It can be used to polymerize electroactive monomers after knowing the oxidation potential of monomers using the CV technique. It can also be used to oxidize and reduce the formed CPs (i.e. redox switching the CP) after knowing the oxidation and reduction potentials from CV.

2.2 Electrochromic Contrast Measurement

After the determination of redox potential from the basic electrochemical study, we will be using spectroelectrochemistry technique to measure the electrochrmic contrast. Spectroelectrochemistry is an optical measurement technique combined with electrochemistry. A lot of useful information can be studied from spectroelectrochemistry. E.G. the band gap of polymers, the absorption characteristics of polymers and it can provide further information on polymer structure-properties relations. Optical measurement is performed on a varian cary 5000 UV-Vis NIR spectrometer shown in **Fig. 2.3**. And it is accomplished in combination with the potentiostat to the internal UV-Vis compartment for real-time scanning.

Fig. 2.3 Image for Varian cary 5000 UV-Vis NIR spectrometer

A typical graph for spectroelectrochemistry study is shown in **Fig. 2.4**.[3]

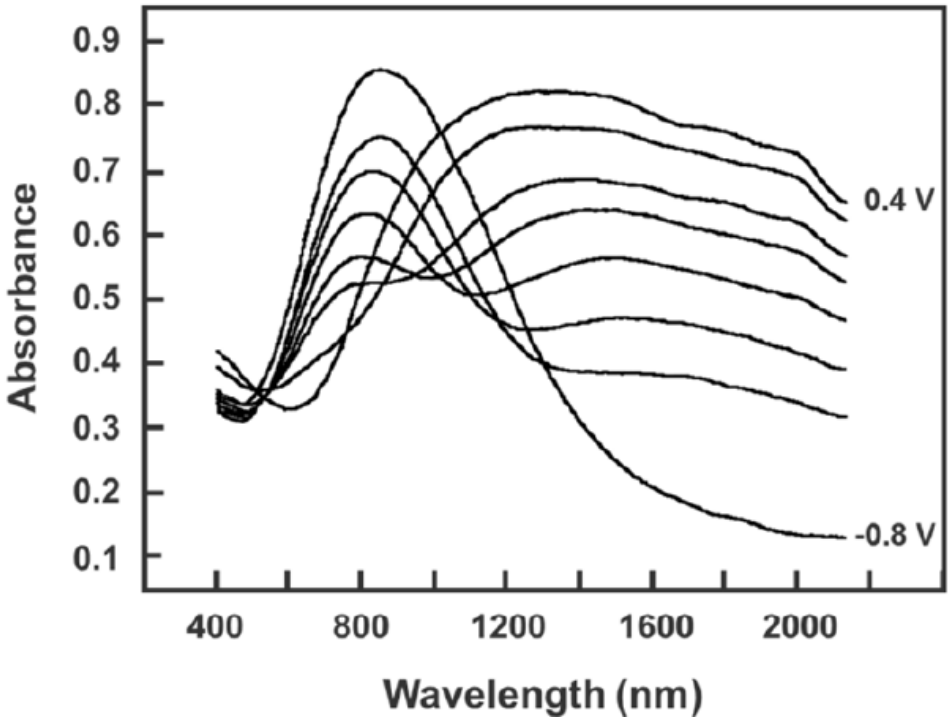

Fig. 2.4 A typical graph for spectroelectrochemistry study

Electrochromic contrast be measured and reported in two ways:

1. At a fixed single wavelength, with potentials switching between different values to completely redox switch the polymer, we measure the UV-vis Absorbance OR transmittance of the CP under this single wavelength. And the electrochromic contrast is reported as single wavelength electrochromic contrast.

$$\Delta T\% = T\%(\text{reduced state}) - T\%(\text{oxidized state})$$

2. Instead of fixing at a single wavelength, we scan the UV-vis spectra from 350 nm~850 nm of the CP in their oxidized and reduced states. And Corresponding photopic transmittance is calculated using **Eq. 2.2**:

$$T_{photopic} = \frac{\int_{350}^{850} T(\lambda)S(\lambda)P(\lambda)d\lambda}{\int_{350}^{850} S(\lambda)P(\lambda)d\lambda} \qquad \textbf{(Eq.2.2)}$$

where T(λ) is the spectral transmittance of the device, S(λ) is the normalized spectral emittance of a 6000 K blackbody and P(λ) is the normalized spectral response of the eye.[2] Photopic contrast is the difference between the photopic transmittance values of the bleached and colored states. Photopic contrast gives a more accurate description than the commonly reported contrast at a single wavelength as it weights all visible wavelengths based upon sensitivity of human eye. In addition, the photopic values reported here are not background corrected and thereby are representative of all absorbance and reflections of through all materials and interfaces of the device.

ΔT photopic % = T photopic %(reduced state) – T photipic %(oxidized state)

2.3 Switching Speed Measurement

For switching speed measurement, a square wave potential is usually applied at different frequencies onto the CP, which allows the CP to switch from one colored state to another state. A typical input for a square wave potential is shown in **Fig. 2.5**.

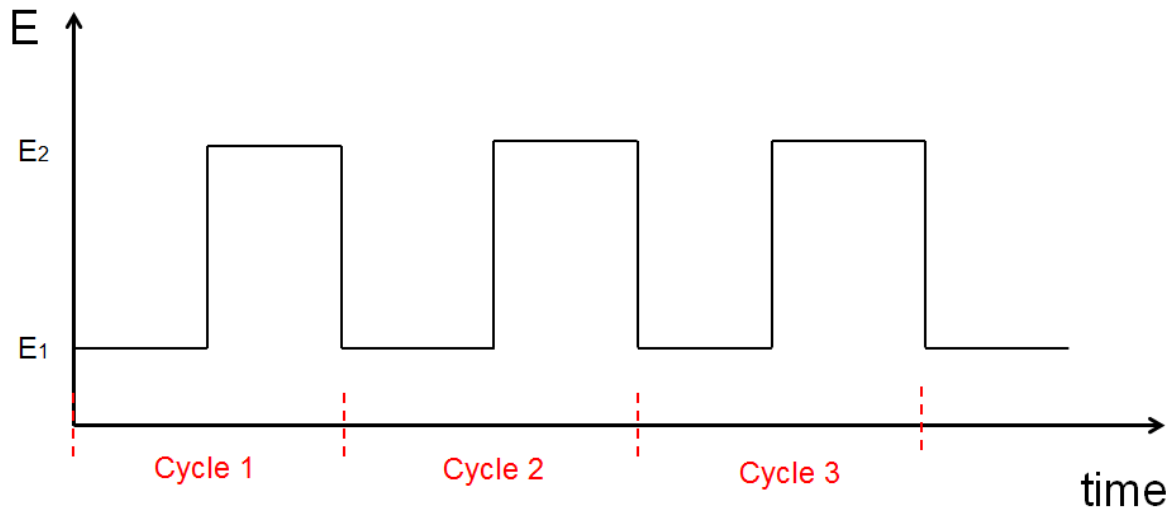

Fig. 2.5 A typical square wave potential graph

And the transmittance change of the material will be monitored at the maximum absorption wavelength (λmax) or 555 nm wavelength where human eye has the highest sensitivity towards using optical instrument. From the T% - time curve, the switching speed is typically determined as the time required for achieving 90% of the full transmittance change. A typical T% - time curve graph and the indication for 90% of the full transmittance change is illustrated in **Fig. 2.6**.

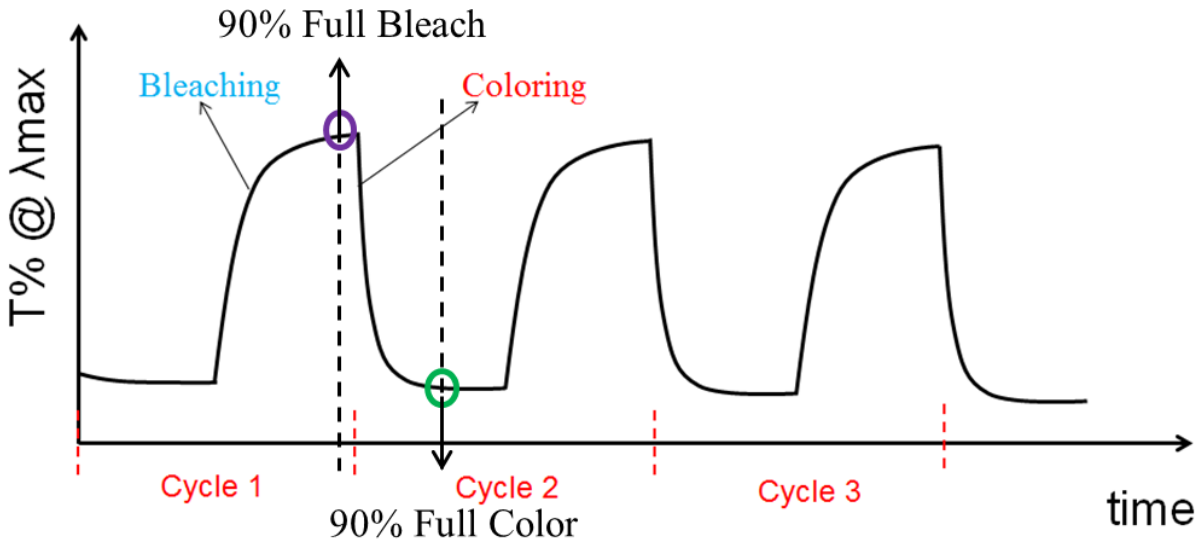

Fig. 2.6 A typical T%-time curve graph and indication of 90% of full transmittance change

2.4 Coloration Efficiency Measurement

Simultaneously, during the measurement of switching speed, a charge-time curve will be recorded by chronocoulometry (CC) during switching process (**Fig. 2.7**). By plotting optical density change as a function of charge density change, the coloration efficiency (CE) can be obtained from the slope of the plot through linear fitting. [4]

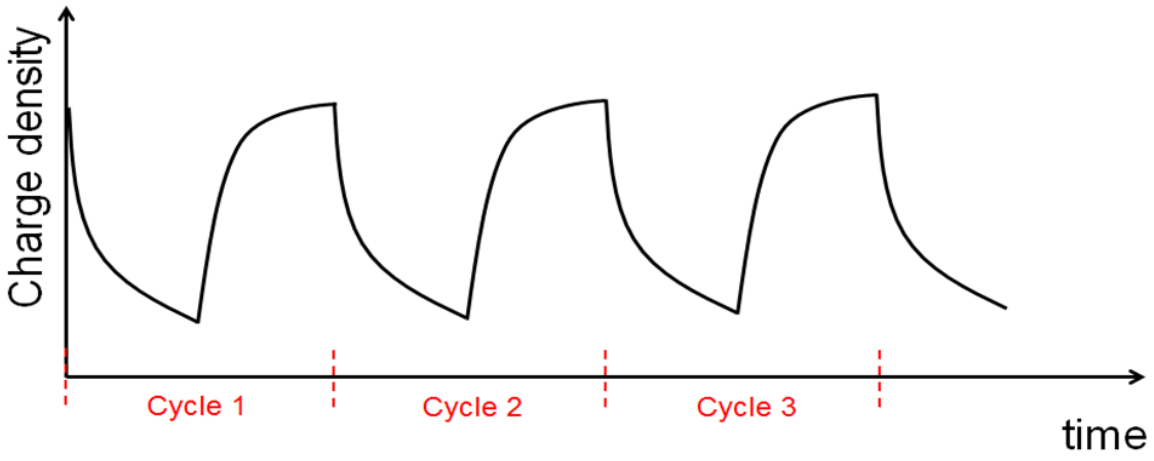

Fig. 2.7. A typical charge - time curve graph

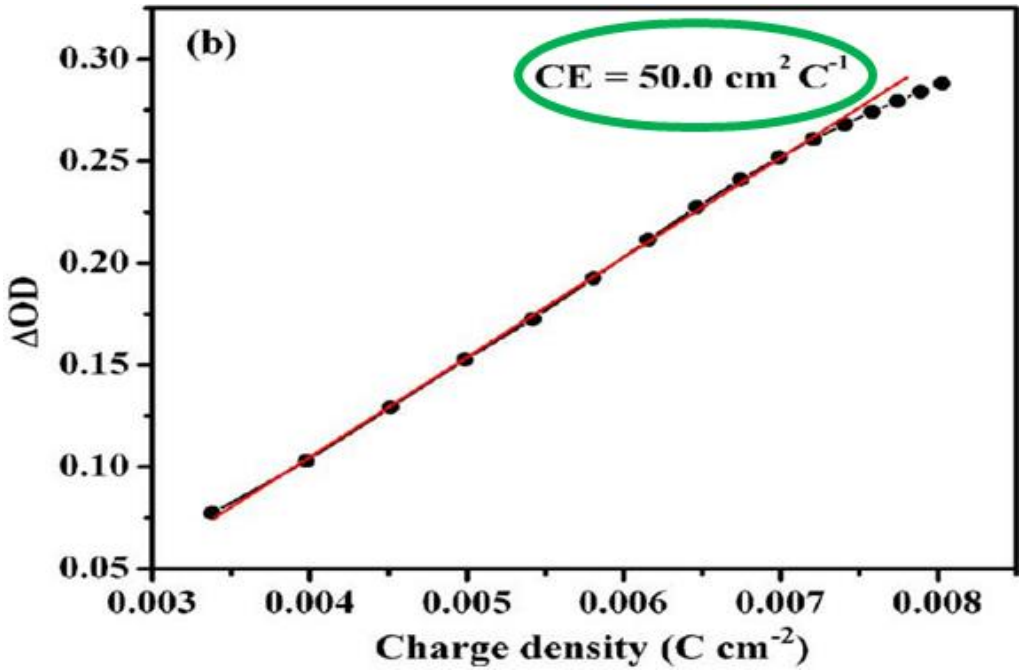

Fig. 2.8. Illustration for coloration efficiency calculation

2.5 Stability Measurement

There are usually two ways to report the long-term switching stability of an electrochromic materials. The experiments will be carried out by repeated switching of the EC material for a long cycles (usually over 10,000 cycles) and the corresponding T%-time curve and charge - time curve will be recorded.

From the T%-time curve, the contrast loss of the material will be determined and from the Charge-time curve, the charge loss of the material can be calculated. Either contrast loss or charge loss can be used to report the stability performance of an EC material.

2.6 Optical Memory Measurement

Optical memory or open circuit memory, is usually defined as the ability of an EC material or built ECD to retain its colored or bleached state, respectively, after the electric field is removed.[5] The optical memory effect originates from the stable electrochemical doping/dedoping process and is an important property of ECDs in eyewear and window applications. Devices that exhibit a higher optical memory will consume less energy for a given application or simplify the electronics.[6] For practical measurement, the hermetically sealed EC devices (to avoid oxygen and moisture effect) are usually placed in open air, under ambient light conditions, and the transmittance of the device is measured as a function of time (can be either single wavelength transmittance or photopic transmittance). When a certain transmittance loss is observed, the time for reaching that loss point is reported as the optical memory.

2.7 Ionic Conductivity Measurement

To measure the ionic conductivity of solid gel electrolyte, the liquid electrolyte is first filled full in a lab made set up shown in **Fig.2.9**. The basic components are: The bottom is aluminum weighing pan, the surrounding is transparent glass cylinder (the height is known which determines the thickness of resulting solid gel electrolyte) sealed with glue onto the aluminum weighing pan. Once the pan is filled full with liquid electrolyte. A piece of parafilm is placed onto the liquid top to form complete seal of the

liquid to avoid air in. Then the liquid fully filled set up is placed into a UVP CL-1000 Crosslinker (365 nm) to cure the liquid monomer electrolyte, shown in **Fig. 2.10**.

Fig. 2.9 Set up for curing liquid electrolyte

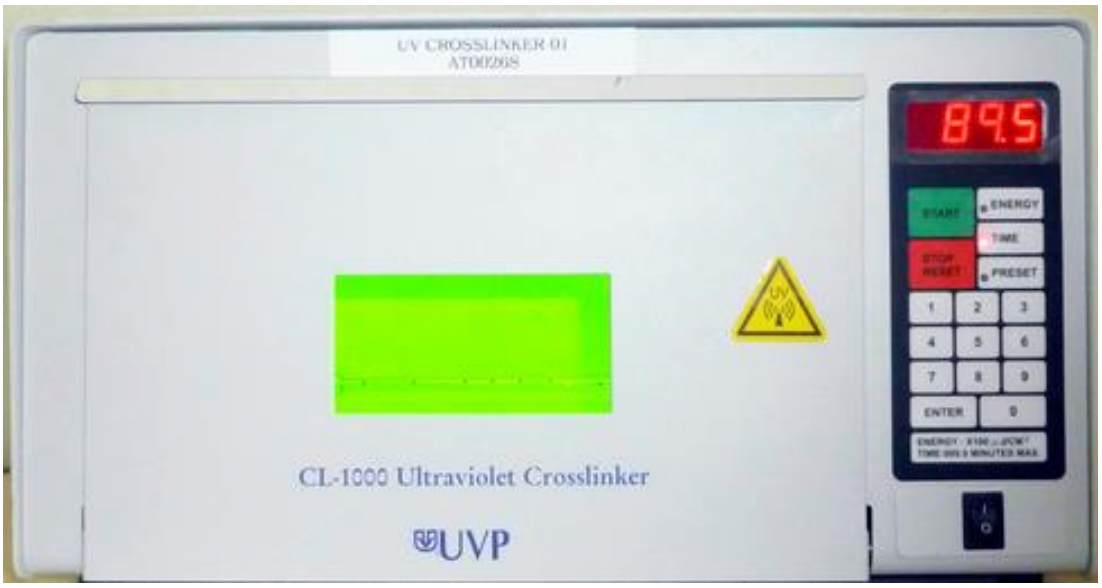

Fig. 2.10 Image for a UVP CL-1000 Crosslinker (365 nm)

Ionic conductivity of the cured solid gel electrolyte is then measured by AC impedance spectroscopy on an HP 4285 A precision LCR meter by placing the sample between two electrodes (see **Figure 2.11**). Then the impedance is recorded as a function of frequency (over a frequency range of 20 Hz to 1 MHz) under ambient room temperature (25 ℃).

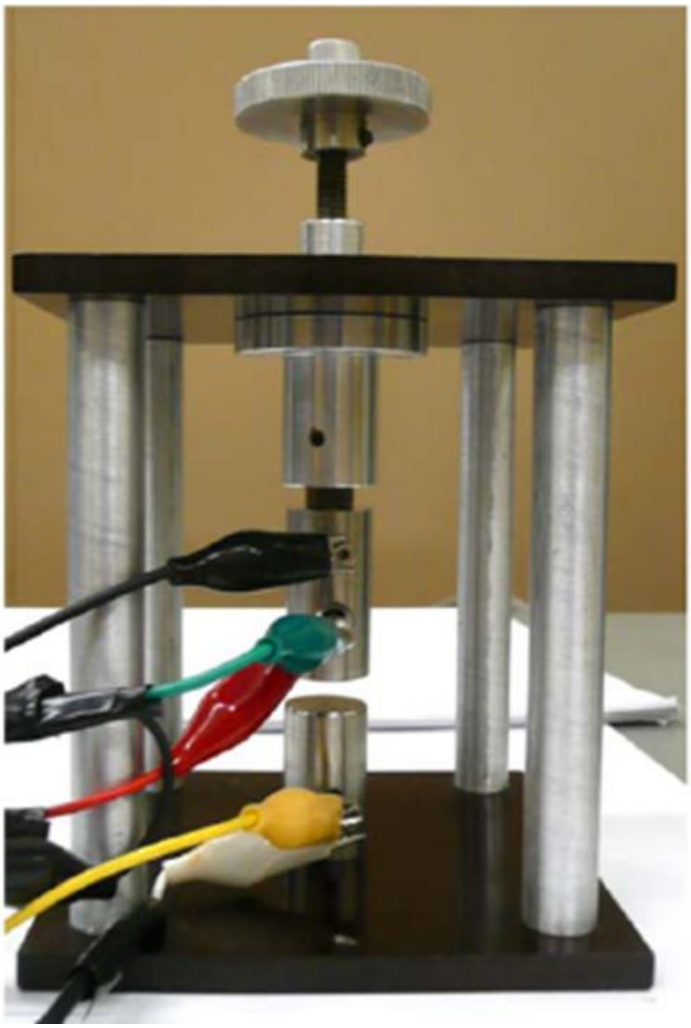

Fig. 2.11 Set up for Ionic conductivity Measurement: Sample is placed between the cylindrical stainless steel electrodes

The solid gel electrolyte resistance, *Rs* is obtained from the plots of *Z* (impedance) and *f* (frequency), known as Bode plots shown in **Fig. 2.12**. The ionic conductivity of the

solid gel electrolyte is then calculated using the **Eq. 2.3**, where t is the thickness of the solid electrolyte (equivalent to the height of the glass cylinder), and A is the area of stainless steel electrode.

$$\sigma = \frac{t}{RA} \quad \textbf{(Eq.2.3)}$$

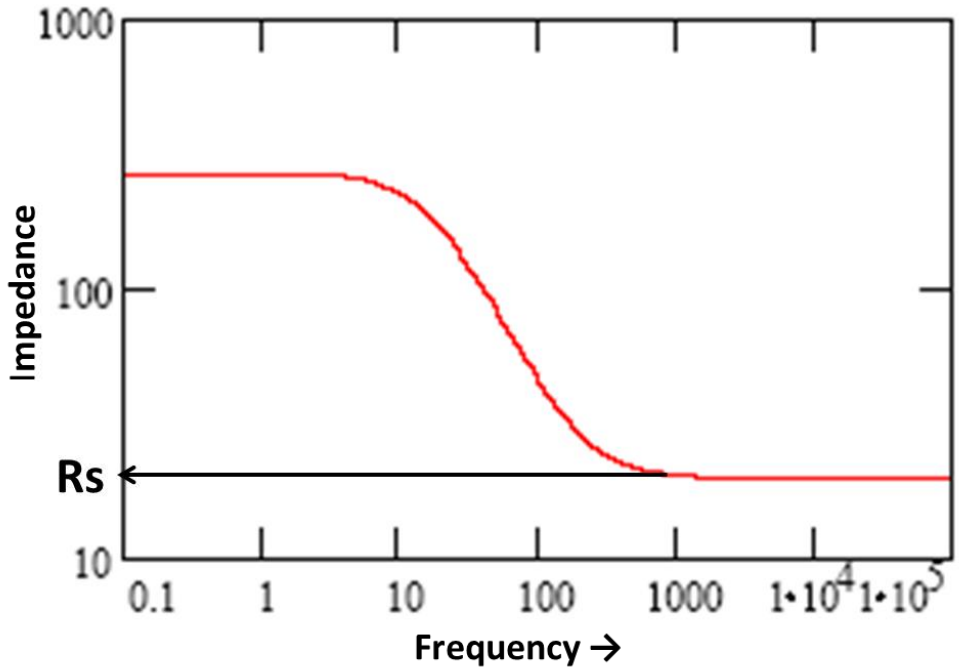

Fig. 2.12 Bode Plot for determining the resistance of solid gel electrolyte

2.8 Thermal Analysis

DSC measurements were performed on a TA Instrument Q100 differential scanning calorimeter following the parameters: 1.Heating from -90 ℃ to 50 ℃ at 5 ℃ /min; 2. Cooling back to -90 ℃ at 20 ℃ /min; 3. reheating to 50 ℃ at 5 ℃ /min. The glass transition temperature (Tg) of the gel polymer electrolyte was determined from the midpoint where the heat capacity changes. [7] A Hi-Res TGA 2950 is used for Thermal Gravimetric Analysis (TGA) and a DMA 2980 Dynamic Mechanical Analyzer was used to perform Stress-strain measurements.

2.9 Colorimetric Analysis

Colorimetric data of assembled electrochromic devices were calculated using the built-in Color software associated with the Varian cary 5000 UV-Vis NIR spectrometer based on a D65 standard illuminant and confirmed by a PR-670 SpectroScan spectroradiometer (Photo Research, Inc.).

For practical measurement using the Spectra Scan PR-670 colorimeter, the devices were held in an lab made dark box which only has two open holes: one hole is on the front of the box, mainly used for focusing the colormeter lens; and the other hole is on top of the box, for the purpose of letting a white lamp to light the inside of the box. After obtaining the color coordinates data, by mapping u′ and v′ or x and Y in the corresponding color space, the exact color of can be defined. **Fig. 2.13** shows the picture of a Spectra Scan PR-670 colormeter.

Fig. 2.13 Image for the Spectra Scan PR-670 colorimeter

2.10 Reference

1. Seshadri, V.; Padilla, J.; Bircan, H.; Radmard, B.; Draper, R.; Wood, M.; Otero, T. F.; Sotzing, G. A. *Organic Electronics*, **2007**, 8(4), 367-381.

2. Padilla, J.; Seshadri, V.; Otero, T. F.; Sotzing, G. A. *Journal of Electroanalytical Chemistry*, **2007**, *609(2)*, 75-84.

3. Sotzing, G.; Lee, K. Macromolecules, 2002, 35, 7281-7286.

4. Huige Wei.et.al. *J. Phys. Chem. C*. **2012**, *116*, 25052−25064

5. A.A. Argun, P.H. Aubert, B.C. Thompson, I. Schwendeman, C.L. Gaupp, J. Hwang, N.J. Pinto, D.B. Tanner, A.G. MacDiarmid, J.R. Reynolds, Chem. Mater. 16 (2004) 4401-4412.

6. H. Shin, Y. Kim, T. Bhuvana, J. Lee, X. Yang, C. Park, E. Kim, ACS Appl. Mater. Interfaces. 4 (2012) 185-191.

7. Zhu, Y.; Otley, M. T.; Zhang, X.; Li, M.; Asemota, C.; Li, G.; Invernale, M. A.; Sotzing, G. A. J. Mater. Chem. C, 2014, 2, 9874-9881

Chapter 3: Electrochromic Properties as a Function of Electrolyte on the Performance of Electrochromic Devices Consisting of a Single-Layer Polymer

Published in *Org. Electron.*, **2014**, 15, 1378-1386

3.1. Introduction and Motivation

Herein, a study on varying salts and their composition used in the gel electrolyte for a one-step lamination assembly procedure for electrochromic devices was carried out to explore their effects on various electrochromic performance parameters, such as color uniformity, photopic contrast, switching speed, and optical memory. Electrochromic polymers formed in different gel electrolyte compositions are highly dependent on the type, amount, and composition of salt used. The following groups of salts were investigated: ionic liquids, ammonium salts, and lithium salts. The lithium salts yielded devices with the best color uniformity, photopic contrast as high as 48%, and a switching response speeds as low as 1 second for 5.5 cm2 devices using the electroactive monomer 2,2-dimethyl-3,4-propylenedioxythiophene (ProDOT-Me2) to generate the electrochromic polymer. Hermetically sealed electrochromic devices exhibited optical memory for up to 270 of 27 hours for a 2% photopic transmittacetransmittance loss under normal laboratory conditions, and a 171 cm^2 electrochromic device was demonstrated upon optimization of the solid gel electrolyte.

Electrochromism (EC) is a color change in response to an applied electrical charge [1,2]. Among the numerous types of electrochromic materials ranging from the inorganic such as tungsten oxide (WO3) and nickel oxide (NiO), organic small molecules like bipyridiliums (viologens) to conjugated polymers, conjugated polymers have are of interest due to their color variety and varibililtyvariability, rapid response time, open air processing, high optical contrast, relatively low cost, and light weight [3,4]. Recent advances in viologen and tungsten oxide electrochromic materials have led to commercialization in rearview mirrors, smart windows, electro-transparent panoramic sunroofs, and more [5-10]. Some high profile examples are the Boeing 787 Dreamliner's windows eliminating the need for manual shades. Also, Maybach has incorporated the use of electrochromics into their roofs, called electro-transparent panoramic glass roof, allowing an open driving experience [11].

Traditionally, electrochromic polymers are prepared via electrochemical deposition, in which monomers are polymerized onto an electrode surface from an electrolyte bath [6,12]. However, due to the nucleation and growth nature of electropolymerization, this method is very sensitive to the substrate surface and any defect will ultimately lead to a defect in the polymer film. Moreover, a largesizeable amount of waste is generated due to leftover monomers and byproducts that are generated during the polymerization that limit the recyclability for further polymerization is a major cost impediment for commercialization.

We previously reported a novel, one-step method to make electrochromic devices, called an the in situ approach [13]. In this method, a liquid monomer electrolyte is first prepared by dissolving electroactive monomers into a liquid electrolyte composed of salt,

solvent, low molecular weight PEG with acrylate end functional groups, and a photoinitiator. The liquid monomer electrolyte is then sandwiched between two electrodes with subsequent photopolymerization of the acrylate end groups under UV light forming a crosslinkedcross-linked gel matrix. Electrochemical conversion of monomer to electrochromic polymer takes place inside the solid gel electrolyte using a potential sufficient to oxidize the monomer. This results in an electrochromic polymer/gel electrolyte composite layer in close proximity to the working electrode rather than a electrochromic polymer film. For simplicity, the electrochromic polymer/gel layer is referred to as a "film" throughout this study. This one-step in situ procedure eliminates the need for an electrolyte bath, and all the electrolyte material is used for the device. A variety of thiophene-based monomers, such as 3,4-ethylenedioxythiophene, 2,2-disubstituted 3,4-propylenedioxythiophenes, and 1,3-disubstituted 3,4-propylenedioxythiophenes have been reported to be viable monomers for in situ polymerization. Previously, we reported a high-throughput screening method using the in situ procedure for several ProDOT monomers within a single electrochromic device (ECD), resulting in a continuum of copolymer compositions that exhibited the full spectral range of subtractive colors [14].

To be useful in eyewear and rearview dimming mirror applications, EC materials must possess color uniformity, greater than 50% photopic contrast, switch speed of less than 1 to 5 seconds, high coloration efficiency, optical memory, and long-g term stability greater than 10,000 cycles. Here, the salts used in the gel electrolyte were varied to determine which will give optimal optimum device performance keeping the monomer 2,2-dimethyl-3,4-propylenedioxythiophene (ProDOT-Me2) constant, poly(2,2-dimethyl-

3,4-propylenedioxythiophene) (PProDOT-Me2) switches between purple in the neutral state and colorless in the oxidized state, and yields a higher photopic contrast than other PProDOT derivatives and PEDOT [12,15]. Commonly used salts in the gel polymer electrolyte were chosen for the study such as lithium trifluoromethansulfonate (LiTRIF), lithium bis(trifluoromethane)sulfonamide (LiTFSI), lithium tetrafluoroborate (LiBF4), tetrabutylammonium hexafluorophosphate (TBAPF6), tetrabutylammonium tetrafluoroborate (TBABF4) and the ionic liquids: 1-butyl-3-methylimidazolium tetrafluoroborate (BMIM BF4), and 1-butyl-3-methylimidazolium hexafluorophosphate (BMIM PF6). Chemical structures for the salts and monomers are shown in **Fig. 3.1**.

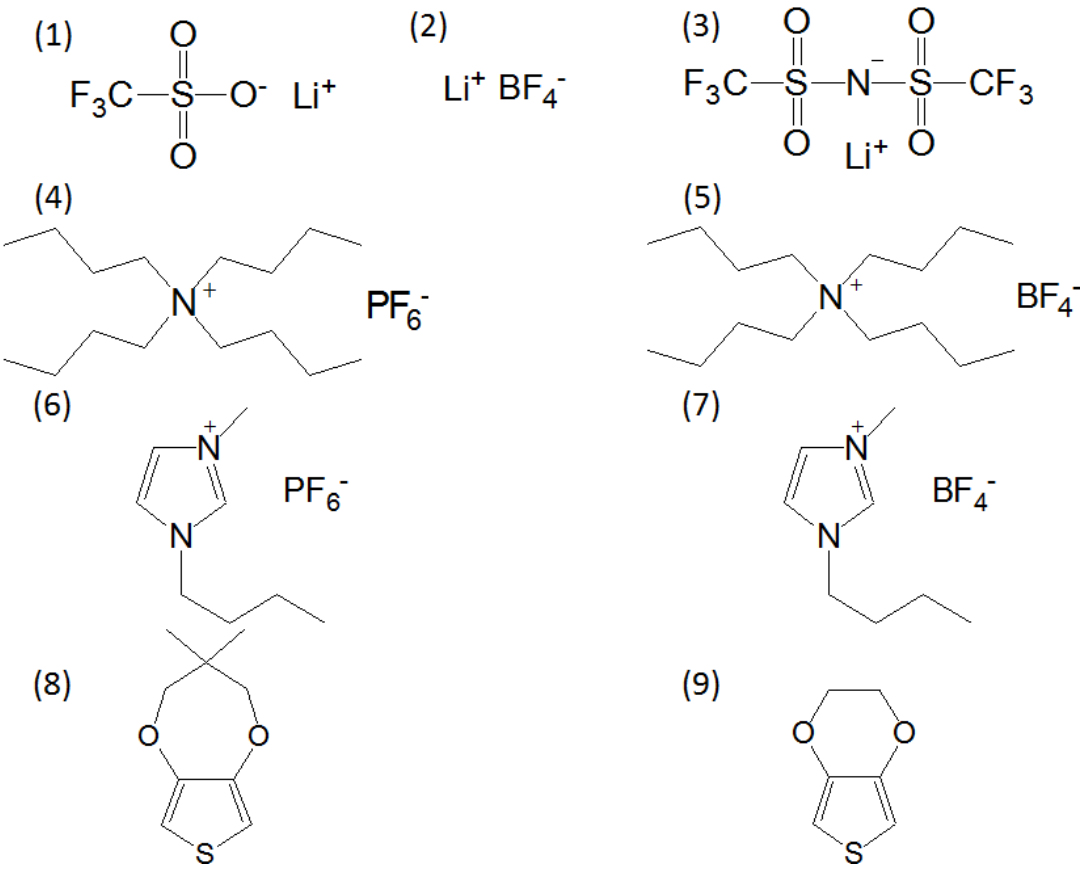

Fig. 3.1. Chemical structures of (1) LiTRIF, (2) LiBF4, (3) LiTFSI, (4) TBAPF6, (5) TBABF4, (6) BMIM PF6, (7) BMIM BF4, and monomers (8) ProDOT-Me2, (9) EDOT

3.2 Experimental

3.2.1 Materials

All aforementioned salts and ionic liquids, propylene carbonate, poly (ethylene glycol) diacrylate (M_n = 700 g/mol) and dimethoxyphenylacetophenone (DMPAP) were purchased from Sigma-Aldrich and used as received. Indium Tin Oxide (ITO) coated glass (sheet resistance 8~12 Ohms/sq) and ITO coated polyethylene terephthalate (PET) substrates (sheet resistance 60 Ohms/sq) were purchased from Delta Tech Inc. and

Bayview Optics Inc., respectively and were cleaned by rinsing with acetone prior to use. UV-sealant (UVS 91) glue was purchased from Norland Products, and a two-component epoxy adhesive (EP41S-1ND) was purchased from Master Bond Products. 2,2-dimethyl-3,4-propylenedioxythiophene (ProDOT-Me_2) was synthesized according to the reported procedure [15]. 3,4-ethylenedioxythiophene (EDOT) was purchased from Heraeus Clevios GmbH and distilled under reduced pressure before use.

3.2.2 Liquid monomer electrolyte

5 g of propylene carbonate, 5 g of poly (ethylene glycol) diacrylate, 17.5 mg of photo-initiator, DMPAP and varying amounts of salts as required for this study were added together and sonicated for 10 minutes until all solids were dissolved. Monomer was then added at 2.5 wt% with respect to the weight of all other components and sonicated for 30 seconds.

3.2.3 Electrochromic device assembly

ITO coated glass (1.91 × 5.1 cm^2) was used as the working electrode and its perimeter was covered with a silicon rubber gasket (0.79 mm) to give an active device area of 5.5 cm^2. The liquid monomer electrolyte was then drop cast onto this active area and ITO coated PET (1.91 × 5.1 cm^2) was placed atop as the counter electrode. The device was then placed inside a UV crosslinker to cure the gel electrolyte under 365 nm UV light for 5 min at 5.8 mW/cm^2 and sealed with UV curable glue. Under a constant potential of +3 V, the monomer was converted to electrochromic polymer for an appropriate conversion time commensurable with our study. Larger devices (9 × 19 cm^2 active area) were fabricated by injecting monomer electrolyte into a preassembled device frame (10.3cm × 20.3 cm) hermetically sealed with Masterbond epoxy adhesive, UV

cured and the monomer was converted to electrochromic polymer as stated above. All electrochromic devices were cycled between their bleached and colored states at ±2 V (pulse width = 2s) five times before data was recorded.

3.2.4 Instrumentation

All electrochemistry was performed using a CHI 700 potentiostat. A UVP CL-1000 Crosslinker (365 nm) was used to cure the liquid monomer electrolyte. Ionic conductivity of the cured solid gel electrolyte was measured by AC impedance spectroscopy on an HP 4285 A precision LCR meter operating in the 20 Hz to 1 MHz frequency range under ambient room temperature (25 ℃). DSC measurements were performed on a TA Instrument Q100 differential scanning calorimeter. 8~10 mg solid gel electrolyte samples were tightly sealed in aluminum pans and the DSC was obtained using the following parameters: step 1 heating scanned from -90 ℃ to 50 ℃ at 5 ℃/min, step 2 cooling back to -90 ℃ at 20 ℃/min, and step 3 heating up again to 50 ℃ at 5 ℃/min. The glass transition temperature (T_g) was determined from the midpoint of the heat capacity changes.

The absorbance spectra of the electrochromic devices in their colored and bleached states were measured from 350 nm to 850 nm using a Varian Cary 5000 UV-Vis-NIR instrument. Corresponding photopic transmittance is calculated using **Eq. (1)**:

$$T_{photopic} = \frac{\int_{350}^{850} T(\lambda)S(\lambda)P(\lambda)d\lambda}{\int_{350}^{850} S(\lambda)P(\lambda)d\lambda} \qquad (1)$$

where T(λ) is the spectral transmittance of the device, S(λ) is the normalized spectral emittance of a 6000 K blackbody and P(λ) is the normalized spectral response of the eye [16]. Photopic contrast is the difference between the photopic transmittance values of the

bleached and colored states. Photopic contrast gives a more accurate description than the commonly reported contrast at a single wavelength as it weights all visible wavelengths based upon sensitivity of human eye. In addition, the photopic values reported here are not background corrected and thereby are representative of all absorbance and reflections of through all materials and interfaces of the device. The photopic transmittance of a blank device consists of both ITO coated substrates and gel electrolyte was determined to be 80% **(Fig. 3.2)**.

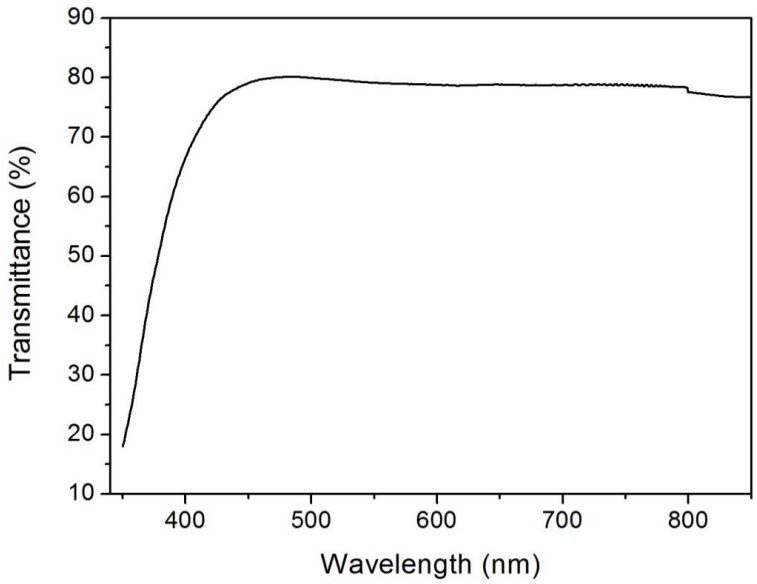

Fig. 3.2 Transmittance spectrum of a blank non-activated device

3.3 Results and Discussion

3.3.1 Gel Polymer Electrolyte Composition and Functions

As an important component of ECDs, one role the gel polymer electrolyte serves is the ionic conduction medium enabling ions to move in and out of the electrochromic polymer. The gel polymer electrolyte is generally a salt-solvent-polymer hybrid system in which the salt is first dissolved in solvent and then immobilized in a polymer matrix [17].

The salt provides free mobile ions for conduction, and the solvent takes part in dissolving the salt as well as acting as the conducting medium for ion movement, while the polymer imparts mechanical stability.

Poly(ethylene glycol)s (PEG) are one of the most widely studied classes of polymers used for gel polymer electrolytes [17,18]. PEG has a wide potential window for operation and due to its polar ether groups and significant segmental mobility, PEG has excellent compatibility for a variety of salts in that the ether oxygens help coordinate to metal cations, which is favorable for compatibility of the salt with the polymer allowing for high ion concentration. In applications, liquid electrolytes are often not desired as they may cause safety issues when used in eyewear if a lens is broken due to proximity[16]. Therefore an acrylate functionalized PEG, PEG-DA, was used for its ability to undergo UV crosslinking in the presence of a photoinitiator to form the solid gel matrix.

The solvent used in the solid gel matrix must possess a high dielectric constant, a wide operating temperature range, a low vapor pressure as well as good electrochemical stability. Propylene carbonate (PC) was chosen as the solvent as it meets all aforesaid requirements: a dielectric constant of 64.42 at 25 ℃, a freezing point of -49 ℃ and a boiling point of 242 ℃ at normal pressure [18,19]. The solvent plays an important role in increasing the degree of dissociation of the salt; that is, solvating the ions thereby reducing ion-ion interactions. The flexibility and segmental motion of the host polymer chains are improved due to the plasticization effect of PC, which in turn enhances the conductivity of the gel electrolyte. In addition to the above properties, PC was chosen

because it has been reported to yield films for electrochromic devices of high optical contrst and color efficiency as reported by Poverenov *et al.* [20].

For experiments, the 1:1 weight ratio of PC and PEG-DA were held constant since this was found to result in the best device performance to date using the *in situ* method [13]. The *in situ* method involves the production of electrochromic polymer inside a solid gel matrix of a constructed device. **Fig. 3.3** shows a schematic for how the *in situ* procedure works. First, a solution consisting of low molecular weight PEG-DA, PC, salt, and electroactive monomer are placed between two ITO substrates. Next, the acrylate functionalities are coupled using UV irradiation to produce a solid gel matrix. In the final step, a positive potential sufficient to polymerize the electroactive monomer is applied, generating the electrochromic polymer within the solid gel matrix nearest the ITO working electrode. The ionic conductivity of the solid gel matrix can serve two important roles. The first role is in the polymerization of the electroactive monomer resulting in the electrochromic polymer which consists of charge compensating anions when first produced. Regardless of how the electrochromic polymer propagates, there will be an increase in density at the surface of the solid gel matrix. Use of different salts and salt concentrations can lead to differences in the density resulting in a shift in ion dominancy during the electrochemical cycling of the electrochromic polymer. The second role the ionic conductivity will have is in the availability of the ions and their mobility during the electrochromic switching process. Higher ionic conductivities translate to faster moving ions. If the electrochromic polymer has a high degree of cation dominancy during the switch, then the switch speed will be rapid. Hence, in order to

improve the electrochromic functionality within this system, the ionic conductivity of the gel electrolyte should be optimized as well as the salt chosen. .

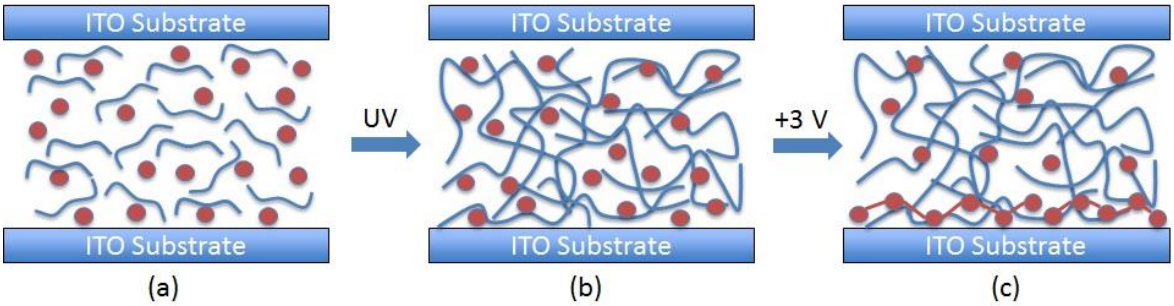

Fig. 3.3 Schematic diagram for *in situ* polymerization (a). Liquid monomer electrolyte was sandwiched between two ITO coated substrates (b). Liquid electrolyte was cured under UV light to produce a solid electrolyte gel (c). Electrochromic polymer/electrolyte blend was generated by converting monomers at a potential of +3 V.

Usually, the conductivity of the gel electrolyte increases with increased salt loading as the number of charge carriers increases. After reaching a maximum in conductivity, there is a drop when more salt is added as a result of ion aggregation. For each particular system, the optimum salt loading corresponds to the salt concentration in its most conductive gel matrix. Monomer loading was maintained at a 2.5 wt% ratio throughout the study unless otherwise specified [21].

In order for the *in situ* method to become beneficial for commercialization the method has to prove that it is scalable to realize these goals. Following the optimization of all the ECD parameters large-scale *in situ* devices were fabricated and tested. Therefore, after introducing all the optimized parameters reported later in this study, *in situ* PProDOT-Me_2 devices with 171 cm^2 active area, larger than goggles (150 cm^2), lenses (40 cm^2), and rearview dimming mirrors (130 cm^2) applications, were successfully fabricated as shown in **Fig. 3.4**. By introducing the optimized gel electrolyte, the device

has a photopic contrast of 48 % and could be colored in 2 s and bleached in 6 s to achieve 90% of its full contrast.

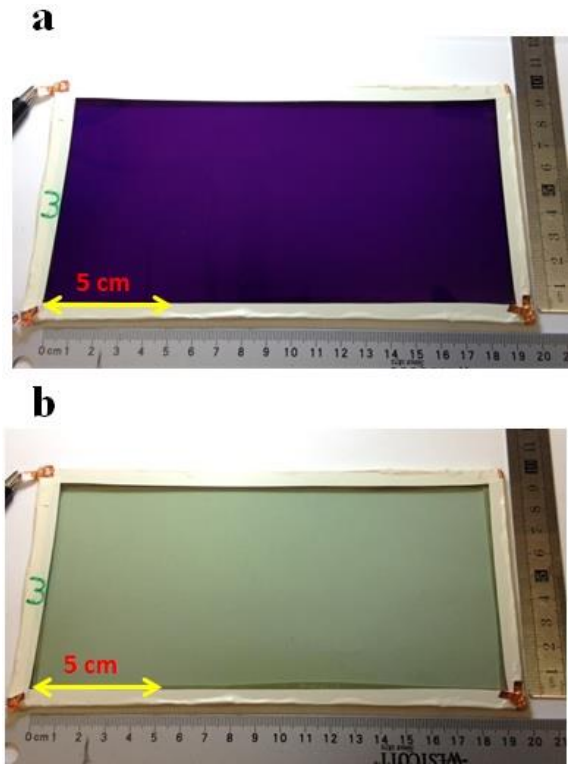

Fig. 3.4 (a) Colored state and (b) Bleached state for an *in situ* PProDOT-Me_2 EC window of 171 cm^2 active area prepared from LiTFSI gel electrolyte

3.3.2 Use of Lithium salt for *in situ* EC Devices

We have previously reported that devices prepared from the most conductive gel matrix will also have the highest contrast [21]. Aiding polymer formation and leading to an increased doping level of the polymer is a more mobile electrolyte contributing to higher charge density during polymerization [22,23]. In addition, switching speed of the devices will also be optimal at this salt loading because of the fastest electrolyte diffusion rate.

For the LiTRIF salt system, the optimal salt concentration was reported at 9.1 wt% with a conductivity value of 5.6×10^{-4} S/cm [21]. To evaluate the optimal amount of salt in LiTFSI and $LiBF_4$ systems, gel electrolyte conductivity and photopic contrast of PProDOT-Me_2 devices prepared from the corresponding gel electrolytes were monitored as a function of salt concentration. **Fig. 3.5** demonstrates the correlation between gel electrolyte conductivity device contrast, and their dependence on the amount of LiTFSI. A similar relationship was seen in $LiBF_4$ system (**Fig. 3.6**). It is clear that for each different salt system, there is an optimal salt loading to yield the highest ionic conductivity. Further, the gel electrolyte with the highest ionic conductivity for each different salt system studied yielded devices with the highest photopic contrast within the given salt system.

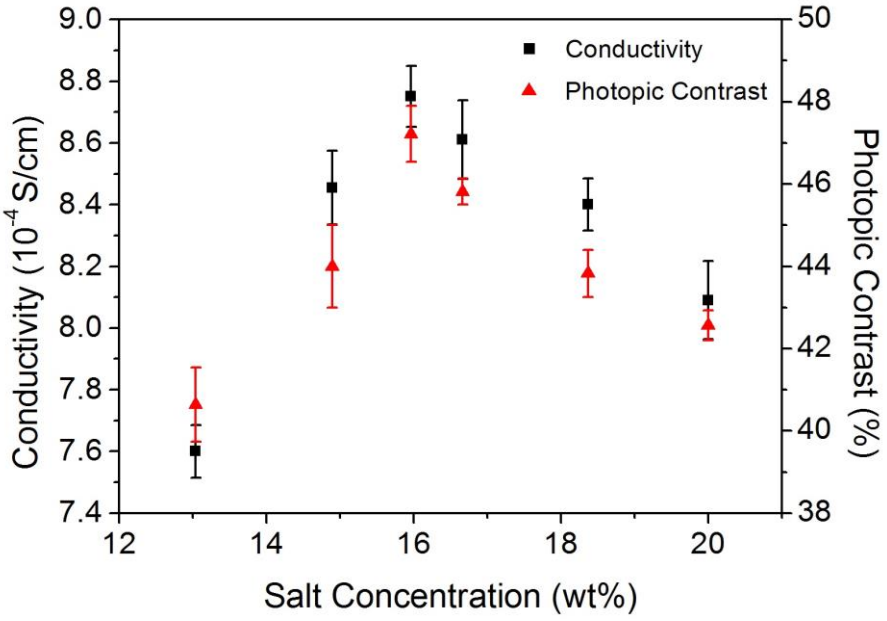

Fig. 3.5 The relationship between *in situ* PProDOT-Me_2 device photopic contrast and ionic conductivity of solid gel electrolytes as a function of LiTFSI concentration.

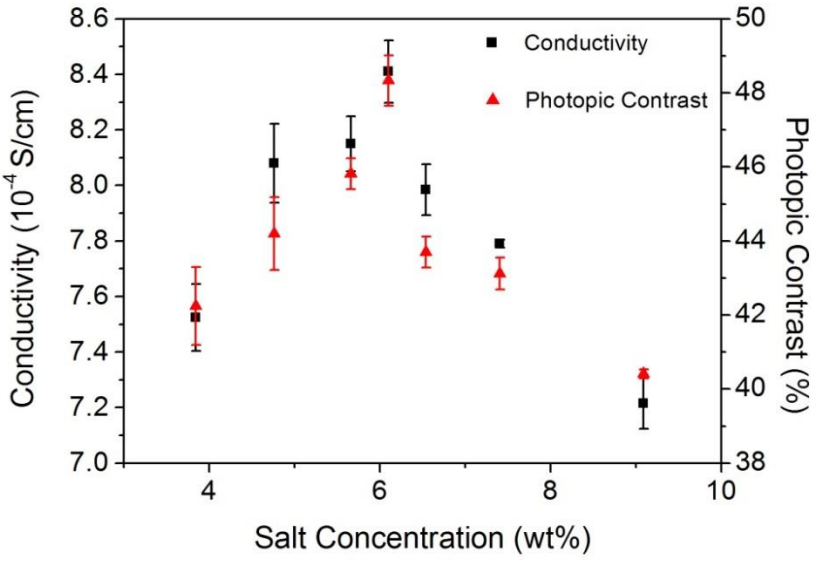

Fig. 3.6. The relationship between *in situ* PProDOT-Me_2 device photopic contrast and ionic conductivity of solid gel electrolytes as a function of $LiBF_4$ concentration.

Table 3.1. Comparison between LiTRIF, LiTFSI and LiBF4 gel electrolytes for in situ device application.

Salt	MW (g/mol)	Optimal weight percentage (%)	Optimal Ionic conductivity (S/cm)	Optimal Photopic Contrast (%)
LiTRIF	156.01	9.1	4.76 E-04	44±1
LiTFSI	287.09	16	8.75E-04	47±1
LiBF4	93.75	6.1	8.41E-04	48±1

A comparison between the three different lithium salts is summarized in **Table 3.1**. The optimal contrast of PProDOT-Me_2 devices achieved by LiTFSI and LiBF4 were 47% and 48%, respectively. Compared with the reported optimal value of 44% for the

LiTRIF system [21], the photopic contrast value was increased by 6.8% and 9% via changing the salt. To confirm the difference in photopic contrast values, the effective polymer layer thickness was calculated following our previously reported procedure [13]. According to the most commonly accepted Diaz mechanism, the mole ratio between electrons transferred and reacted monomers is 2 to 1, therefore the number of moles of monomer converted during the device activation process can be calculated from the polymerization charge collected. The calculations were also based upon assumptions that no side reactions or overoxidation occurred. The density of PProDOT-Me_2 is estimated to be 1 g/cm^3, for a device with active area of *ca.* 5.5 cm^2, the film thickness was estimated to be 177 nm, 200 nm, and 215 nm for LiTRIF, LiTFSI and $LiBF_4$ deposited film, respectively (**Table 3.2**).

Table 3.2. *In situ* ProDOT-Me_2 polymerization charge density from LiTRIF, LiTFSI and $LiBF_4$ based gel electrolyte

Salt	**Polymerization Charge density (mC/cm^2)**	**Equivalent Film Thickness (nm)**
LiTRIF	18.7	177
LiTFSI	21.1	200
$LiBF_4$	22.7	215

Compared with the triflate anion, the bulky imide anion in LiTFSI has two strong electron-withdrawing triflate groups, the conjugation between them and the lone electron pair on the nitrogen leads to an extensive dispersion of formal negative charge in the anion. This higher level of charge delocalization results in a higher degree of dissociation

of LiTFSI and a lower extent of ion pairing than in the LiTRIF electrolyte. Availability of free mobile ions is increased therefore a higher ionic conductivity is achieved [19,24]. As a result, devices prepared from a LiTFSI electrolyte have a higher contrast. $LiBF_4$ electrolytes were found to have similar ionic conductivity to that of the LiTFSI system. However, due to its small size, the tetrafluoroborate anion has a much higher mobility [25], which promotes the easier migration of anions inside the crosslinked gel matrix during the course of polymerization. Within the same amount of polymerization time, there is a larger amount of BF_4^- anions available at the working electrode than $TRIF^-$ and $TFSI^-$ anions, leading to a higher polymerization charge density. A thicker polymer film was formed; therefore the highest contrast of 48% was achieved in $LiBF_4$ electrolyte.

3.3.3 Use of Ionic Liquids for *in situ* EC Devices

Ionic liquids (ILs) were included in this study of EC devices due to advantages such as low volatility, excellent thermal stability, high conductivity, and a wide electrochemical potential window [17,18]. Our recent work has demonstrated devices built with EDOT monomers have an improved photopic contrast of 42% when the IL BMIM PF_6 is employed as the salt in the gel electrolyte attributed to an enhanced conductivity (optimal $\sigma = 12.9\times10^{-4}$ S/cm at 8.3 wt% IL loading) greater than the LiTRIF gel electrolyte (optimal $\sigma = -5.6\times10^{-4}$ S/cm at 9.1 wt% salt loading) [21]. To further explore the utilization of ILs for *in situ* devices, the same experiments were performed using ProDOT-Me_2 as the monomer with BMIM BF_4 as the salt in addition to BMIM PF_6, with the resulting polymers were found to be non-uniform in contrast to the uniform polymers of PEDOT as shown in **Fig. 3.7**.

Through the incorporation of IL, accompanied with the conductivity increment is an increased viscosity of the gel electrolyte that limits monomer diffusion for film growth. A less uniform polymer was observed when the more viscous IL BMIM PF_6 [26] was employed, and when the IL weight percent was increased in the gel electrolyte, the PProDOT-Me_2 film quality became worse due to the rise in viscosity, see **Fig. 3.8**. However, when a less viscous solvent diethyl carbonbate (DEC), of which the viscosity equals 0.75 cP at 25 ℃ as compared to a viscosity of 2.53 cP for PC [18], was loaded into the gel electrolyte to lower the overall viscosity of the gel electrolyte, a uniform PProDOT-Me_2 film was seen which could be attributed to improved monomer diffusion (**Fig. 3.8**).

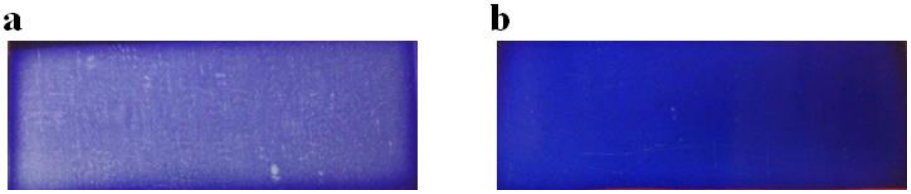

Fig. 3.7 A color uniformity comparison between two *in situ* devices in their colored state with 8.3% BMIM BF_4 with an electrochromic polymer (a) PProDOT-Me_2 (b) PEDOT.

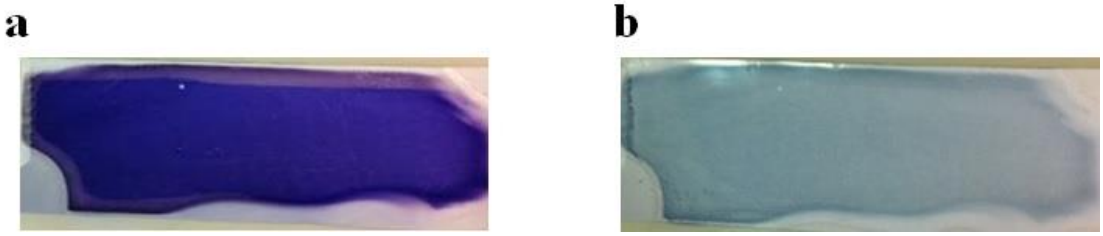

Fig. 3.8 (a). Colored State and (b). Bleached state for *In situ* ProDOT-Me_2 device prepared from a gel electrolyte of 8.3 wt% BMIM PF_6: solvent for the gel electrolyte was a mixture of PC and DEC at a 1 to 2 mass ratio.

Previously reported, the diffusion coefficient of EDOT (9.57×10-11 m^2/s) inside the crosslinked gel matrix was 8 times larger than ProDOT-Me_2 (1.21 $\times 10^{-11}$ m^2/s) due to its smaller molecular size [14]. The formation of uniform films of PEDOT in gel electrolytes with BMIM BF_4, BMIM PF_6, but not PProDOT-Me_2 was a result of this difference in diffusion rates between the two monomers. The higher viscosity induced by ILs does not hinder the diffusion of EDOT in the gel matrix as it does with ProDOT-Me_2. To confirm the diffusion rate difference was the cause of the uneven film formation, two different monomers, pyrrole (D = 2.95×10^{-9} m^2/s) and ProDOT-tBu_2 (D = 4.63×10^{-12} m^2/s) [14], where the diffusion coefficient is a three-order magnitude difference, were tested in the IL gel electrolyte. As expected, pyrrole was found to polymerize evenly producing uniform films while ProDOT-tBu_2 exhibited films of poor quality (**Fig.3.9**).

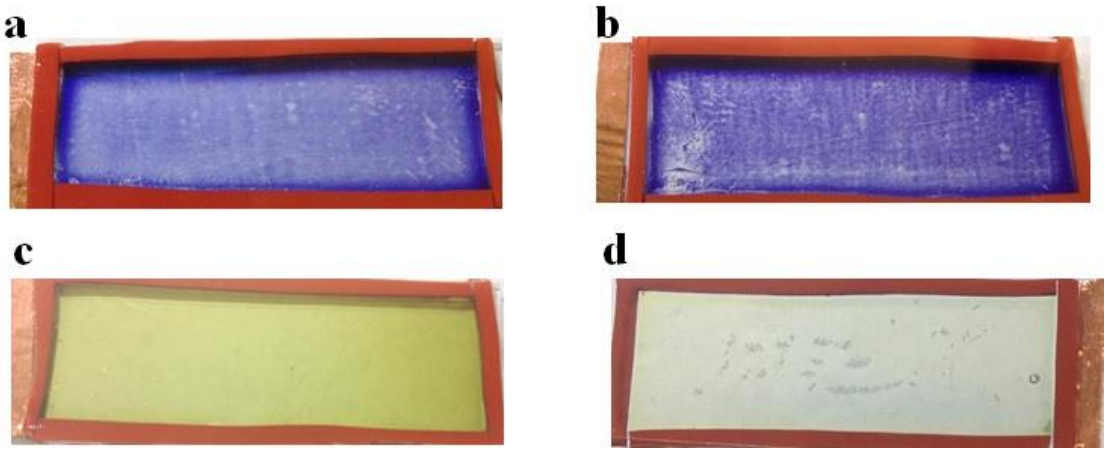

Fig. 3.9 (a). *In situ* ProDOT-Me_2 device prepared from a gel electrolyte of 8.3 wt% BMIM PF_6. (b). *In situ* ProDOT-Me_2 device prepared from a gel electrolyte of 16.6 wt% BMIM PF_6. (c). *In situ* pyrrole device prepared from a gel electrolyte of 8.3 wt% BMIM PF_6. (d). *In situ* ProDOT-tBu_2 device prepared from a gel electrolyte of 8.3 wt% BMIM PF_6.

3.3.4 Use of Ammonium Salt for in situ EC Devices

Ammonium salts are another commonly used salt in gel polymer electrolytes [27]. Compared with ILs and lithium salts, they are less hygroscopic and more chemically inert, which allows the salts to serve as an inert electrolyte over a wide potential window. Quaternary ammonium salts were reported to have higher molar conductivities in propylene carbonate than the corresponding lithium salts having the same anion due to the electrostatic shielding effect of alkyl groups [25].

However, the film quality of polymers prepared from the ammonium salt based gel electrolytes were found to be worse than those prepared from IL gel electrolytes. Observed in this study, neither EDOT nor ProDOT-Me_2 was found to polymerize uniformly inside assembled devices as shown in **Fig. 3.10**.

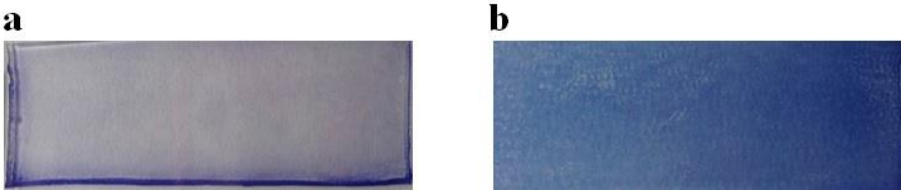

Fig. 3.10 A color uniformity comparison between two *in situ* devices in their colored state with 2.7% $TBABF_4$ with an electrochromic polymer (a) PProDOT-Me_2 (b) PEDOT.

Moreover, an opaque yellow color gradually came out as the weight percent of ammonium salt was increased. In order to be applicable in electrochromic devices, gel polymer electrolytes must possess high optical transparency, thus limiting the use of ammonium salts in this system for EC devices [12,17-19]. When the salt concentration exceeded 16.6 wt%, $TBAPF_6$ salt recrystallized out from the gel electrolyte overnight. Higher salt concentrations (23.0 wt% salt loading) started to crash out immediately when

the gel was being cured (**Fig. 3.11** and **Fig. 3.12**). As a result of aggregation, ammonium salts were not well dispersed in the gel matrix which led to the uneven film formation inside devices, and this phenomenon was more severe in gel electrolytes at higher ammonium salt loading owing to the larger extent of aggregation, see **Fig. 3.13**.

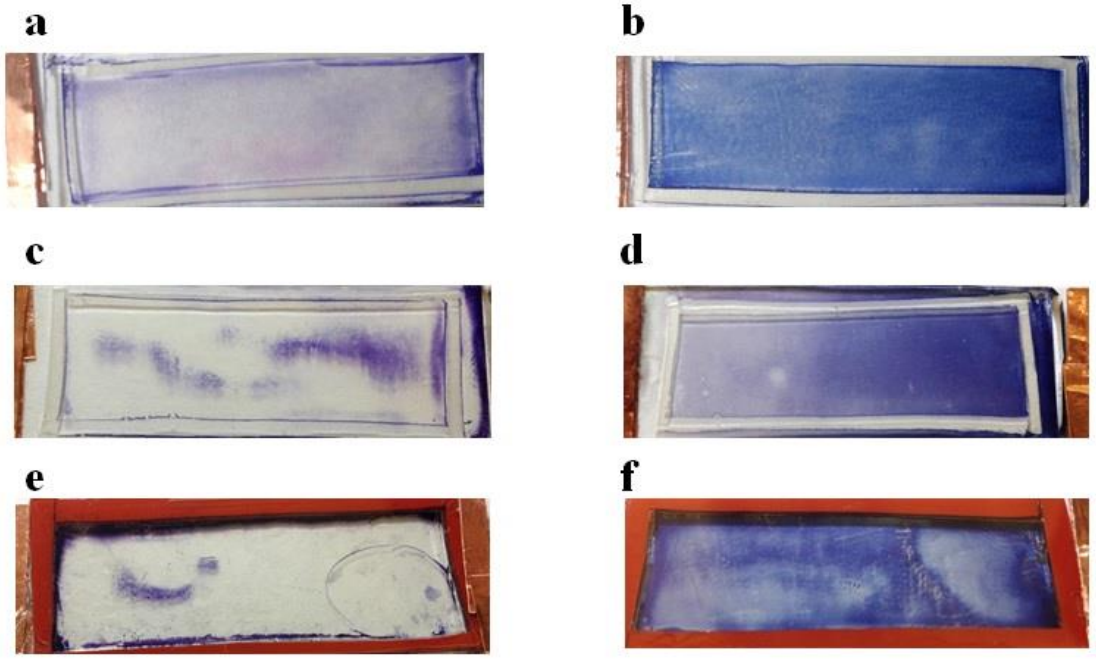

Fig. 3.11 (a). *In situ* PProDOT-Me_2 device prepared from a gel electrolyte of 4.8 wt% $TBABF_4$. (b). *In situ* PEDOT device prepared from a gel electrolyte of 4.8 wt% $TBABF_4$. (c). *In situ* PProDOT-Me_2 device prepared from a gel electrolyte of 9.1 wt% $TBABF_4$. (d). *In situ* PEDOT device prepared from a gel electrolyte of 9.1 wt% $TBABF_4$. (e). *In situ* PProDOT-Me_2 device prepared from a gel electrolyte of 16.6 wt% $TBABF_4$. (f). *In situ* PEDOT device prepared from a gel electrolyte of 16.6 wt% $TBABF_4$.

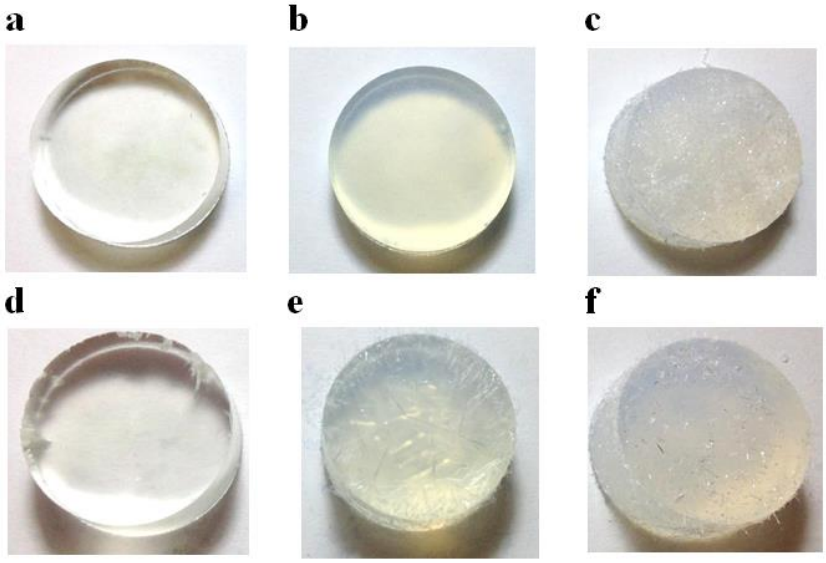

Fig. 3.12 (a). Cured gel electrolyte of 9.1 wt% $TBAPF_6$ after curing. (b). Cured gel electrolyte of 16.6 wt% $TBAPF_4$ after curing. (c). Cured gel electrolyte of 23.0 wt% $TBAPF_6$ after curing. (d). Cured gel electrolyte of 9.1 wt% $TBAPF_6$ after overnight. (e). Cured gel electrolyte of 16.6 wt% $TBAPF_6$ after overnight. (f). Cured gel electrolyte of 23.0 wt% $TBAPF_6$ after overnight.

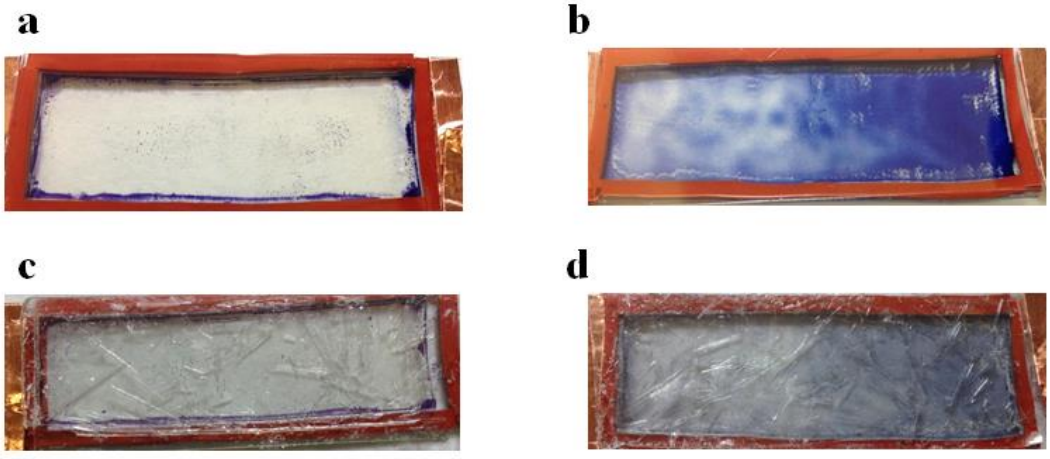

Fig. 3.13. (a). *In situ* ProDOT-Me_2 device prepared from a gel electrolyte of 16.6 wt% $TBAPF_6$. (b). *In situ* PEDOT device prepared from a gel electrolyte of 16.6 wt%

$TBAPF_6$. (c). *In situ* PProDOT-Me_2 device prepared from a gel electrolyte of 16.6 wt% $TBAPF_6$ after overnight. (d). *In situ* PEDOT device prepared from a gel electrolyte of 16.6 wt% $TBAPF_6$ after overnight.

On the other hand, due to the relatively large size of tetra-n-butylammonium cation, it may get trapped inside the cross-linked gel matrix, and thus its diffusion is limited. During electropolymerization, counter anions diffuse towards the working electrode to neutralize the positive charges formed on the polymer chain while cations diffuse to the counter electrode for charge compensation. This is potentially due to the imbalance between the movements of bulky cations and the mobile anions that resulted in the nonuniform streaky film quality since it has not been observed in solution electrodeposition where both TBA^+ and BF_4^- (or PF_6^-) are highly mobile (**Fig.3.14**). For solution based electropolymerization, ITO coated glass (1.91 × 5.1 cm2) was used as the working electrode, a Pt flag (1 × 2.5 cm2) was used as the counter electrode, and a silver wire was used as the pseudo-reference electrode. A constant potential of +2.0 V vs. Ag wire was applied for 6 s and the electropolymerized films were switched between -0.5 V to +0.5 V for 4 steps at a 0.5 s pulse width inside the solution. Polymer films were then thoroughly washed with propylene carbonate.

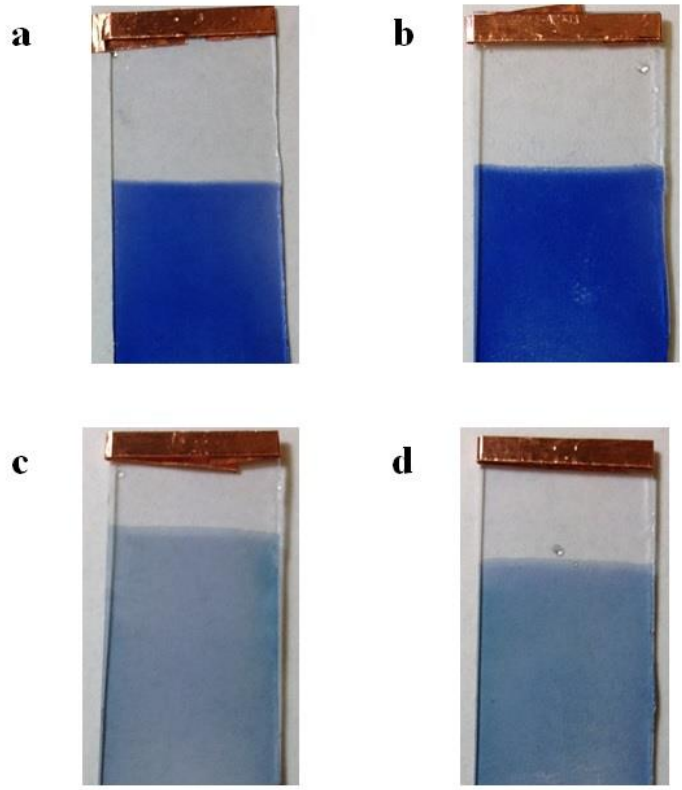

Fig. 3.14 PProDOT-Me_2 film electrodeposited from (a). 0.10 M $TBAPF_6$/PC and (b). 0.10 M $TBABF_4$/PC solution; PEDOT film electrodeposited from (c). 0.10 M $TBAPF_6$/PC solution and (d). 0.10 M $TBABF_4$/PC solution.

3.3.5 Switching Speed

The switching speed of *in situ* PProDOT-Me_2 devices prepared from lithium salt gel electrolytes were studied by UV-Vis spectrophotometry upon the application of a square wave chronocoulometry. Devices were switched between −2 V and +2 V and a percentage transmittance (%T) at 575 nm, was recorded as a function of time (**Fig. 3.15**). Switching speeds of the devices here were defined as the time required to achieve 90% of full ΔT at the λ_{max} [6,16,29]. The results of the study are summarized in **Table 3.3**.

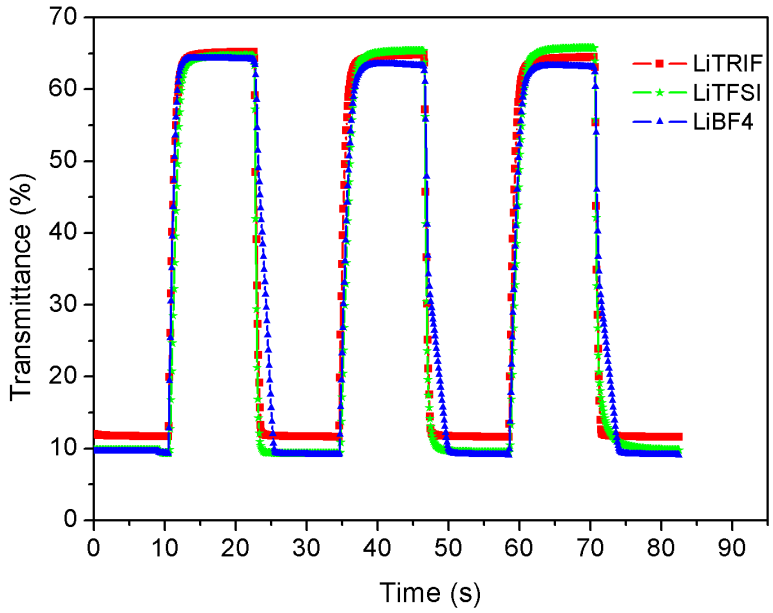

Fig. 3.15 Percent transmittance change at 575 nm for *in situ* PProDOT-Me_2 devices prepared from LiTFSI, LiBF4 and LiTRIF electrolytes during constant potential stepping between -2 V and +2 V at a 12s pulse width.

Table 3.3 The effect on switching speed between differing lithium salt compositions with PProDOT-Me_2 devices of 5.5 cm^2.

Salt	**Photopic Contrast**	**Contrast at 575 nm**	**Time to Color (s)**	**Time to Bleach (s)**
LiTRIF	44%	53%	1.0	1.5
LiTFSI	47%	55%	0.8	1.8
$LiBF_4$	48%	55%	2.5	1.4

Generally, switching a device from one state to the other is an electrochemical process dependent on several factors, such as the ionic conductivity of the gel electrolyte, ion diffusion in the polymer itself, and polymer film thickness and morphology [3]. An electrochromic polymer/gel electrolyte composite layer was formed during *in situ* polymerization, Entanglement with the cross-linked PEG chains may restrict the motion of polymer chains within this thin layer of gel electrolyte. During the course of polymerization, bulkier anions such as $TRIF^-$ and $TFSI^-$, which are 1.7 and 2.9 times larger than BF_4^- anions, respectively, are more likely to get trapped onto the polymer chains. In contrast, lithium cations are one order of magnitude smaller than the abovementioned anions, thus could easily diffuse through the cross-linked composite layer, which, will ultimately lead to the cation dominance during the electrochemical switch. **Fig. 3.16** shows the charge as a function of time during electrochemical switch. The resulting curve of LiBF4 system differs from those of LiTRIF and LiTFSI, which indicate both cations and anions were moving during the electrochemical switch of $LiBF_4$ device as seen in **Fig. 3.16** .

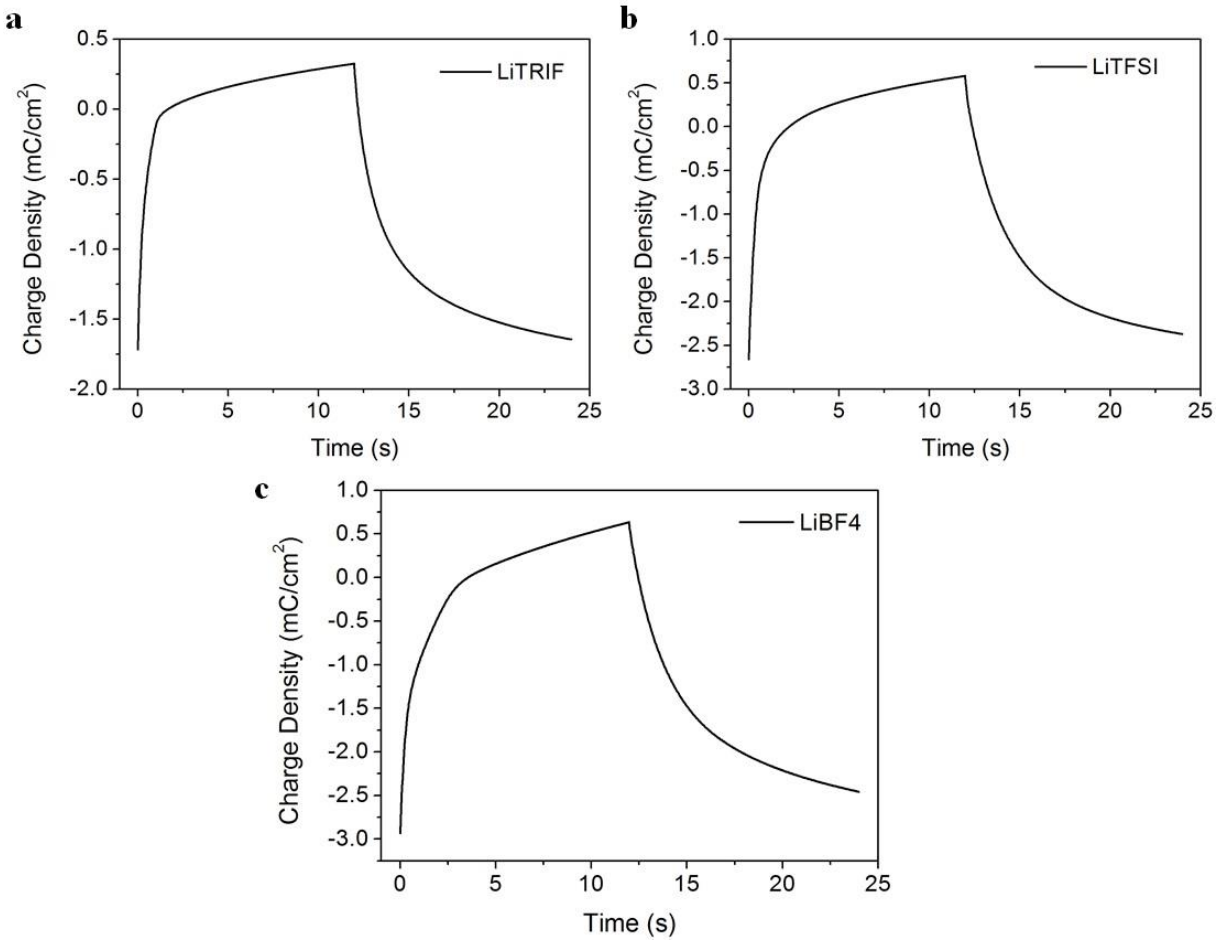

Fig. 3.16 Chronocoulometry of *in situ* ProDOT-Me_2 device prepared from (a) LiTRIF, (b) LiTFSI, and (c) $LiBF_4$ based gel electrolytes during constant potential stepping between -2 V and +2 V.

Higher ionic conductive gel electrolytes yield faster switching speeds due to the presence of mobile lithium cations. The difference between the LiTFSI electrolyte and the LiTRIF electrolyte illustrates the conductivity of the gel electrolyte was increased by replacing LiTRIF with LiTFSI, which, in turn, shortened the amount of time for coloring. The longer bleaching time associated with the LiTFSI gel electrolyte is a result of the thicker polymer film formed in LiTFSI gel electrolyte.

Ion diffusion of counter anions is another important factor that affects the switching kinetics for cathodically coloring polymers. During the device bleaching process, conjugated polymers undergo an oxidation reaction, forming positive charges along the chain. Concurrently, the counter anions have to diffuse into the polymer for charge neutralization, which defines the bleaching time. Tetrafluoroborate, which has the highest mobility among the three anions, easily diffusing through the gel matrix, therefore it required the shortest bleaching time of 1.4 s. $LiBF_4$ shows a slower coloring speed compared with its bleaching speed, which is conflicting to the typically observed behavior reported in literature [30,31]. This result may be explained by fast ion insertion and accumulation. As previously mentioned, BF_4^- has a high mobility, and thus, the polymer film could be easily charged with a large amount of BF_4^- anions during the bleaching process. As a result, it takes a longer time for these accumulated anions to diffuse out of the polymer film in comparison to the time it would take for the diffusion of lithium ions for complete reduction to the neutral state of the polymer, leading to a slower coloring speed.

3.3.6 Optical Memory

Another parameter for ECDs is the optical memory or open circuit memory, defined as the ability of the ECD to retain its colored or bleached state, respectively, after the electric field is removed [3]. The optical memory effect originates from the stable electrochemical doping/dedoping process and is an important property of ECDs in eyewear and window applications. Devices that exhibit a higher optical memory will consume less energy for a given application or simplify the electronics. [32]. **Fig. 3.17** shows the optical memory effect for PProDOT-Me_2 devices prepared from different salt-based gel electrolytes. The devices were placed in open air, under ambient light conditions, and the photopic transmittance loss was monitored as a function of time. Where a 2% photopic transmittance loss was chosen as our upper limit for this study.

Table.3.4 The effect on Bleach and Dark state retention time between different lithium salt compositions with PProDOT-Me_2 devices

Salt	**Bleach state retention Time (min)**	**Dark State retention Time (min)**
LiTFSI	5	33
LiTRIF	25	60
$LiBF_4$	125	1620

Exhibited in **Table. 3.4**, as the size of anions decrease, devices have improved optical memory. One possible explanation is the electrochromic polymer formed in the gel electrolyte with the bulkier anions has a larger inter-chain distance. A larger inter-chain distance will facilitate the movement of lithium cations through the polymer and

result in a loss of photopic transmittance as the electrochromic polymer transitions to its resting potential.

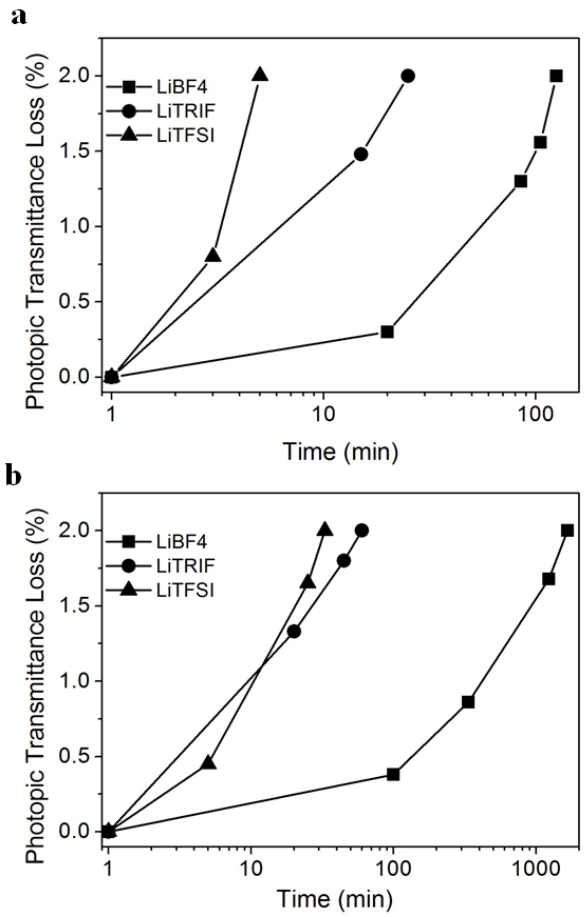

Fig. 3.17 Memory effect for the *in situ* ProDOT-Me_2 device prepared from $LiBF_4$, LiTRIF, and LiTFSI based gel electrolyte.

3.4 Conclusion

Different salts were found to affect the quality and efficiency of the electrochromic polymer “film” formation for single layer devices wherein lithium based salts showed the best film quality, whereas electrochromic devices assemble using ILs and ammonium salts resulted in more heterogenous films. Lithium salts were found to work best with ProDOT-Me_2, resulting in ECDs with defect-free color uniformity, 48% photopic contrast, switching speeds as low as 1 second, and optical memory up to 27 hours for a 2% photopic transmittance loss. The optimal parameters were demonstrated on an electrochromic device having an active area of 171 cm^2, surpassing the active area of a goggle, 2 sunglass lenses, or rearview dimming mirror. Apart from the effects that the salt has on ionic conductivity or on ion movement into the electrochromic polymer upon switching, Monomer diffusion is another property that is affected through changing salt for the *in situ* polymerization to generate electrochromic polymer. EDOT was found to polymerize more uniformly in the presence of ionic liquids and ammoniums salts, which could be attributed to its faster diffusion rate than ProDOT-Me_2 within these salt systems. The ionic conductivity of the solid gel matrix is significant for device electrochromic performance. For each particular salt system, its most conductive gel electrolyte yielded devices with the highest contrast and the most rapid switch speed. Primarily, for devices made in the one film process, the optical memory was found to be dependent on the size of the anion wherein smaller anions contribute to enhanced optical memory.

3.5 References

[1] P.M.S. Monk, R.J. Mortimer, D.R. Rosseinsky, Electrochromism: Fundamentals and Applications, VCH, Weinheim, Germany, 1995.

[2] P.M.S. Monk, R.J. Mortimer, D.R. Rosseinsky, Electrochromism and Electrochromic Devices, Cambridge University Press, Cambridge, UK, 2007.

[3] A.A. Argun, P.H. Aubert, B.C. Thompson, I. Schwendeman, C.L. Gaupp, J. Hwang, N.J. Pinto, D.B. Tanner, A.G. MacDiarmid, J.R. Reynolds, Chem. Mater. 16 (2004) 4401-4412.

[4] G. Gunbasab, L. Toppare, Chem. Commun. 48 (2012) 1083–1101.

[5] M.A. Invernale, Y. Ding, G.A. Sotzing, ACS Appl. Mat. Interfaces.2 (2010) 296-300.

[6] C. Ma, J. Zheng, S. Yang, D. Zhu, Y. Bin, C. Xu, Org. Electron. 12 (2011) 980-987.

[7] S. Kim, X. Kong, M. Taya, Sol. Energy Mater. Sol. Cells. 7 (2013) 183-188.

[8] P. A. Ersman, J. Kawahara, M. Berggren, Org. Electron. 14 (2013) 3371-3378.

[9] E. Detsi, P. R. Onck, J. T. M. De Hosson, Appl. Phys. Lett. 103 (2013) 193101-193101

[10] B. B. Carbas, D. Asil, R. H. Friend, Ahmet M. Önal, Org. Electron. 15 (2014) 500-508

[11] A. Pawlicka, Recent Patents on Nanotechnology. 3 (2009) 177-181.

[12] M.A. Invernale, V. Seshadri, D.M.D. Mamangun, Y. Ding, J. Filloramo, G.A. Sotzing, Chem. Mater. 21 (2009) 3332-3336.

[13] Y. Ding, M.A. Invernale, D.M.D. Mamangun, A. Kumar and G.A. Sotzing, J. Mater. Chem. 21 (2011) 11873-11878

[14] F.A. Alamer, M.T. Otley, Y. Ding, G.A. Sotzing, Adv. Mater. 25 (2013) 6256-6260.

[15] D.M. Welsh, A. Kumar, E.W. Meijer, J.R. Reynolds, Adv. Mater. 11 (1999) 1379-1382.

[16] V. Seshadri, J. Padilla, H. Bircan, B. Radmard, R. Draper, M. Wood, T.F. Otero, G.A. Sotzing, Org. Electron. 8 (2007) 367-381.

[17] V.K. Thakur, G. Ding, J. Ma, P.S. Lee, X. Lu, Adv. Mater. 24 (2012) 4071-4096.

[18] S. Ahmad, Ionics. 15 (2009) 309-321.

[19] S.A. Agnihotry, P. Pradeep, S.S. Sekhon, Electrochim. Acta. 44 (1999) 3121-3126

[20] E. Poverenov, M. Li, A. Bitler, M. Bendikov, Chem. Mater. 22 (2010), 4019-4025.

[21] A. Kumar, M.T. Otley, F.A. Alamar, Y. Zhu, B.G. Arden, G.A. Sotzing, J. Mater. Chem. C. (2014) DOI:10.1039/C3TC32319F

[22] J. Padilla, V. Seshadri, G.A. Sotzing, T.F. Otero, Electrochem. Commun. 9 (2007) 1931-1935.

[23] A.L. Holt, J.M. Leger, S.A. Cartera, Appl. Phys. Lett. 86 (2005) 123504-123504.

[24] S. Besner, A. Vallée, G. Bouchard, J. Prud'homme', Macromol. 25 (1992) 6480-6488.

[25] M. Ue, J. Electrochem. Soc. 141 (1994) 3336-3342.

[26] D. Tomida, A. Kumagai, K. Qiao, C. Yokoyama, Int. J. Thermophys. 27 (2006) 39-47.

[27] A. Cirpan, A.A. Argun, C.R.G. Grenier, B.D. Reeves, J.R. Reynolds, J. Mater. Chem. 13 (2003) 2422-2428.

[28] S.K. Fullerton-Shirey, J.K. Maranas, Macromol. 42 (2009) 2142-2156.

[29] L. Huang, H. Yen, J. Wu, G. Liou Org. Electron.13 (2012) 840-849.

[30] T.F. Otero, H.J. Grande, J. Rodriguez, J. Phys. Chem. B. 101 (1997) 3688-3697.

[31] T.F. Otero, M. Bengoechea, Langmuir. 15 (1999) 1323-1327.

[32] H. Shin, Y. Kim, T. Bhuvana, J. Lee, X. Yang, C. Park, E. Kim, ACS Appl. Mater. Interfaces. 4 (2012) 185-191.

Chapter 4: Neutral Color Tuning of Conjugated Polymer Electrochromic Devices Using a Commercial Solvent Dye

Published in *Chem. Commun.*, **2014**, 50, 8167-8170

4.1 Introduction and Motivation

Herein, we present a facile, one-step method to color tune electrochromic devices (ECDs) that switch between two neutral colors via *in situ* polymerization of electroactive monomers in the presence of a small molecule organic yellow dye. These devices exhibited photopic contrasts of *ca.* 30% without background correction when assembled on flexible PET-ITO substrates. In addition, devices exhibited switching speeds as low as 1 second, color uniformity, and stability. In addition, large defect free ECDs of 100 cm^2 were fabricated exceeding the active switch area required for goggles, lenses, and small display applications.

Electrochromic materials that exhibit the necessary colors for RGB and CMYK color replication have been sought after by the display industry for the fabrication of lower-power, thinner, flexible, and less complex displays. Among the numerous types of electrochromic materials, conjugated polymers (CPs) have aroused significant interest due to their high optical contrasts, fast switching speeds, and the multitude of colors achievable through chemical structure modifications.[1,2] This has led to the wide applicability of CPs in a variety of electrochromic display devices, such as eyewear,

goggles, anti-glare mirrors, sunroofs, automotive windows, architectural glass, smart windows, displays, sensors, OLEDs, solar cells, and color change fabrics.[3] A neutral color is a color not associated with any single hue. Some common neutral colors are beige, ivory, grey, taupe, black, and white. The most extensively studied and reported neutral color polymeric electrochromes are near-black electrochromic polymers utilizing the donor-acceptor approach with an appropriate ratio of donors and acceptors in a random DA polymer backbone, synthesized through various procedures.[4-7] Our group recently realized a random copolymerization approach by blending two precursor polymers possessing both DA and donor-only groups. The conversion of the precursor blends in the appropriate ratios resulted in an entirely new donor-acceptor electrochromic polymer that switched between black to sky blue in its neutral and oxidized states, respectively, with a photopic contrast of 30%.[8] In addition, other reported methods, to date, for achieving black EC polymers involve electrochemical copolymerization of two DA electroactive groups inside an electrolyte solution[9] and multilayers of several polymer electrochromes with complementary color absorption.[10]

ECDs that exhibit neutral color transitions are of special interest in the current eyewear industry. Neutral grey lenses for use in military and consumer applications have dominated a large portion of the sunglass market as neutral colors provide an unmitigated view of the environment without distorting original colors or affecting contrast. Their low brightness minimizes eye fatigue and develops a calm, non-distractive atmosphere.[6]

Our group previously developed and optimized a one-step procedure to make ECDs.[11,12] With this *in situ* process, monomers are first dissolved into a liquid electrolyte and assembled into devices. With subsequent exposure to UV light, a solid electrolyte

matrix is formed, where conversion of monomers takes place with the application of an appropriate potential. Recent applications of this one-step lamination procedure involve high-throughput color screening, which utilized the diffusion of two monomers to generate a full subtractive color spectrum between yellow and blue,[13] the locking of acrylated ProDOT monomers into the gel matrix for device lifetime and stability enhancement,[14] and the assembly of larger-area EC windows for real world applications.[12]

Instead of synthesizing electrochromic polymers with the desired color transitions, a neutral color can also be achieved by mixing corresponding hues following the "subtractive color mixing" theory. For example, red can be made by blending green and blue absorbing materials, leaving only red light transmission or reflection. Herein, we demonstrate the ability to tune optical and colorimetric properties of electrochromic devices by adding a dye to the monomer gel electrolyte. By *in situ* polymerizing EDOT in the presence of a yellow solvent dye, ECDs that exhibit color neutrality were prepared using balanced yellow solvent dye and polymer absorbance intensities. Although the yellow solvent dye is conjugated, it does not disrupt the electropolymerization of EDOT, nor does it affect the redox process of the PEDOT responsible for its electrochromic functionality.

4.2 Experimental

4.2.1 Materials

The Solvent yellow dye (YG) was a sample received from Lanxess, Inc.; its molecular weight is 289.28 g/mol. 3,4-ethylenedioxythiophene (EDOT) was purchased from Heraeus Clevios GmbH and was distilled under vacuum prior to use. Lithium

trifluoromethane sulfonate (LiTRIF), propylene carbonate (PC), poly (ethylene glycol) methyl ether acrylate (M_n = 480 g/mol) (PEG-MA) and dimethoxyphenylacetophenone (DMPAP) were purchased from Sigma-Aldrich and used as received. Indium Tin Oxide (ITO) coated glasses (sheet resistance 8-12 Ohm/sq) were purchased from Delta Technologies and cleaned by acetone, isopropanol and methanol prior to use. ITO coated polyethylene terephthalate (PET) substrates were purchased from Bayview Optics and were cleaned by acetone prior to use. Copper tape was purchased from Newark and UV-sealant glue was purchased from Norland Optics.

4.2.2 Gel polymer electrolyte

1 g of LiTRIF, 3 g of PC, 7 g of PEG-MA and 17.5 mg of DMPAP were added together and sonicated for 10 minutes until fully dissolved. Monomer gel electrolyte was prepared by dissolving a 2.5 wt% ratio of EDOT monomers into the gel electrolyte.

4.2.3 Electrochromic device assembly

For small area device fabrication, ITO coated PET (2 cm × 5 cm) was used as both working electrode and counter electrodes. The perimeter of one ITO/PET piece was covered with a rubber gasket (0.8 mm) to form the device active area (1.5 × 4.5 cm^2). The liquid monomer gel electrolyte (or YG-incorporated gel electrolyte) was then drop cast onto this active area and another ITO/PET piece was placed atop. The device was placed inside an UV crosslinker (UVP CL-1000, 5.8 mW/cm^2) to cure the gel electrolyte under 365 nm UV light for 20 min and sealed with UV curable glue. Under a constant potential of +3 V, the device was activated for an appropriate conversion time to achieve its optimal performance.

For large area device fabrication, a preassembled device frame sealed with epoxy adhesive was first built using 7.6 cm × 20 cm ITO coated glass for both substrates. The YG-incorporated gel electrolyte was then injected into the device frame and followed by UV curing and an activation process as stated above.

All activated devices were switched between ±2 V (pulse width = 2 s) for five cycles to switch the electrochromic polymer between its oxidized and neutral states before optical characterization.

4.2.4 Electrochemistry

Electrochemical conversions and spectroelectrochemistry were carried out with a CHI 700 potentiostat.

4.2.5 Optical Characterization

Optical properties of assembled devices were measured with a Varian Cary 5000 UV-Vis-NIR spectrophotometer and corresponding built-in Color software. Colorimetric data were collected using a 10 degree standard observer angle in measurement range of 360-860 nm at 1 nm intervals based on a D65 standard illuminant.

4.3 Results and Discussion

4.3.1 Material Selection

In order to achieve neutrality, an ECD must exhibit absorption of light across all or near all wavelengths of the visible spectrum. Our approach to solving this requirement is to use a polymer that has broad visible absorption and combine it with a dye of a complimentary color, such that most of the visible region is absorbed, which, will in turn result in a neutral color. PEDOT is a good candidate for this study as its absorption in the neutral state spans from 500 nm to 700 nm with a maximum absorption peak at ca. 610 nm, giving it a deep blue color. In the oxidized state, it exhibits a transmissive sky blue color. A yellow dye was chosen because its absorption in and around the 450 nm region will complement the absorption of PEDOT. The yellow solvent dye, YG, used for this study was received from Lanxess, Inc (Macrolex Yellow G, C.I. Solvent Yellow 114 CAS # 17772-51-9). It was found to have solubility in the electrolyte and have an absorption peak at 442 nm. The yellow dye must not undergo reduction or oxidation in the range of -2 V to 3 V in the electrolytic medium, it must be soluble in the electrolyte precursor solution, and the spectral overlap with the PEDOT conjugated polymer must be complimentary resulting in a 'neutral' coloration in both the bleached and colored states. In addition, this YG dye was chosen over other commercially available yellow dyes because it allowed for both the bleached and colored states to stay within eyewear neutral chromaticity specifications, shown in **Fig. 4.1**.

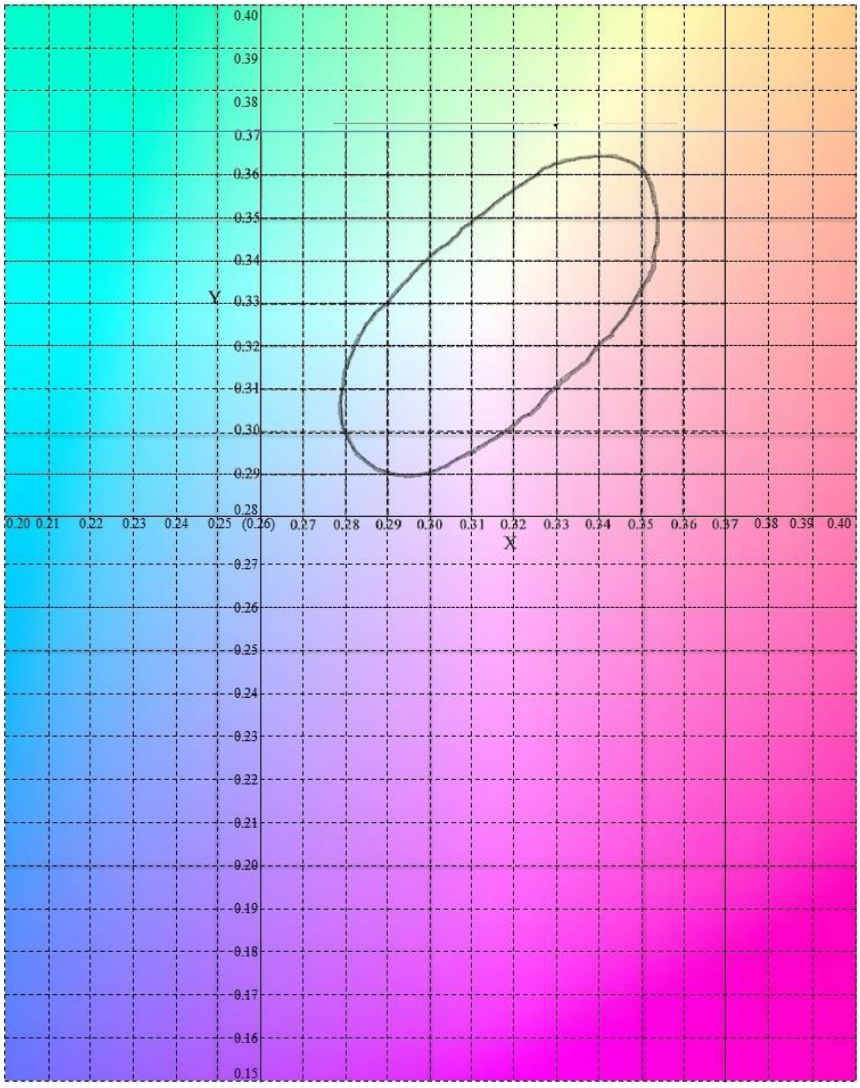

Fig. 4.1. Eyewear neutral chromaticity specifications (This color coordinate figure listed here defines the neutral color target: Whatever color with color coordinates inside the circle is considered as a neutral color.)

4.3.2 Molar Absorptivity of Yellow Dye

The YG-incorporated gel electrolytes were then used to build devices according to reported procedures.[11,15] A critical step for achieving neutral grey coloration in assembled devices is to balance YG and polymer absorbance intensities. A too-high yellow intensity is not desirable as it distorts the perception of color by the human eye and will affect the device's bleach state color. Device contrast will also be decreased due to the enhanced absorbance intensity in the bleached state. Conversely, a too-low yellow intensity will not be enough to tune the deep blue color of PEDOT towards neutral. Therefore, to determine the optimal amount of YG to be placed within the gel electrolyte, the molar absorptivity of YG was first measured.

Molar absorptivity of YG was determined by monitoring the absorbance at 442 nm as a function of YG concentration in PC, solvent for the gel electrolyte. Results are shown below in **Fig. 4.2**. The molar absorptivity is determined to be 27,231 M^{-1} cm^{-1} under this wavelength.

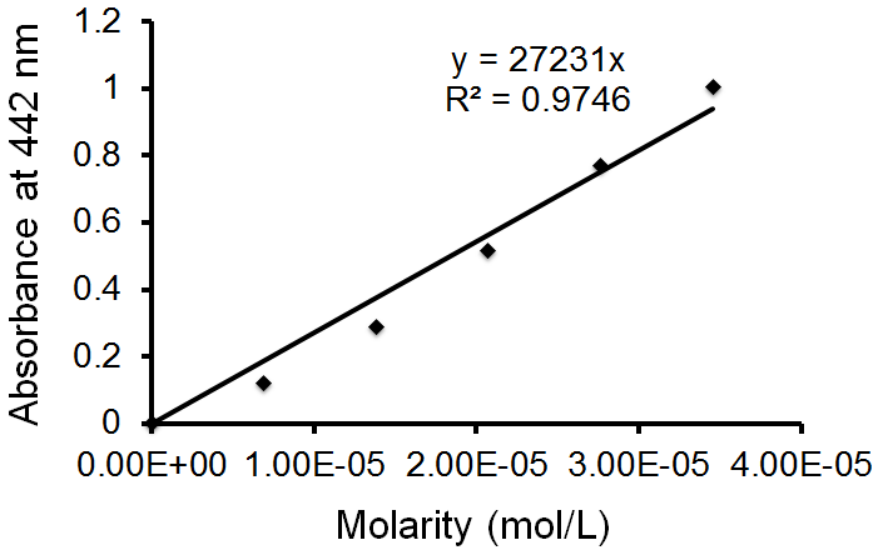

Fig. 4.2. Absorbance of YG at 442 nm as a function of YG molarity.

To prepare the YG-incorporated gel electrolyte, a YG stock solution was first prepared by dissolving 5 mg of YG into 5 g of PC. 205 mg of YG stock solution was then added into 10 g of the monomer gel electrolyte mentioned above. Number of moles of YG loaded was calculated to be 7.08×10^{-6} mol. Volume of the gel electrolyte was determined to be 8.5 mL. Thickness of gel layer was 0.8 mm. Therefore, the concentration of the YG = $\frac{\text{number of moles of YG}}{\text{Volume}} = 8.34 \times 10^{-5}$ M.

According to the Beer-Lambert law, the absorbance of YG at 442 nm wavelength inside an assembled device = $\varepsilon \times b \times c = 0.182$. For further confirmation, absorbance at 442 nm of EDOT device (Abs = 0.467) shown in **Fig. 4.3** was subtracted from that of EDOT + YG device (Abs = 0.279), giving the background corrected absorbance of YG. This absorbance is calculated to be 0.188, which agrees well with the calculated value.

4.3.3 Spectral Behavior

Devices were assembled on flexible ITO-coated polyethylene terephthalate (PET) substrates, as detailed in the Experimental section. **Fig. 4.3 a** and **Fig. 4.3 b**, respectively, show the spectral behavior of an in situ PEDOT device and an in situ PEDOT + YG device in the two extreme redox states. These two devices were activated for the same time, 30 seconds, under a constant potential of +3 V versus ground. As can be seen from **Fig. 4.3 b**, PEDOT absorption and YG absorption were balanced to about the same intensity. Compared with a normal PEDOT device, the PEDOT + YG device exhibits a broadened absorption, spanning the visible spectrum from 400 nm to 700 nm except for a gap from 460 nm to about 530 nm. Photopic contrasts were calculated for the two devices. The PEDOT + YG device has a photopic contrast of 30% (65.5%T to 35.5%T) as compared to the control PEDOT device photopic contrast of 30.5% (66.5%T to

36%T). Only a 0.5% photopic contrast loss was observed, which indicates that the application of YG did not sacrifice the original contrast of the polymer.

The UV-Visible absorption spectra of this dye, PEDOT, and the combination of the two within an assembled device are shown in **Fig. 4.3**.

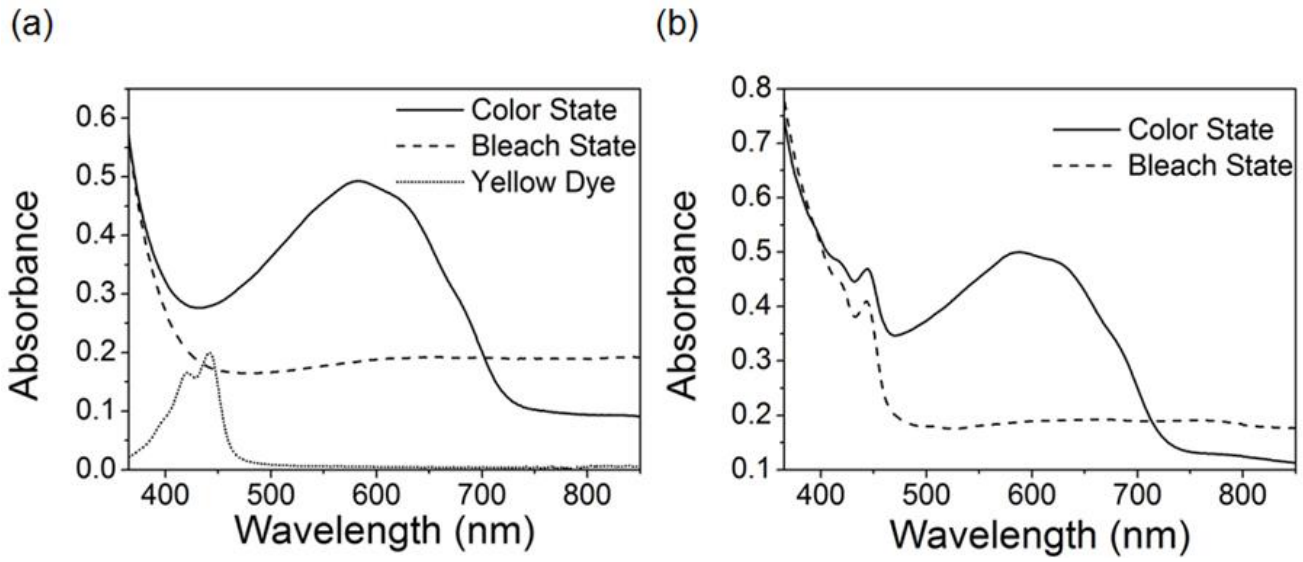

Fig. 4.3. UV-Vis absorption spectra of (a). in situ PEDOT device and yellow dye (background corrected) and (b).in situ PEDOT with YG device

Table 4.1. Photopic Contrast Comparison between normal PEDOT devices and PEDOT + YG Devices

Device	T% photopic Color	T% photopic Bleach	Photopic Contrast
PEDOT	36%	66.5%	**30.5%**
PEDOT + YG	35.5%	65.5%	**30%**

4.3.4 Color Analysis

To evaluate the color changes, the colorimetric properties for each device were characterized by CIE 1931 xyY color space based on the standard D65 illuminant. The white point for this color space is x = y = 0.333, which is equivalent to "black" at zero luminance, or white at high luminance. This central point is the target for neutral grey color electrochromics. The color coordinates for the PEDOT + YG device in the neutral state was determined to be x = 0.291, y = 0.317. As shown in **Fig. 4.4** , the device exhibits a dark bluish-black color which is similar to that reported by Reynolds.[4,6] Upon oxidation, it bleaches to a transmissive pale yellow tint with color coordinates of x = 0.332, y = 0.359, very close to the white point. The color of the PEDOT device in the neutral state was blue, with x = 0.226, y = 0.216. Its transmissive sky blue oxidized state had color coordinates of x = 0.309, y = 0.329. As seen in **Fig. 4.5**, there is a clear color shift from the blue region to the yellow region. It is also clear that, with the aid of the YG, the neutral state of the device is moving towards the white point where the true color neutrality lies.

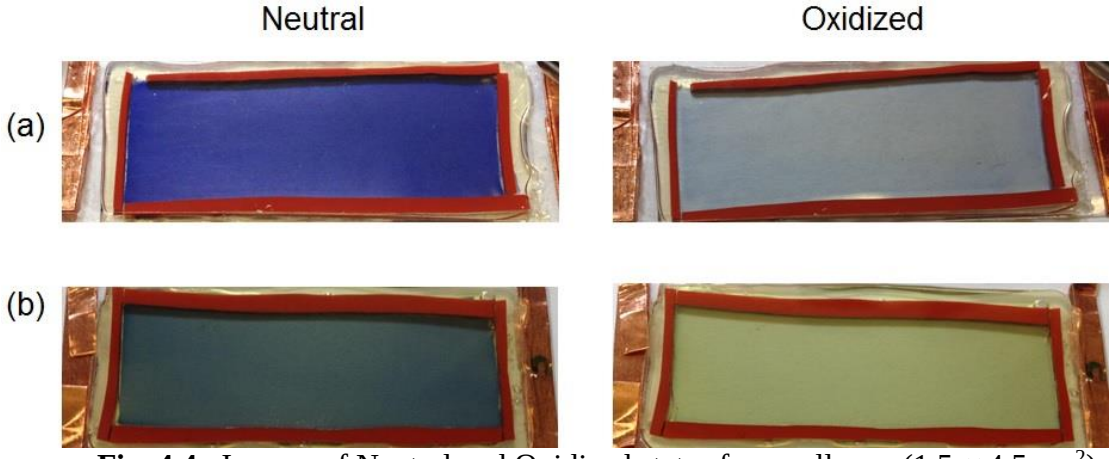

Fig. 4.4 . Images of Neutral and Oxidized states for small area (1.5 × 4.5 cm^2) devices: (a) *in situ* PEDOT device and (b) *in situ* PEDOT + YG device

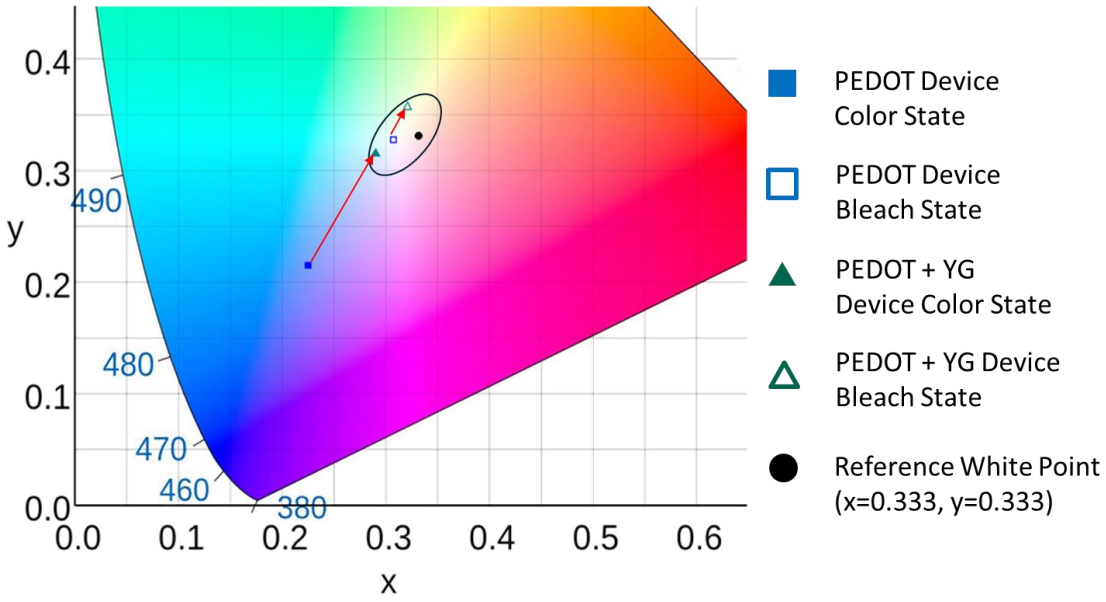

Fig. 4.5 Color coordinates of *in situ* PEDOT device neutral state (solid blue square) and oxidized state (open blue square), *in situ* PEDOT + YG device neutral state (solid dark cyan triangle) and oxidized state (open dark cyan triangle), reference white point (solid black circle).

Table 4.2. Color Coordinates Comparison between normal PEDOT devices and PEDOT + YG Devices

PEDOT Device	X	Y	PEDOT+YG Device	X	Y
Color State	0.226	0.216	Color State	0.291	0.317
Bleach State	0.309	0.329	Bleach State	0.322	0.359

4.3.5 Switching Speed

The switching kinetics of the PEDOT+ YG device was studied by UV-Vis spectrophotometry upon the application of a double-potential step from −2 V to +2 V. Devices were repeatedly switched between their fully neutral and oxidized states using an

8 s time interval. The percent transmittance (%T) change at 555 nm, where the human eye has its highest sensitivity, was monitored as a function of time. As shown in **Fig. 4.6**, the device shows a full optical contrast of 30% (63.5%T to 33.5%T) at this wavelength. Switching speeds of the devices, here, were defined as the time required to achieve 95% of the full color change, since the human eye is sensitive up to 95% of the full contrast.[7] Under these conditions, for a device with 1.5 × 4.5 cm^2 active area, the time required for coloring the device was calculated to be 1.5 s and the device exhibited a switch time to bleached state of 2.7 s. These values are comparable to the switching speed of the control PEDOT device of the same active area size, 1s for coloring and 2.5 s for bleaching, summarized in **Table. 4.3**.

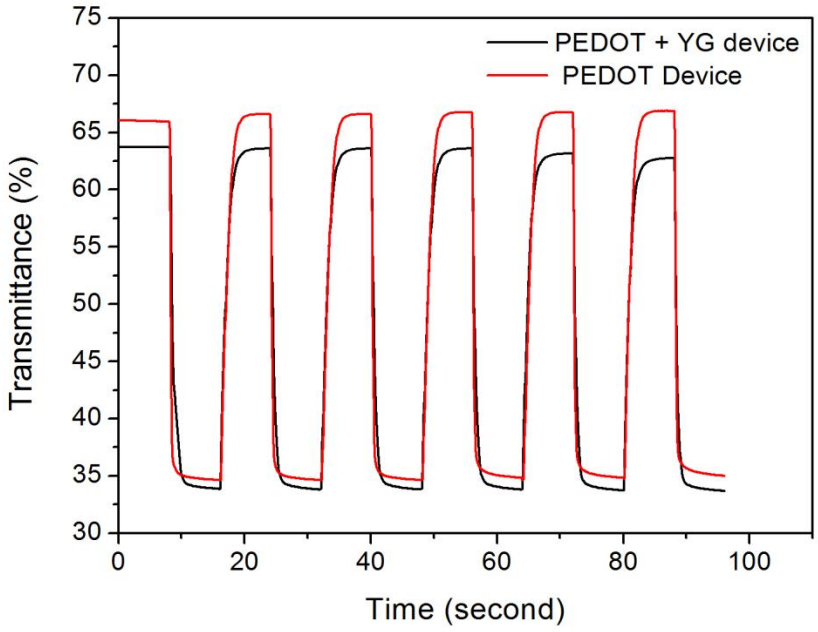

Fig. 4.6. Percent transmittance change at 555 nm for *in situ* PEDOT device and *in situ* PEDOT + YG device during constant potential stepping between -2 V to +2 V at an 8 s pulse width.

Table 4.3. Redox switching speeds for *in situ* PEDOT device and *in situ* PEDOT + YG device

Device	Color state photopic transmittance	Bleach state photopic transmittance	Coloring Time (s)	Bleaching Time (s)
PEDOT	34.5%	66.5%	1	2.5
PEDOT + YG	33.5%	63.5%	1.5	2.7

4.3.6 Large Area Device Fabrication

Another advantage of the *in situ* method is that it facilitates the preparation of large area devices, which is an essential component for commercialization of EC sunglasses, goggles, and windows, among other applications. To date, common active switching area sizes for ECDs have been on the order of 2.5 × 2.5 cm^2. A PEDOT + YG optical defect-free ECD with 100 cm^2 (6 cm × 16.7 cm) active area was prepared by injecting YG-dissolved monomer infused liquid electrolyte into preassembled device frames (Figure 3b). ITO coated glass was used for both substrates. The percent transmittance of the device in the colored and bleached states across the visible region (380 nm to 780nm) is shown in **Fig. 4.7**. In the colored state, at a device cell potential of -2 V vs. ground, the device exhibits a 39% photopic transmittance and in the bleached state, upon oxidation at + 2 V vs. ground, the device exhibits a photopic transmittance of 70%. Thus, a photopic contrast of 31% was achieved, equivalent to that of the smaller-area 6.75 cm^2 devices.

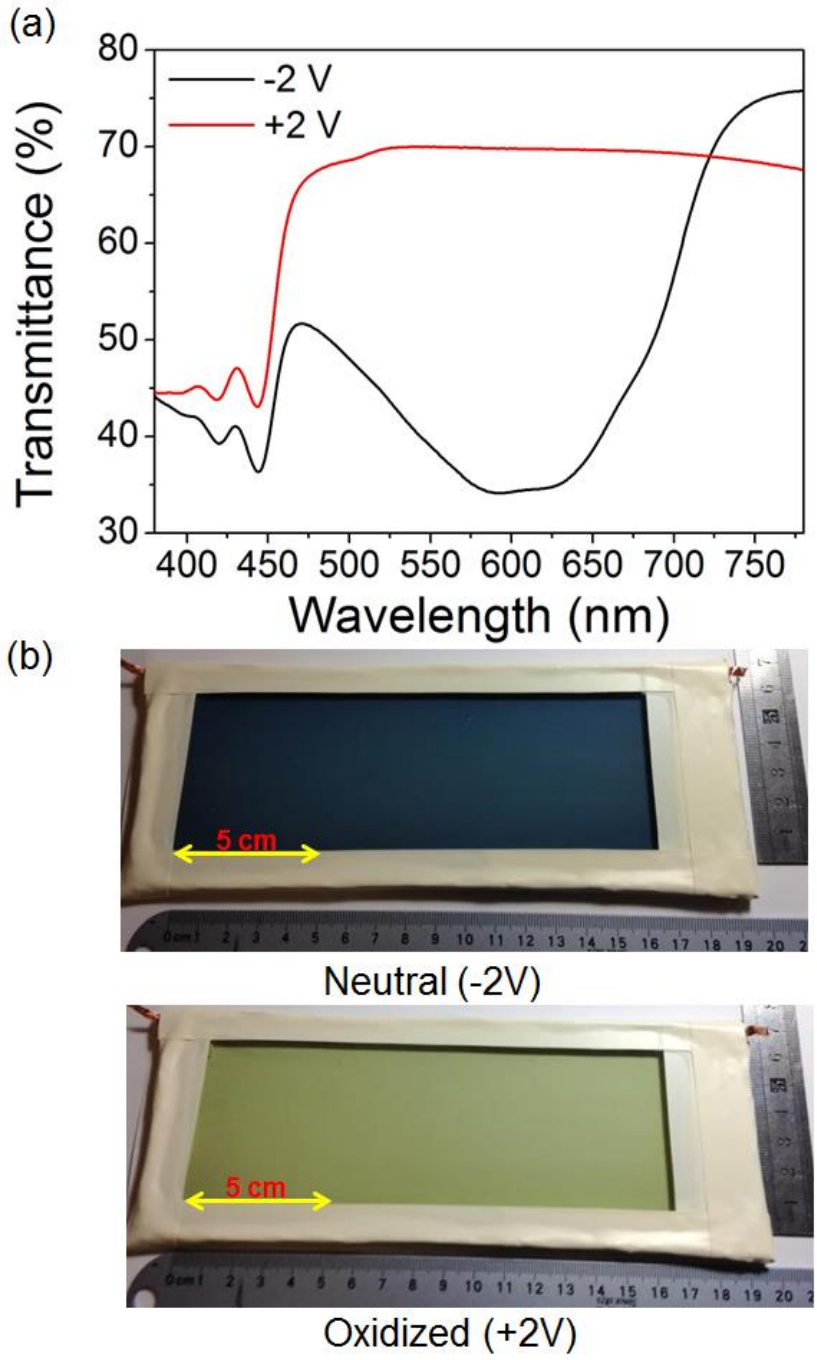

Fig. 4.7. (a) Percent Transmittance of a 100 cm^2 *in situ* PEDOT + YG device in the neutral (-2 V) and oxidized (+2 V) states. (b). Images of the 100 cm^2 *in situ* PEDOT + YG device in the neutral and oxidized states.

4.4 Conclusion

In conclusion, utilizing the *in situ* device fabrication approach, we have demonstrated the ability to achieve neutral color ECDs by adding a commercially available yellow dye into the gel polymer electrolyte. The conjugated dye was shown to not interfere with the electropolymerization of EDOT, which is known to follow the Diaz mechanism, allowing a combinatorial effect in the subtractive color spectrum. Optimized polymer and yellow dye absorption intensities yielded neutral grey color ECDs with 30% photopic contrast and switch speeds as low as 1 second on flexible PET substrates. A defect-free 100 cm^2 active area ECD, as analyzed by optical microscopy, was demonstrated in this study using this method exhibiting both color uniformity and stability. In addition, this study opens up new directions to tune optical and colorimetric properties of EC polymers in combination with the use of commercially available dyes for increased contrast. This approach could be adapted for the real-world production of EC sunglasses, goggles, and windows.

4.5 Reference

1 A. A. Argun, P. H. Aubert, B. C. Thompson, I. Schwendeman, C. L. Gaupp, J. Hwang, N. J. Pinto, D. B. Tanner, A. G. MacDiarmid and J. R. Reynolds, *Chem. Mater.*, 2004, **16**, 440-4412.

2 G. Gunbasab and L. Toppare, *Chem. Commun.*, 2012, **48**, 1083-1101.

3 J. L. Boehme, D. S. K. Mudigonda and J. P. Ferraris, *Chem. Mater.*, 2001, **13**, 4469-4472; V. Seshadri, J. Padilla, H. Bircan, B. Radmard, R. Draper, M. Wood, T. F. Otero and G. A. Sotzing, *Org. Electron.*, 2007, **8**, 367-381; P. Tehrani, L. O. Hennerdal, A. L. Dyer, J. R. Reynolds and M. Berggren, *J. Mater. Chem.*, 2009, **19**, 1799-1802; M. A. Invernale, Y. Ding and G. A. Sotzing, *ACS Appl. Mat. Interfaces*, 2010, **2**, 296-300; J. Kim, J. You, B. Kim, T. Park, and E. Kim, *Adv. Mater.*, 2011, **23**, 4168-4173; D. Navarathne and W. G. Skene, *J. Mater. Chem. C*, 2013, **1**, 6743-6747; S. Kim, X. Kong and M. Taya, *Sol. Energy Mater. Sol. Cell.*, 2013, **7**, 183-188; T. Bhuvana, B. Kim, X. Yang, H. Shin, and E. Kim, *Angew. Chem. Int. Ed.*, 2013, **52**, 1180-1184.

4 P. M. Beaujuge, S. Ellinger and J. R. Reynolds, *Nat. Mater.*, 2008, **7**, 795-799.

5 P. J. Shi, C. M. Amb, E. P. Knott, E. J. Thompson, D. Y. Liu, J. G. Mei, A. L. Dyer and J. R. Reynolds, *Adv. Mater.*, 2010, **22**, 4949-4953.

6 S. V. Vasilyeva, P. M. Beaujuge, S. Wang, J. E. Babiarz, V. W. Ballarotto and J. R. Reynolds, *ACS Appl. Mater. Interfaces*, 2011, **3**, 1022-1032.

7 G. Oktem, A. Balan, D. Baran and L. Toppare, *Chem. Commun.*, 2011, **47**, 3933-3935.

8 K.-R. Lee and G.A. Sotzing, *Chem. Commun.*, 2013, **49**, 5192-5194.

9 M. Icli, M. Pamuk, F. Algi, A. M. Onal and A. Cihaner, *Org. Electron.*, 2010, **11**, 1255-1260.

10 H. Shin, Y. Kim, T. Bhuvana, J. Lee, X. Yang, C. Park and E. Kim, *ACS Appl. Mater. Interfaces,n* 2012, **4**, 185-191.

11 Y. Ding, M. A. Invernale, D. M. D. Mamangun, A. Kumar and G. A. Sotzing, *J. Mater. Chem.*, 2011, **21**, 11873-11878.

12 A. Kumar, M. T. Otley, F. A. Alamar, Y. Zhu, B. G. Arden and G.A. Sotzing, *J. Mater. Chem. C*, 2014, **2**, 2510-2516.

13 F. A. Alamer, M. T. Otley, Y. Ding and G. A. Sotzing, *Adv. Mater.*, 2013, **25**, 6256-6260.

14 M. T. Otley, F. A. Alamer, Y. Zhu, A. Singhaviranon, X. Zhang, M. Li, A. Kumar and G. A. Sotzing, *ACS Appl. Mater. Interfaces*, 2014, **6**, 1734-1739.

15 M. A. Invernale, Y. Ding, D. M. D. Mamangun, M. S. Yavuz and G. A. Sotzing, *Adv. Mater.*, 2010, **22**, 1379-1382.

Chapter 5: Polyelectrolyte Exceeding ITO Capabilities in Flexible Electronics

Published in *J. Mater. Chem. C*, **2014**, 2, 9874-9881

5.1. Introduction and Motivation

Utilizing the *in situ* method, developed by our group in 2011, we report the fabrication of flexible electrochromic (EC) displays in a one-step lamination procedure. We undertook a study to optimize device performance via the optimization of new gel polymer electrolyte (GPE) materials based on poly(ethylene glycol) dimethacrylate (PEGDMA) in conjunction with poly(ethylene glycol) methyl ether acrylate (PEGMA), containing lithium trifluoromethanesulfonate (LiTRIF) as the salt and propylene carbonate (PC) as solvent; we investigated varying electrolyte parameters, including salt loading, the mono/di-functional PEG ratio, and solvent to PEG ratio. Optimized gel systems exceed the mechanical flexibility of indium tin oxide (ITO) coated polyethylene terephthalate (PET) substrates in sustainable minimum bending radius of curvature, exhibit an ionic conductivity up to 1.36×10^{-3} S/cm, and yield electrochromic devices (ECDs) with photopic contrasts as high as 53% (without background correction) using poly(2,2 dimethyl-3,4-propylenedioxythiophene) (PProDOT-Me2) as the standard electrochromic material. In addition to ionic conductivity, the crosslink density of the gel polymer electrolytes was found to have an important effect on photopic contrast of resulting ECDs. Using these results, 110 cm^2 flexible EC displays with high resolution patterns were assembled as a demonstration of their potential in real world applications.

Polymeric electrochromic devices (ECDs) have found a wide applicability in eyewear, architectural windows, automotive mirrors, aircraft, color changing fabrics and display panels,[1] owing to their high optical contrast, fast response time, and the color multitude achievable via polymer structure modification.[2] Whereas, the traditional flat screen displays are currently used in most electronics devices, there has been a significant growing demand for flexible displays because of their advantages in flexibility, conformability, and light weight, which are considered as the next generation of electronics. As opposed to previous work on solid electrochromic devices which were built on rigid glass substrates, more recent studies have been devoted to flexible plastic substrates [3] for their potential applications in paper like products such as e-papers, e-books, and even flexible cellphone screens that can be frequently bended and folded. For more sophisticated needs, the electrochromic displays would require stretchability for future wearable smart clothing.[4]

However, to date, no commercially available flexible electrochromic displays are mass produced due to a number of problems and challenges to be solved, such as the limitation of low cost, high volume manufacturability, device stability/ruggedness, and relatively low device contrast for practical use, to name a few. We have developed and optimized a one-step *in situ* device fabrication to improve device performance towards meeting the demands of commercialization.[5,6] Unlike conventional device fabrication processes, where electrochromic polymer films are electrodeposited from solution, this is a technique where electrochemical conversion of monomers into electrochromic polymers takes place inside a cross-linked polyelectrolyte matrix within assembled devices. This cross-linked polyelectrolyte is formed upon UV curing of an all-in-one

liquid monomer electrolyte composed of acrylate end functionalized low molecular weight poly(ethylene glycol) (PEG), salt, plasticizer, electroactive monomers, and a photoinitiator. Electrochromic polymers formed by this approach are highly dependent on the properties of the polyelectrolyte. [7,8]

Generally speaking, GPEs are generally a salt-solvent-polymer hybrid system formed by dissolving salt in solvent and then incorporated into a polymer matrix. Among numerous GPE materials, acrylate and methacrylate-based PEG oligomers are widely used as polymer hosts due to their excellent compatibility for a variety of salts, wide operation potential window, and low cost and toxicity.[9,10] Photo-polymerization of the PEG oligomers or their combinations under UV irradiation is one of the most practical curing methods to form these polyelectrolytes which have already been applied in such areas as vapor separation membrane materials, drug delivery hydrogels, lithium ion batteries, and dye-sensitized solar cells. [11]

Herein, we report the optimization of new GPE materials formed by UV curing of liquid electrolytes composed of salt lithium trifluoromethanesulfonate (LiTRIF), solvent propylene carbonate (PC) in polymer host consisting a di-methacrylate PEG oligomer (poly(ethylene glycol) dimethacrylate) (PEGDMA) and a mono-acrylate PEG oligomer (poly(ethylene glycol) methyl ether acrylate) (PEGMA), and their applications in electrochromic devices. Electrolyte composition parameters including salt weight percentage, mono-acrylate/di-methacrylate PEG weight ratio, the solvent to PEG weight ratio were studied to maximize performance of ECDs fabricated via the *in situ* method. Optimal polyelectrolyte demonstrated a high ionic conductivity of 1.36×10^{-3} S/cm and yielded ECDs with a photopic contrast up to 53% (nonbaseline corrected). In addition, a

systematic study was carried out on the mechanical flexibility properties of the gel electrolytes by comparing with commercial indium doped tin oxide (ITO) coated polyethylene terephthalate (PET) substrates dominantly used in flexible electronics. Optimized GPEs were found to withstand a much larger bending extent, exceeding that of ITO coated PET. After introducing all these optimized parameters, large-area optical defect-free flexible ECDs with high resolution patterns were successfully assembled and demonstrated.

5.2 Experimental

5.2.1 Materials

Poly (ethylene glycol) dimethacrylate (PEGDMA) (Mn = 550 g/mol), poly(ethylene glycol) methyl ether acrylate (PEGMA) (Mn = 480 g/mol), lithium trifluoromethanesulfonate (LiTRIF), propylene carbonate(PC), dimethoxyphenylacetophenone (DMPAP) were purchased from Sigma-Aldrich and used as received. Indium Tin Oxide (ITO) coated glass (sheet resistance 8-12 Ohms/sq, Part Number: CG-50IN) were purchased from Delta Tech Inc.. Two different ITO coated PET substrates of which sheet resistance are 60 Ohms/sq and 20 Ohms/sq (Part Number: LR-15/CP54/500) were purchased from Bayview Optics Inc. and CP Films Inc., respectively. UV-sealant glue (UVS 91) was purchased from Norland Products. Conductive copper adhesive tape and transparent silicone rubber gasket (0.02 inch thick) were purchased from 3M Inc. and used as received. 2,2-dimethyl-3,4-propylenedioxythiophene (ProDOT-Me2) was synthesized according to the reported procedure.[12] 3,4-ethylenedioxythiophene (EDOT) was purchased from Heraeus Clevios GmbH and distilled under reduced

pressure prior to use. Hydrochloric acid (HCl) was purchased from Fisher Scientific and diluted to 6 M with DI water for use.

5.2.2 Preparation of Gel Polymer Electrolyte

All liquid electrolytes were prepared by mixing a total of 5 g propylene carbonate, 5 g of PEG oligomers (PEGDMA and PEGMA binary mixtures in various weight ratios: 100:0, 75:25, 50:50, 25:75, 10:90, 5:95, 2.5: 97.5, 1:99, 0:100), LiTRIF at different weight loading (0.5 g to 1.5 g), 17.5 mg of photoinitiator (DMPAP) and then sonicated for 15 minutes until fully dissolved. Prepared liquid electrolytes were subjected to UV curing in N_2 atmosphere inside a UV crosslinker under 365 nm UV light (5.8 mW/cm^2) according to reported procedure to form the gel polymer electrolyte. [13,14]

5.2.3 Electrochromic Device Assembly

For *in situ* ECD construction, an all-in-one liquid monomer electrolyte was first prepared by loading monomer at a 2.5 wt% with respect to abovementioned liquid electrolytes, and was then sandwiched between two ITO coated substrates (cleaned by sonicating with acetone and air dried before use). A silicon rubber gasket (0.02 inch thick) was placed between the two ITO coated substrates to serve as the spacer. Sequentially, the device was placed inside the UV crosslinker and underwent the same curing process as stated above and sealed with UV curable glue. After photo-curing, a constant potential of +3 V was applied to the solid state assembled devices to electrochemically couple monomers to make the electrochromic polymer and then the device was cycled between ±2 V for 5 times before data acquisition.

For large area flexible patterned ECD fabrication, ITO coated PET (6 × 20cm) was first etched with 6 M HCl aqueous solution using a stencil to form the patterned ITO area

and then rinsed with DI water to remove acid residue. Patterned substrates were used for device assembly following abovementioned procedures.

5.2.4 Instrumentation and Methods

A UVP CL-1000 Crosslinker (365 nm) was used to cure the liquid electrolytes. The ionic conductivity of the gel polymer electrolyte was measured using a HP 4284A precision LCR meter operating from 20 Hz to 100 KHz frequency range under ambient room temperature (25 ℃) and evaluated by AC impedance spectroscopy. DSC measurements were performed on a TA Instrument Q100 differential scanning calorimeter following the parameters: 1.Heating from -90 ℃ to 50 ℃ at 5 ℃ /min; 2. Cooling back to -90 ℃ at 20 ℃ /min; 3. reheating to 50 ℃ at 5 ℃ /min. The glass transition temperature (Tg) of the gel polymer electrolyte was determined from the midpoint where the heat capacity changes. Crosslink density of GPEs was determined by equilibrium swelling experiments placing a small sample of gel electrolyte in propylene carbonate at room temperature for three days. According to Flory-Rehner's theory, the degree of swelling is dependent upon the crosslink density of the gel matrix. The greater the degree of swelling, the less the crosslink density. For a cross-linked gel formed in the presence of solvent, an extended form of Flory-Rehner equation was used. [15] The number average molecular weight between cross-links, M_c, can be determined from Eq. (1):

$$M_c^{-1} = \frac{\frac{\upsilon}{V_s}\left[\ln\left(1-V_{p,s}\right)+V_{p,s}+\chi V_{p,s}^{2}\right]}{V_{p,0}\left[\left(\frac{V_{p,s}}{V_{p,0}}\right)^{\frac{1}{3}}-\frac{1}{2}\left(\frac{V_{p,s}}{V_{p,0}}\right)\right]} \qquad (1)$$

where υ is specific volume of polymer, V_s is molar volume of solvent, $V_{p,0}$ and $V_{p,s}$ are polymer volume fractions of gel samples in initial and swollen state, respectively. χ is the

polymer-solvent interaction parameter. The crosslink density, defined as 1/2*Mc*, can be obtained.

All electrochemistry was performed on a CHI 720c potentiostat. All optical studies were carried out using a Varian Cary 5000 UV-vis-NIR instrument. The absorbance spectra of assembled electrochromic devices in their colored and bleached states were measured from 350 nm to 850 nm and corresponding photopic transmittance value was calculated using Eq. (2):

$$T_{photopic} = \frac{\int_{350}^{850} T(\lambda)S(\lambda)P(\lambda)d\lambda}{\int_{350}^{850} S(\lambda)P(\lambda)d\lambda} \qquad (2)$$

where T(λ) is the spectral transmittance of the device, S(λ) is the normalized spectral emittance of the light source, and P(λ) is the normalized spectral response of the eyes.[7,8,13] Photopic contrast value equals the difference between the photopic transmittance of the two extreme device redox states and was monitored as a function of polymerization time to ensure the optimal contrast was achieved.[7] All photopic contrast values reported here are without background correction as it represents all absorbance and reflections through all materials and interfaces of the device, giving the most real perception of human eyes.

5.3 Results and Discussion

5.3.1 Optimization of salt concentration

As an important component of gel polymer electrolyte, the salt provides free mobile ions for conduction and as dopants during the formation and redox switching of EC polymers. Generally speaking, the conductivity of the gel electrolyte increases with increased salt concentration as the number of charge carriers increases. After reaching a maximum point, the conductivity drops upon further salt addition due to ion aggregation or crystallization. We have previously reported and demonstrated that for each particular GPE system, its most conductive gel matrix yielded devices with the highest photopic contrast as a more mobile electrolyte contributed to a higher charge density during polymerization, thus aiding polymer formation and leading to an enhanced doping level of the polymer.[7,8,16] Hence, in order to optimize the electrochromic performance across these GPE systems, the polyelectrolyte ionic conductivity should be optimized.

All GPEs for experiments were started with 1:1 weight ratio of PC to PEG as this ratio was found to give best device performance to date,[6,7] and conductivity was monitored as a function of salt concentration. As can be seen in in **Fig.5.1 (a)**, there is an optimal salt loading (9.1 wt%) which yields the highest ionic conductivity of 9.14×10^{-4} S/cm in 100% PEGMA system. Similar trends were also found in other systems. The optimum salt concentration was determined for each GPE and corresponding optimal ionic conductivity with respect to the PEGDMA wt% in overall PEG amount is shown in **Fig.5.1 (b)**. Upon UV curing, PEGDMA forms a rigid cross-linked polymer which is much harder than the gooey linear polymer obtained from photopolymerization of PEGMA. A lower PEGDMA loading within the mixed PEG systems will produce a

polymer of fewer cross-links and as a result, flexibility and mobility of PEG chains will be enhanced, thus contributing to an enhanced ionic conductivity. Further, DSC was employed to compare Tg of these GPEs. The glass transition temperature measures the polymer chain mobility in the amorphous domain. Below Tg, polymer relaxation stops which drastically lowers ionic conductivity and increases brittleness. In general, low Tg polymers are more flexible and have higher conductivity. The same behavior was observed in our systems. Tg value decreases from -67.5 ℃ to -84 ℃ while optimal ionic conductivity value improves from 3.74×10^{-4} S/cm to 9.14×10^{-4} S/cm when the PEGDMA wt% drops from 100 wt% to 0 wt%. For practical applications of ECDs, a lower Tg is also usually desired for GPEs as it suggests ECDs can function in low temperature environments.

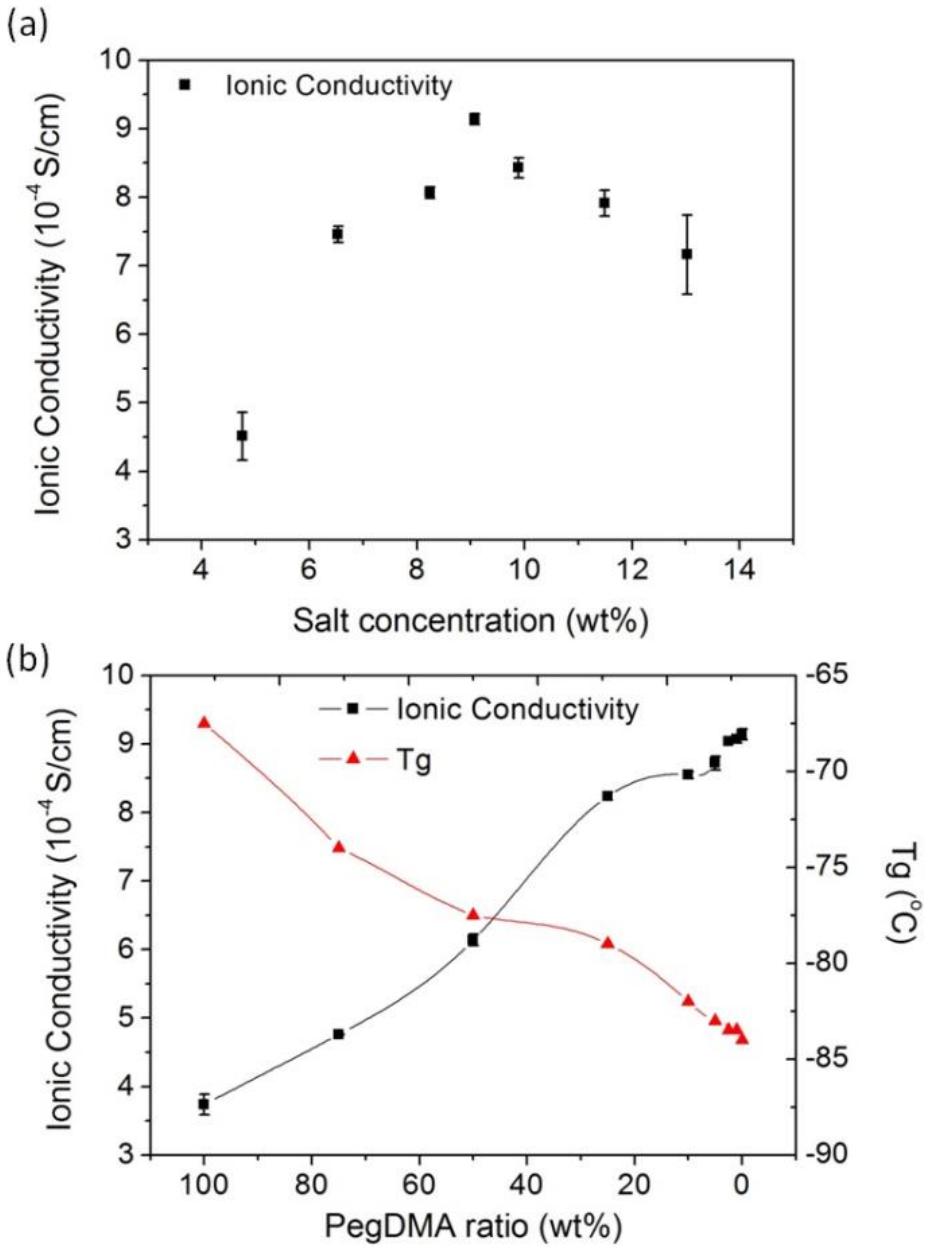

Fig. 5. 1 (a). Ionic conductivity as a function of LiTRIF concentration for GPE consisting of 100% PEGMA as the host polymer; (b). Ionic conductivity and glass transition temperature as a function of PEGDMA wt% in PEG across studied GPEs.

Table 5.1 The optimum salt concentration for each GPE (under 1 to 1 PC to PEG ratio) and corresponding optimal ionic conductivity

PEGDMA wt% in PEG (%)	**Optimal Salt wt% (%)**	**Optimal Ionic conductivity (mS/cm)**
100	9.1	0.374
75	9.1	0.476
50	9.1	0.614
25	9.1	0.824
10	9.9	0.855
5	9.1	0.872
2.5	9.1	0.904
1	9.1	0.907
0	9.1	0.914

3.2 Optimization of the mono/di-functional PEG ratio

High contrast have always been the main demand in the development of ECDs. To evaluate the electrochromic functionality within these gel electrolytes, *in situ* PProDOT-Me_2 devices were built and characterized. ProDOT-Me_2 was chosen as the standard monomer as PProDOT-Me_2, which switches between purple and colorless in the neutral and oxidized state respectively, were found to have a higher contrast than PEDOT and other PProDOT derivatives in the visible and NIR regions due to that oxidized PProDOT-Me_2 lacks the typical large NIR absorption, translating to a more transparent oxidized state.[12,17,18]

ECDs were assembled using ITO coated glass (8-12 ohms/sq) as working electrode and ITO coated PET (60 ohms/sq) as counter electrode. **Fig. 5.2** demonstrates the relationship between optimal device contrast and corresponding PEGDMA weight percentage (with respect to total PEG amount) in the GPEs used for device preparation. An interesting phenomenon observed here is that it is not the most conductive gel electrolyte that yield the highest device contrast. Device contrast was found to first increase to a maximum value with increased ionic conductivity then decreased upon further conductivity increase. Polyelectrolyte in which PEG was consisted of 25 wt% PEGDMA ($\sigma = 8.24\times10^{-4}$ S/cm) gave the highest photopic contrast of 52%, ca. 4% higher than that of devices prepared from the most conductive gel matrix (100 wt% PEGMA in PEG). Possible explanation could be related to the polymer matrix structure, namely the crosslink density of the polymer network. We have reported that the for ECDs prepared using the *in situ* procedure, monomer diffusion through the gel matrix is a key factor that affects the devices' quality.[8,19] A too high crosslink density of the

polyelectrolyte will result in a short inter-chain distance and a restricted mobility of PEG segments which will limit the monomer diffusion rate for polymer film growth. In contrast, too few cross-links will produce a very loose network in which the highly mobile PEG chains will interfere the monomer diffusion during the course of polymerization. Polyelectrolyte with a moderate crosslink density, can provide a adequate inter-chain distance while stabilize the movement of PEG chains, which will lead to a facilitated monomer diffusion, thereby, a higher polymerization charge density could be achieved under the same polymerization time, yielding a thicker polymer film. As can be seen in **Table 5.2**, the highest polymerization density was seen in the system which gave the highest photopic contrast.

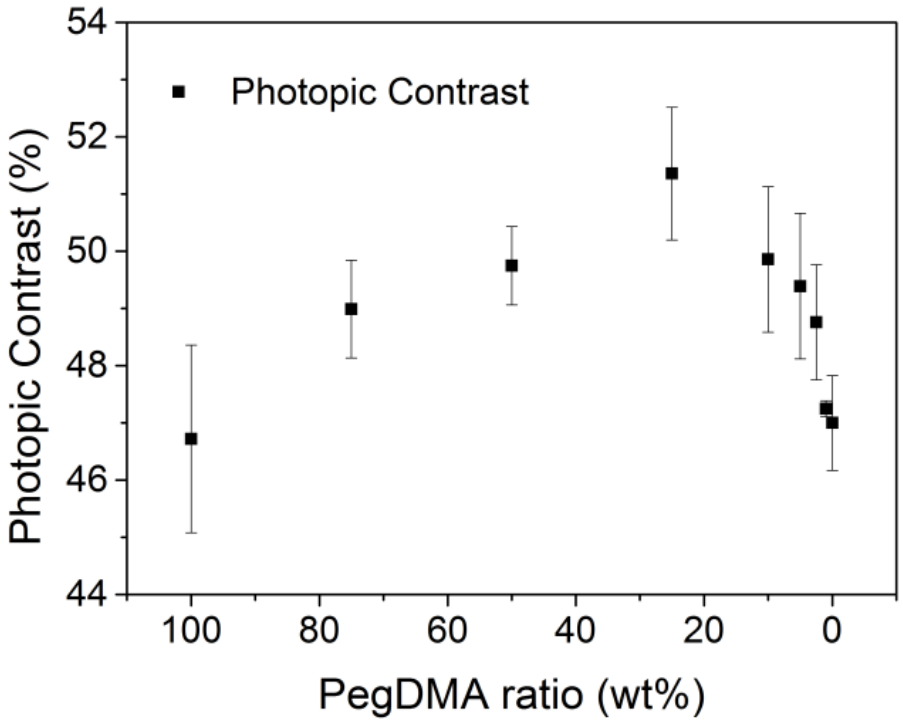

Fig. 5.2 Optimal device photopic contrast as a function of PEGDMA wt% in PEG across studied GPEs

Table 5.2. In situ ProDOT-Me2 polymerization charge density from studied GPEs with different crosslink densities

PEGDMA wt% in PEG (%)	Crosslink Density (mol/cm^3)	Polymerization Charge Density (mC/cm^2)
100	1.16 E-03	13.01
75	1.11 E-03	15.05
50	8.65 E-04	15.25
25	4.59 E-04	19.08
10	2.12 E-04	18.01
5	1.04 E-04	16.62
2.5	5.22 E-05	14.44
1	2.02 E-05	14.42
0	0	13.42

3.3 Optimization of Solvent to PEG ratio

The solvent used in GPEs serve two main important roles. First, it aids dissolving the salt and serve as the conducting medium for ion movement. Second, it acts to plasticize the host polymer chains to enhance the flexibility and mobility which in turn improves the conductivity of the polyelectrolyte. Upon determination of the optimal PEGDMA fraction in PEG (25 wt%), the solvent to PEG ratio was varied to further optimize the gel electrolyte. Keeping the total mass of solvent and PEG constant, four more different weight ratios (0 to 1, 3 to 7, 2 to 3, and 3 to 2) were studied in addition to

the aforesaid 1: 1 ratio. **Fig. 5.3 (a)** illustrates the correlation between the optimal gel electrolyte conductivity, optimal device contrast, and their dependence on the solvent to PEG weight ratio. As expected, addition of solvent improves the ionic conductivity of the gel electrolyte. The maximum value was achieved at the highest solvent to PEG ratio (3 to 2) within our study (σ=1.36 × 10^{-3} S/cm), which was two orders of magnitude higher than gel electrolyte with no solvent added (σ=1.24 × 10^{-5} S/cm), and, as a result, the optimal device photopic contrast was boosted up to 53%, which is 18% higher compared to the contrast value of 35% when no solvent was added. The 53% photopic contrast is the highest value for *in situ* ECDs reported to date. Solvent to PEG ratio higher than 3 to 2 was not considered, since preliminary experiments had shown that the gel electrolytes were not well cured due to too much solvent in presence. Result of subsequent DSC measurement was also in accordance with the trend of ionic conductivity: addition of solvent lowers the Tg of gel electrolyte while improves the conductivity. Images of a 53% photopic contrast *in situ* ECD in its colored and bleached states were shown in **Fig.5.3 (b)** and **Fig.5.3 (c)**.

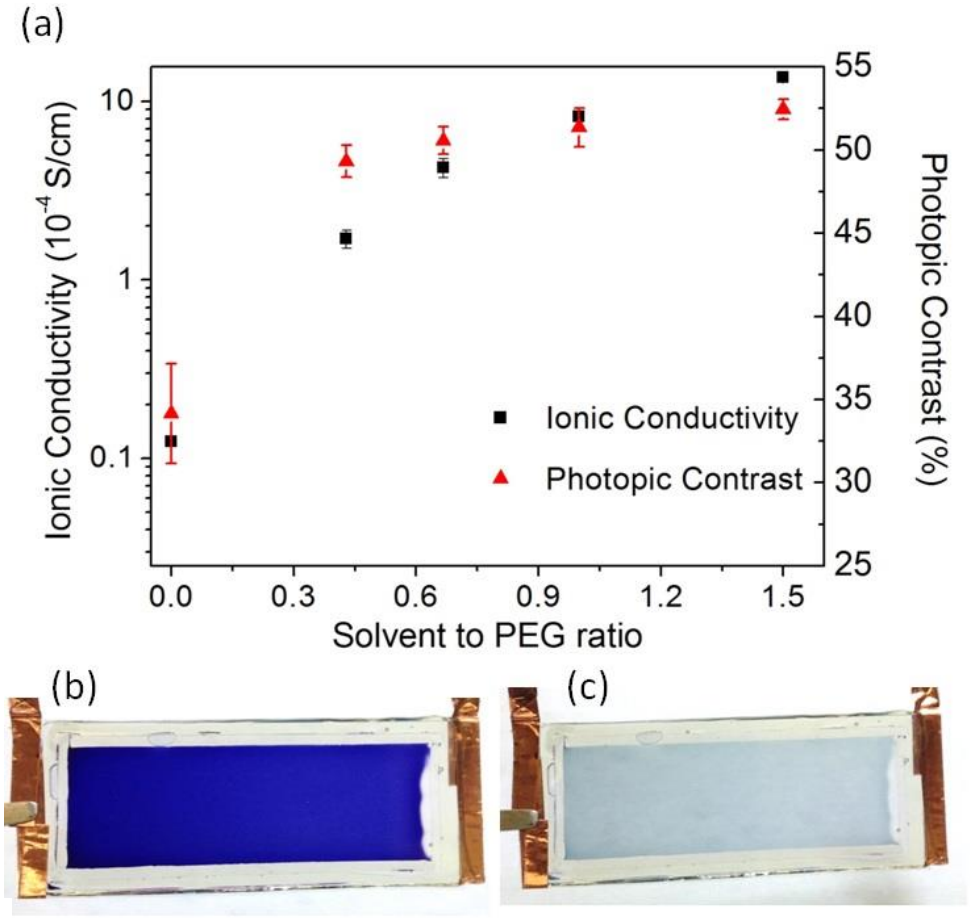

Fig. 5.3 (a).The relationship between in situ PProDOT-Me2 device photopic contrast and ionic conductivity of GPE consisting of 25 wt% PEGDMA in PEG as a function of PC to PEG ratio; (b). Colored state and (c). Bleached state for a 1.9 × 5 cm2 in situ PProDOT-Me2 ECD of 53% photopic contrast.

Table 5.3. The optimum ionic conductivity, glass transition temperature and flexibility for GPEs (The total mass of solvent and PEG was constant and the amount of PEDMA was fixed at 25% in PEG) under different solvent to PEG ratio

PC to PEG ratio	Optimal Ionic conductivity (S/cm)	Glass transition Temperature (℃)	Sustainable minimum bending radius of curvature (mm)
0 : 1	1.24E-05	-48	8
3 : 7	1.70E-04	-65	7
2: 3	3.96E-04	-74	6.25
1: 1	8.24E-04	-79	5.5
3 : 2	1.36E-03	-84	5

3.4 Mechanical Flexibility of ITO coated PET

ITO coated PET is currently the dominating substrate used for the fabrication of flexible electronics. A thorough investigation of the substrates will contribute to a better device design and handling to withstand everyday use. The mechanical flexibility test was performed on two commercial ITO/PET substrates (Sample A purchased from CP Film Inc.: sheet resistance 20 Ohms/sq, ITO layer thickness 278 nm; Sample B purchased from Bayview Optics Inc.: sheet resistance 60 Ohms/sq, ITO layer thickness 95 nm;) based on literature reported procedures.[20] The samples (2.54 cm × 2.54 cm) were conformally applied to cylinders of different radius ranging from 16.5 to 3 mm. Two types of bending tests were involved: tensile and compressive stress mode where the ITO surface was facing externally and internally from the cylindrical surface respectively.

Sheet resistance of substrates was measured before and after 100 bending cycles and evaluated as a function of bending radius of curvature (r) under the two stress modes.

Results of flexibility test of sample A was shown in **Fig. 5.4 (a)**. Under tensile bending mode, when the r reaches 11 mm, there is slightly sheet resistance increase (ca. 3 Ohms/sq). A more noticeable increase occurred under tensile stress was observed when r drops to 9.25 mm, the sheet resistance went up to 134 Ohms/sq. A significant increase was seen at 7.5 mm bending radius, it increased by two orders of magnitude (1500 Ohms/sq) compared to the initial value. ITO is a rigid and brittle inorganic material, frequent flexing will produce surface cracks as indicated in optical microscopy images in **Fig. 5.4 (b)**. As the bending radius decreases, number of cracks aggregates, leading to a drastic conductivity degradation. On the other hand, the compressive bending was found to give a much slower damage in conductivity: a noticeable sheet resistance change didn't occur until bending radius went down to 6.25 mm. Similar phenomenon was also seen and confirmed by previously reported studies.[21] Nevertheless, most flexible electronics require two opposite electrodes. When one substrate is subjected to compressive stress, the opposite one will simultaneously undergo tensile bending. Thus, in order to avoid any mechanical flexibility failure, the bending radius of curvature must be no smaller than 11 mm in the case for sample A. In comparison, sample B was found to withstand a larger bending extent as a result of a thinner conductive coating layer. The result is summarized in **Fig. 5.5**.

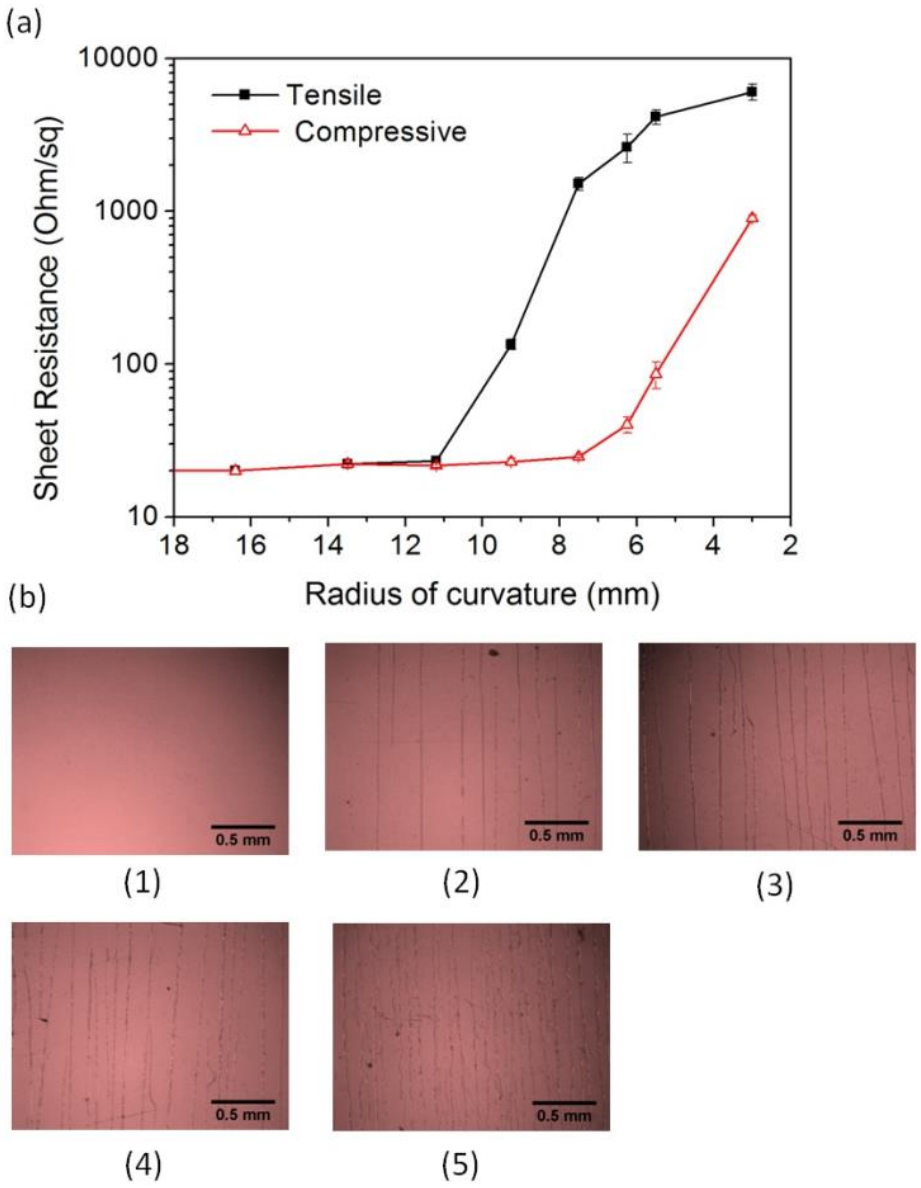

Fig. 5.4 (a). Sheet resistance of Sample A ITO/PET as a function of bending radius of curvature under tensile (solid black square) and compressive (open red triangle) stress after 100 bending cycles; (b).Optical microscopy images (×5 magnification) of the ITO surface (1) before bending; and after 100 bending cycles under (2) 7.5 mm; (3) 6.25 mm; (4) 5.5 mm; (5) 3.0 mm.

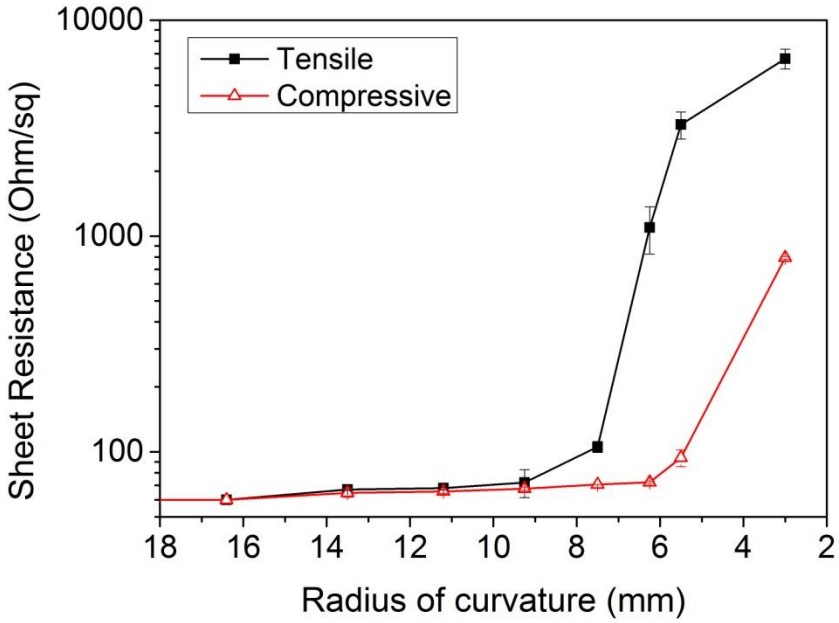

Fig. 5.5. Sheet resistance of Sample B ITO/PET as a function of bending radius of curvature under tensile (solid black square) and compressive (open red triangle) stress after 100 bending cycles.

Under tensile stress, when the radius of curvature reaches 11 mm, there is slightly increase in the sheet resistance value. When radius of curvature reaches 9.25 mm, the sheet resistance value increases to 72 ohms/sq. Upon further radius of curvature decrease to 7. 5 mm, there is an more obvious increase in sheet resistance value. It increases from 60 to 105 ohms/sq. Under compressive bending mode, there wasn't an obvious sheet resistance change until the bending radius drops to 5.5 mm (sheet resistance increases from 60 to 93 ohms/sq).

3.5 Mechanical Flexibility of Gel Polymer Electrolytes and Applications in Flexible ECDs

To gauge the mechanical properties of gel polymer electrolytes in our study, the same flexibility tests mentioned above was carried out. Gel sample length and width were kept the same as ITO/PET samples (2.54 cm × 2.54 cm) while the thickness was held at 0.51 mm as this was the gel layer thickness used for device fabrication. Exhibited in **Table 5.4** was the flexibility for each GPE system (under 1 to 1 PC to PEG ratio) depicted as the sustainable minimum bending radius of curvature.

Table 5.4 Mechanical flexibility of studied GPE systems

PEGDMA wt% in PEG (%)	Sustainable minimum bending radius of curvature (mm)
100	Hard, rigid
75	10
50	9.25
25	5.5
10	< 3
5	< 3
2.5	< 3
1	< 3
0	Sticky, stretchable

When the polymer host was consisted of 100 wt% PEGDMA, the polyelectrolyte tended not to be bendable which was found to easily break apart under the maximum studied radius of curvature. On the other hand, although gel electrolyte using 100 wt% PEGMA as the host polymer has good stretchability, resulting devices, however, easily delaminate during flexing, which was not preferred for practical application as well. Our results indicate that, the gel electrolyte composed of a binary mixture of PEGDMA and PEGMA are more suitable for flexible ECD fabrication. Under the 1 to 1 solvent to PEG ratio, when the PEGDMA weight percentage decreases to 75%, the gel electrolyte flexibility has already surpassed that of examined ITO coated PET substrates. Upon further decease of PEGDMA amount, the gel electrolyte flexibility improved as a result of enhanced polymer chain mobility. Gel electrolytes in which PEG has 10 wt% or lower PEGDMA were found to be able to tolerate the smallest bending radius within our study. No cracks could be observed even under more bending cycles as analyzed by optical microscopy shown in **Fig. 5.6 (a)**.

Other advantages associated with the *in situ* method are that it facilitates the manufacture of large area devices towards commercialization,[7,8] simplifies complex patterning by substrate blockage/or etching,[6] and color selection could be easily tuned through copolymerization of different monomers[19] or adding a solvent dye[22] within a single device. After introducing all the optimized parameters reported earlier in this study, high resolution patterned flexible in situ devices with up to 110cm2 area were successfully fabricated and exhibited in **Fig. 5.7**. These devices surpass the active switching area for sunglass lenses (40 cm^2), automotive mirrors (100 cm^2) and small

display applications, demonstrating the *in situ* method a good candidate for flexible ECD fabrication.

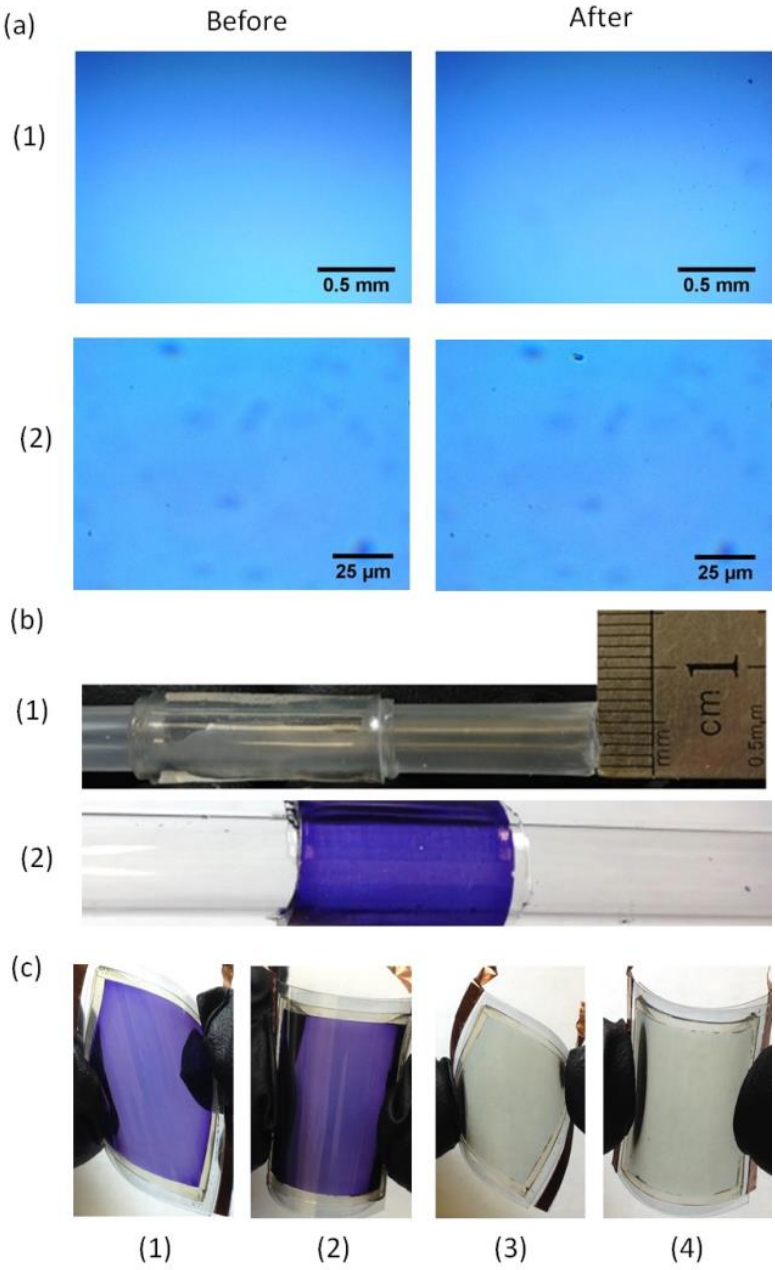

Fig. 5.6 (a) Optical microscopy images (×5 and ×100 magnification) of GPE consisting of 10wt% PegDMA in PEG before and after bending under 3 mm radius of curvature for 500 cycles; (b) (1) GPE consisting of 10wt% PegDMA in PEG and (2) corresponding PProDOT-Me2/gel electrolyte composite conformally bended to cylinder

with 3 mm radius; (c) A 3 cm × 3 cm flexible *in situ* ProDOT-Me_2 ECD bended diagonally and from the middle line its colored (1) (2) and bleached (3) (4) states.

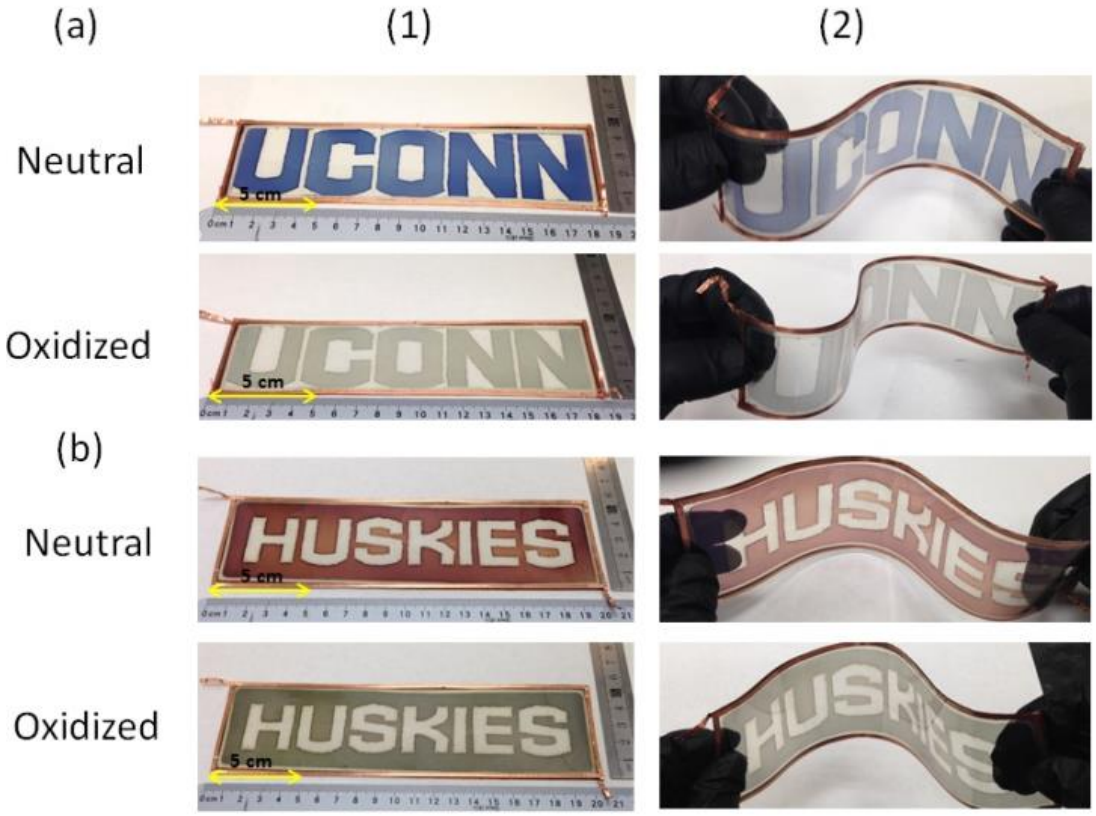

Fig. 5.7 Images of 110 cm^2 *in situ* flexible ECDs patterned with (a) UCONN logo employing PEDOT and (b) HUSKY logo employing a copolymer *in situ* copolymerized from Pyrrole and EDOT (monomer feed ratio 99 wt%:1 wt%) in their neutral and oxidized states under (1) unbent and (2) bended states, respectively.

5.4. Conclusion

We have studied and optimized a new GPE material formed by the photopolymerization of liquid gel electrolyte consisting of PEGDMA, PEGMA or their mixtures as host polymer with LiTRIF as the salt and PC as solvent for the application of ECDs using the *in situ* approach. Gel electrolyte composition parameters, including the salt concentration, PEGDMA to PEGMA ratio and solvent to PEG ratio were extensively studied towards the optimization of ECD performance. Both ionic conductivity and crosslink densities of GPEs were found to affect resulting device photopic contrast and a highest value of 53% to date was achieved upon optimization of abovementioned parameters. A thorough investigation on mechanical flexibility of GPEs was also conducted through a side by side comparison with commercial ITO coated PET substrates. Our results indicate that optimized gel electrolyte exceeded the flexibility of ITO/PET in sustainable minimum bending radius of curvature. Utilizing these results, large area flexible ECDs with high resolution patterns were assembled and tested, showing the versatility of the *in situ* method for flexible display manufacture and application.

5.5. Reference

1 (a) J. L. Boehme, D. S. K. Mudigonda and J. P. Ferraris, *Chem. Mater.*, 2001, **13**, 4469–4472; (b) A. Pawlicka, *Recent Patents on Nanotechnology*, 2009, **3**, 177-181. (c) P. Tehrani, L. O. Hennerdal, A. L. Dyer, J. R. Reynolds and M. Berggren, *J. Mater. Chem.*, 2009, **19**, 1799–1802; (d) M. A. Invernale, Y. Ding and G. A. Sotzing, *ACS Appl. Mater. Interfaces*, 2010, **2**, 296–300; (e) J. Kim, J. You, B. Kim, T. Park and E. Kim, *Adv. Mater.*, 2011, **23**, 4168–4173; (f) D. Navarathne and W. G. Skene, *J. Mater. Chem. C*, 2013, **1**, 6743–6747; (g) S. Kim, X. Kong and M. Taya, *Sol. Energy Mater. Sol. Cells*, 2013, **7**, 183–188; (h) T. Bhuvana, B. Kim, X. Yang, H. Shin and E. Kim, *Angew.Chem., Int. Ed.*, 2013, **52**, 1180–1184; (i) A. S. Shaplov, D. O. Ponkratov, P. Aubert, E. I. Lozinskaya, C. Plesse, F. Vidalb and Y. S. Vygodskiia, *Chem. Commun.*, 2014, **50**, 3191-3193; (j) E.L. Runnerstrom, A. Llordes, S. D. Lounisac and D. J. Milliron, *Che*m. Commun., DOI: 10.1039/c4cc03109a.

2 (a) A. A. Argun, P. H. Aubert, B. C. Thompson, I. Schwendeman, C. L. Gaupp, J. Hwang, N. J. Pinto, D. B. Tanner, A. G. MacDiarmid and J. R. Reynolds, *Chem. Mater.*, 2004, **16**, 440–4412; (b) P. M. Beaujuge and J. R. Reynolds, *Chem. Rev.*, 2010, **110**, 268–320; (c) G. Gunbasab and L. Toppare, *Chem. Commun.*, 2012, **48**, 1083–1101.

3 (a) W. A. Gazotti, G. Casalbore-Miceli, A. Geri, A. Berlin, and M. A. De Paoli, *Adv. Mater.*, 1998, 10, 1522-1524; (b) A.A. Argun, A. Cirpan and J.R. Reynold, *Adv. Mater.* 2003, **15**,1338; (c) L.-M. Huang, C.-H. Chen and T.-C.Wen, *Electrochim. Acta*, 2006, **51**, 5858; (d) N. Kobayashi, S. Miura, M. Nishimura and G. Yutaka, *Electrochim. Acta*, 2007, **53**, 1643; (e) C. Ma, M. Taya and C. Xu, *Electrochim. Acta*,

2008, **54**, 598-605; (f) W.-R. Lian , Y.-C. Huang , Y.-A. Liao ,K.-L. Wang , L.-J. Li , C.-Y. Su ,D.-J. Liaw, K.-R. Lee, and J.-Y. L, *Macromolecules*, 2011, **44**, 9550–9555; (g) K. Wang, H. Wu, Y. Meng, Y. Zhang and Z. Wei, ***Energy Environ. Sci.***, 2012, **5**, 8384-8389; (h) M. Layani, P. Darmawan, W. L. F, L. Liu, A. Kamyshny, D. Mandler, S. Magdassi and P. S. Lee, *Nanoscale*, 2014, **6**, 4572; (i) H.-J. Yen, H. Tsai, C.-Y. Kuo, W. Nie, A. D. Mohite, G. Gupta, J. Wang, J.-H. Wu, G.-S. Liou and H.-L. Wang, *J. Mater. Chem. C*, 2014, **2**, 4374.

4 (a) C.Yan, W. Kang, J. Wang, M. Cui, X.Wang, C. Y. Foo, K. J.Chee, and P. S. Lee, *ACS Nano*, 2014, **8**, 316–322 (b) W. M Kline, R. G. Lorenzini and G. A Sotzing, *Color. Technol.*, 2014, **130**, 73–80.

5 M. A. Invernale, Y. Ding, D. M. D. Mamangun, M. S. Yavuz and G. A. Sotzing, *Adv. Mater.*, 2010, **22**, 1379–1382.

6 Y. Ding, M. A. Invernale, D. M. D. Mamangun, A. Kumar and G. A. Sotzing, *J. Mater. Chem.*, 2011, **21**, 11873–11878.

7 A. Kumar, M. T. Otley, F. A. Alamar, Y. Zhu, B. G. Arden and G. A. Sotzing, *J. Mater. Chem. C*, 2014, **2**, 2510–2516.

8 Y. Zhu, M. T. Otley, F.A. Alamer, A. Kumar, X. Zhang, D. M.D. Mamangun, M. Li, B. G. Arden and Gregory A. Sotzing, *Org. Electron.*, 2014, **15**, 1378–1386.

9 V.K. Thakur, G. Ding, J. Ma, P.S. Lee, X. Lu, *Adv. Mater.* , 2012, **24**, 4071-4096.

10 S. Ahmad, *Ionics*, 2009, **15**, 309-321

11 (a) H. Lin, T. Kai, B. D. Freeman , S. Kalakkunnath and D. S. Kalika, *Macromolecules*, 2005, **38**, 8381-8393; (b) J.M. Teijón, R.M. Trigo, O. García and M.D. Blanco, *Biomaterials*, 1997. **18**, 383-388; (c) M.-H. Ryou, Y. M. Lee, K. Y.

Cho, G.-B. Han, J.-N. Lee, D. Jin Lee, J. W. Choi and J.-K. Park, *Electrochim. Acta*, 2012, **60**, 22-30; (d) F. Bella, D. Pugliese, J. R. Nair, A. Sacco, S. Bianco,C. Gerbaldi, C. Baroloc and R. Bongiovanni, *Phys. Chem. Chem. Phys.*, 2013, **15**, 3706; (e) M. Echeverri, C. Hamad and T. Kyu, *Solid State Ionics*, 2014, **254**, 92-100; (f) F. Bella, E. D. Ozzello, A. Sacco, S. Bianco and R.Bongiovanni, *Int. J. Hydrogen Energy*, 2014, **39**, 3036-3045.

12 D.M. Welsh, A. Kumar, E.W. Meijer, J.R. Reynolds, *Adv. Mater.* , 1999, **11**, 1379–1382.

13 V. Seshadri, J. Padilla, H. Bircan, B. Radmard, R. Draper,M. Wood, T. F. Otero and G. A. Sotzing, *Org. Electron.*, 2007, **8**, 367–381

14 (a) H. Bircan, V. Seshadri, J. Padilla, M. A. Invernale, T.F. Otero, G.A. Sotzing, *J. Phys.: Conf. Ser.*, 2008, **127**,012011;(b) H. Bircan, M.S. Dissertation, University of Connecticut, 2006.

15 (a) P. J. Flory and J. R. Rehner, *J. Chem. Phys.*, 1943, **11**, 521; (b) J. C. Bray and E. W. Merrill, *J. Appl. Polym. Sci.*, 1973, **17**, 3779; (c) N. A. Peppas, E. W. Merrill, *J. Polym. Sci., Polym. Chem. Ed.*, 1976, **14**, 441.

16 (a) J. Padilla, V. Seshadri, G.A. Sotzing and T.F. Otero, *Electrochem. Commun.*, 2007, **9**, 1931-1935; (b) A. L. Holt, J. M. Leger and S. A. Cartera, *Appl. Phys. Lett.* , 2005, **86**, 123504.

17 M. A. Invernale, V. Seshadri, D. M. D. Mamangun, Y. Ding, J. Filloramo and G. A. Sotzing, *Chem. Mater.*, 2009, **21**, 3332–3336.

18 I. Schwendeman, J. Hwang, D. M. Welsh, D. B. Tanner, and J. R. Reynolds, *Adv. Mater.* **2001**, 13, 634-637.

19 F. A. Alamer, M. T. Otley, Y. Ding and G. A. Sotzing, *Adv. Mater.*, 2013, **25**, 6256–6260.

20 (a) V. Zardetto, T. M. Brown, A. Reale and A. D.Carlo, J. Polym. Sci., Part B: Polym. Phys., 2011, **49**, 638-648; (b) H. J. Lee, T. H. Park, J. H. Choi, E. H. Song, S. J. Shin, H. Kim, K. C. Choi, Y. W. Park, B.-K. Ju, *Org. Electron.*, 2013, **14**, 416-422; (c) X. Wu, J. Liu, D. Wu, Y. Zhao, X. Shi, J. Wang, S. Huang and G. He, ***J. Mater. Chem. C***, 2014, **2**, 4044-4050; (d) P. Q. M. Nguyen, L-P. Yeo, B.-K. Lok and Y.-C. Lam, *ACS Appl. Mater. Interfaces*, 2014, **6**, 4011–4016.

21 (a) Z. Chen, B. Cotterell, W. Wang, E. Guenther and S. J. Chua, *Thin Solid Films*, 2001, **394**, 202-206; (b) Z. Chen, B. Cotterell and W. Wang, *Eng. Fract. Mech.*, 2002, **69**, 597-603.

22 Y. Zhu, M. T. Otley, A. Kumar, M. Li, X. Zhang, C. Asemota and G. A. Sotzing, *Chem. Commun.*, **2014**, 50, 8167-8170

Chapter 6: Color Tuning Neutrality for Flexible Electrochromics via a Dual Copolymer Approach

Published in *Adv. Mater.*, **2014**, 26, 8004-8009

6.1 Motivation and Introduction

Flexible display devices that can be easily manufactured in a method exhibiting low cost, low waste, and cover large areas have yet to be realized consisting of electrochromic polymers. Electrochromic devices traditionally have been fabricated by depositing the electrochromic polymer onto the electrode via electrodeposition that can be a costly and inefficient procedure for manufacturing. Color tuning for architectural windows, smart glass/privacy glass, automotive, aerospace, and contrast-enhancement for see-through displays all require grey/black/neutral colors. Herein, a method to color-tune electrochromic devices using a single-lamination procedure, where the monomers are electrochemically polymerized *in situ*, is demonstrated to achieve neutrality using three monomers to form two distinct copolymers. The monomer ratios for the conjugated random copolymers were predetermined and optimized via theoretical calculations to provide the most desirable optical properties when combined within an electrochromic device. These devices exhibited photopic contrasts up to *ca*. 38%, 2% neutrality, color uniformity across a 75 cm^2 active area device, haze below 2%, and switch speeds of less than 1 second.

Electrochromic materials hold potential as becoming the next generation of flexible displays due to their ability to work on flexible substrates and low power

consumption.[1] Recent high-profile commercialization of electrochromics includes the Boeing 787 Dreamliner windows manufactured by Gentex.[2] Electrochromic materials consist of inorganics,[3] small molecule organics,[4] and conjugated polymers.[5] Electrochromic materials made from π–conjugated polymers (CP)s have been gaining in popularity due to fast switch speeds, color variability, and high optical memory that results in low power consumption. CPs extended π-conjugation along the polymer backbone allow for its spectral absorption, and the energy gap between the HOMO and LUMO for CPs changes with an applied voltage due to the ability of the CP to change from an insulator to a semiconductor. The effect is a difference in absorption shifts resulting in visible color changes. A full visible spectral range of colors for CPs have been reported.[6] These optical properties make CPs of significant interest for applications such as displays, windows, OLEDs or anywhere the optical variation of transmittance and/or reflectance is required.

The benchmark electrochromic polymer poly(3,4-ethylenedioxythiophene) (PEDOT) has been extensively studied since it was first reported in 1994.[7] Poly(3,4-propylenedioxythiophene) P(ProDOT) and its derivatives, demonstrate higher contrasts than PEDOT due to a more transmissive bleached state.[8] This is due, in part, to PEDOT's six-membered planar ring in comparison to PProDOT's non-planar seven-membered ring resulting in increased spacing along the polymer backbone, which minimizes the stacking of the polymers, and thus decreasing electron chain hopping. Therefore, the absorption in the near infrared (NIR) is reduced along with the tail into the visible region, making them more transmissive in their oxidized state. By modifying the R groups on P(ProDOT), the color transitions can be tuned across the visible spectrum.

For example, poly(2,2-dimethyl-3,4-propylenedioxythiophene) P(ProDOT-Me_2) transitions between purple and sky blue while poly(1,3-di-*tert*-butyl-3,4-propylenedioxythiophene) P(1,3-PProDOT-tBu_2) transitions between yellow and sky blue.[9] ProDOT-Me_2 and ProDOT-tBu_2 were previously reported in a copolymerization study where high-throughput screening of the two ProDOT monomers exhibited a continuum of single-wavelength colors spanning the entire subtractive visible spectrum.[6] This study revealed the color variability of ProDOTs where two monomers, when copolymerized, can achieve the entire single-wavelength spectrum, but more importantly went to the same clear transparent color when oxidized. An earlier study demonstrated the electrochemical copolymerization of EDOT and thieno[3,4-*b*]thiophene (T34bT) that resulted in a red shift of the EDOT λ_{max}.[10]

A neutral color is a color not associated with any single hue, but is a color close to the white point for emittance and black point for absorbance. Recent efforts in fabricating ECDs that display neutral color transitions are of special interest in the current architectural window, smart glass/privacy glass, automotive, and aerospace industry. Currently, neutral color or near-black electrochromic polymers are highly researched in the academic and industrial community. Several published studies have utilized the donor-acceptor (DA) approach to broaden the absorbance spectra of these polymers to obtain neutrality including a notable study by Reynolds *et. al.* who published the first neutral or "black" electrochrome. Reynolds' method consists of soluble CPs that can be spray coated onto tin-doped indium oxide (ITO) coated substrates.[11] Our group published a random copolymerization method using two precursor polymers that was comprised of both DA and donor-only groups.[12] The precursor blends were

electrochemically converted into a donor-acceptor electrochromic polymer that switched between black to sky blue in its neutral and oxidized states, respectively, with a photopic contrast of 30%. In a more recent study from our group, a method was demonstrated using all commercially available materials to achieve neutrality with EDOT and an organic solvent dye using the "subtractive color mixing" theory.[13] In addition, the recent literature includes studies comprising of copolymers on two separate electrodes, and multiple layers of several polymer electrochromes with complementary color absorption.[14]

Previously reported from our research group was a one-step procedure to simplify the fabrication and enhance the success rate of constructing ECDs.[15] The *in situ* method dissolves the monomers directly into a liquid electrolyte and this solution is sandwiched between two ITO coated substrates. Next, the device is exposed to UV light, forming a solid electrolyte matrix, where conversion of the electroactive monomers to electrochromic polymers happens with the application of an appropriate potential. This method was developed as an alternative to electrodepositing the electroactive monomer onto the ITO coated substrate inside an electrolyte bath, thus eliminating a step. In the electrodeposition procedure an ITO coated substrate is placed into an electrolyte bath containing monomers. Then the electroactive monomers are converted to electrochromic polymers on the ITO coated substrate for an electrochromic polymer layer or film on the ITO. The bath has a limited lifespan for producing pristine films, normally one or two depositions, thus increasing solvent and waste consumption. Recently reported from our group using the one-step lamination procedure was high-throughput screening of

electroactive monomers,[6] long-term stability of acrylated ProDOTs in high-contrasting ECDs,[16] and ProDOT-Me_2 was used in several optimization studies for ECDs.[17]

Initially, the copolymerization of three monomers 2,2-dimethyl-3,4-propylenedioxythiophene (ProDOT-Me_2), 1,3-di-*tert*-butyl-3,4-propylenedioxythiophene (ProDOT-tBu_2), and thieno[3,4-*b*]thiophene (T34bT) in two separate copolymerizations were studied. The monomers were chosen due to their visible absorbance where ProDOT-tBu_2 has a λ_{max} at 392 nm at the extreme low end of the visible spectrum, ProDOT-Me_2 has a λ_{max} of 575 nm, and T34bT is in the near infrared (NIR) with a broad absorbing λ_{max} at 850 nm so that a combination of these could cover the entire visible spectrum. Then theoretical calculations were performed combining the different copolymer compositions of the two copolymer systems to determine the best combination to achieve neutrality without sacrificing contrast using the "subtractive color mixing" theory. The most promising were experimentally evaluated using the *in situ* approach, but with a slight modification to allow copolymerization of the two different copolymer systems to form a single electrochromic layer within the device. Once the procedure was optimized, a flexible device was fabricated on ITO coated polyethylene terephthalate (PET) to demonstrate the broad utility of this procedure.

6.2 Experimental

6.2.1 Materials

Lithium trifluoromethanesulfonate (LiTRIF), propylene carbonate (PC), poly (ethylene glycol) methyl ether acrylate (Mn = 480 g/mol) (PEG-MA), poly (ethylene glycol) dimethacrylate (Mn = 550g/mol) (PEG-DMA) and dimethoxyphenylacetophenone (DMPAP) were purchased from Sigma-Aldrich and used

as received. Indium Tin Oxide (ITO) coated glasses (sheet resistance 8-15Ohms/sq, Part Number: CH-50IN) were purchased from Delta Technologies and cleaned by acetone, isopropanol and methanol prior to use. ITO coated polyethylene terephthalate (PET) substrates (sheet resistance 60 Ohms/sq, Part Number: OC50/CP54/500) were purchased from CP Films Inc. and were cleaned by acetone prior to use. UV-sealant glue (UVS 91) was purchased from Norland Optics Inc. and conductive copper adhesive tape was purchased from Newark and used as received. Transparent silicone rubber gasket (0.508 mm thickness) was purchased from 3M Inc.

Monomer synthesis: 2,2-dimethyl-3,4-propylenedioxythiophene (ProDOT-Me_2, 1,3-di-*tert*-butyl-3,4-propylenedioxythiophene (ProDOT-tBu_2), and thieno[3,4-*b*]thiophene was synthesized according to the reported procedures.[9, 18]

6.2.2 Gel polymer electrolyte

Standard Gel polymer electrolyte was prepared by adding 1g of LiTRIF, 3g of PC, 7g of PEG-MA and 17.5mg of DMPAP together and sonicated until fully dissolved.

Gel polymer electrolyte used for flexible electrochromic device fabrication was composed of 1g of LiTRIF, 4g of PC, 0.12g of PEG-DMA, 5.88g of PEG-MA and 17.5mg of DMPAP and sonicated until fully dissolved.

6.2.3 Electrochromic device (ECD) assembly

A liquid Monomer electrolyte was first prepared by loading an overall 2.5 wt% ratio of monomers into the abovementioned gel polymer electrolyte.

Fabrication of ECD involves the following two steps:

Step 1. Liquid State Copolymerization of ProDOT-Me_2 and T34bT:

ProDOT-Me_2/T34bT dissolved liquid monomer electrolyte was drop casted onto a piece of ITO coated glass (2 ×4 cm^2) of which the perimeter was covered with a silicon rubber gasket (0.508 mm thickness) to give an active device area of ~5 cm^2 and to serve as the spacer. Another piece of ITO coated PET (2 × 4 cm^2) was then placed atop. A constant potential of +3 V was applied to the device for an appropriate conversion time (30 seconds to 60 seconds), converting the monomers in the liquid state to form the copolymer film onto ITO coated glass. The ITO coated PET was then removed and resulting copolymer film was rinsed with PC to wash off the leftover monomers and air dried.

Step 2. Solid State copolymerization of ProDOT-Me_2 and ProDOT-tB_2:

Liquid monomer electrolyte containing ProDOT-Me_2 and ProDOT-tB_2 was drop casted onto the active area of the DMP/TT copolymer deposited ITO coated glass obtained in Step 1. Another piece of ITO coated glass was covered atop. The device was then placed inside a UV crosslinker and exposed to UV light (365 nm, 5.8 mW/cm^2) for 20 mins and sealed with UV curable glue. Cured devices were subjected to the same polymerization process as stated above, converting the monomers in the solid state to form the copolymer film onto the previously formed copolymer layer.

Relatively Larger flexible devices (7.5 ×10 cm^2) were fabricated following the same procedure mentioned above except that the both substrates used were ITO coated PET. All assembled ECDs were cycled between their neutral and oxidized states between +2 V ~-2 V (pulse width = 3 s) five times before data was recorded.

6.2.4 Equipment

A UVP CL-1000 Crosslinker (365 nm) was used for UV curing. All electrochemistry was carried out using a CHI 720c potentiostat. Optical studies were performed on a PerkinElmer Lambda 1050 UV/VIS/NIR spectrometer. Colorimetric data of assembled devices were calculated using corresponding color software based on a D65 standard illuminant and confirmed by a PR-670 SpectroScan spectroradiometer (Photo Research, Inc.).

6.3 Results and Discussion

Initially, the copolymerization of three monomers 2,2-dimethyl-3,4-propylenedioxythiophene (ProDOT-Me_2), 1,3-di-*tert*-butyl-3,4-propylenedioxythiophene (ProDOT-tBu_2), and thieno[3,4-*b*]thiophene (T34bT) in two separate copolymerizations were studied. The monomers were chosen due to their visible absorbance where ProDOT-tBu_2 has a λ_{max} at 392 nm at the extreme low end of the visible spectrum, ProDOT-Me_2 has a λ_{max} of 575 nm, and T34bT is in the near infrared (NIR) with a broad absorbing λ_{max} at 850 nm so that a combination of these could cover the entire visible spectrum. Then theoretical calculations were performed combining the different copolymer compositions of the two copolymer systems to determine the best combination to achieve neutrality without sacrificing contrast using the "subtractive color mixing" theory. The most promising were experimentally evaluated using the *in situ* approach, but with a slight modification to allow copolymerization of the two different copolymer systems to form a single electrochromic layer within the device. Once the procedure was optimized, a flexible device was fabricated on ITO coated polyethylene terephthalate (PET) to demonstrate the broad utility of this procedure.

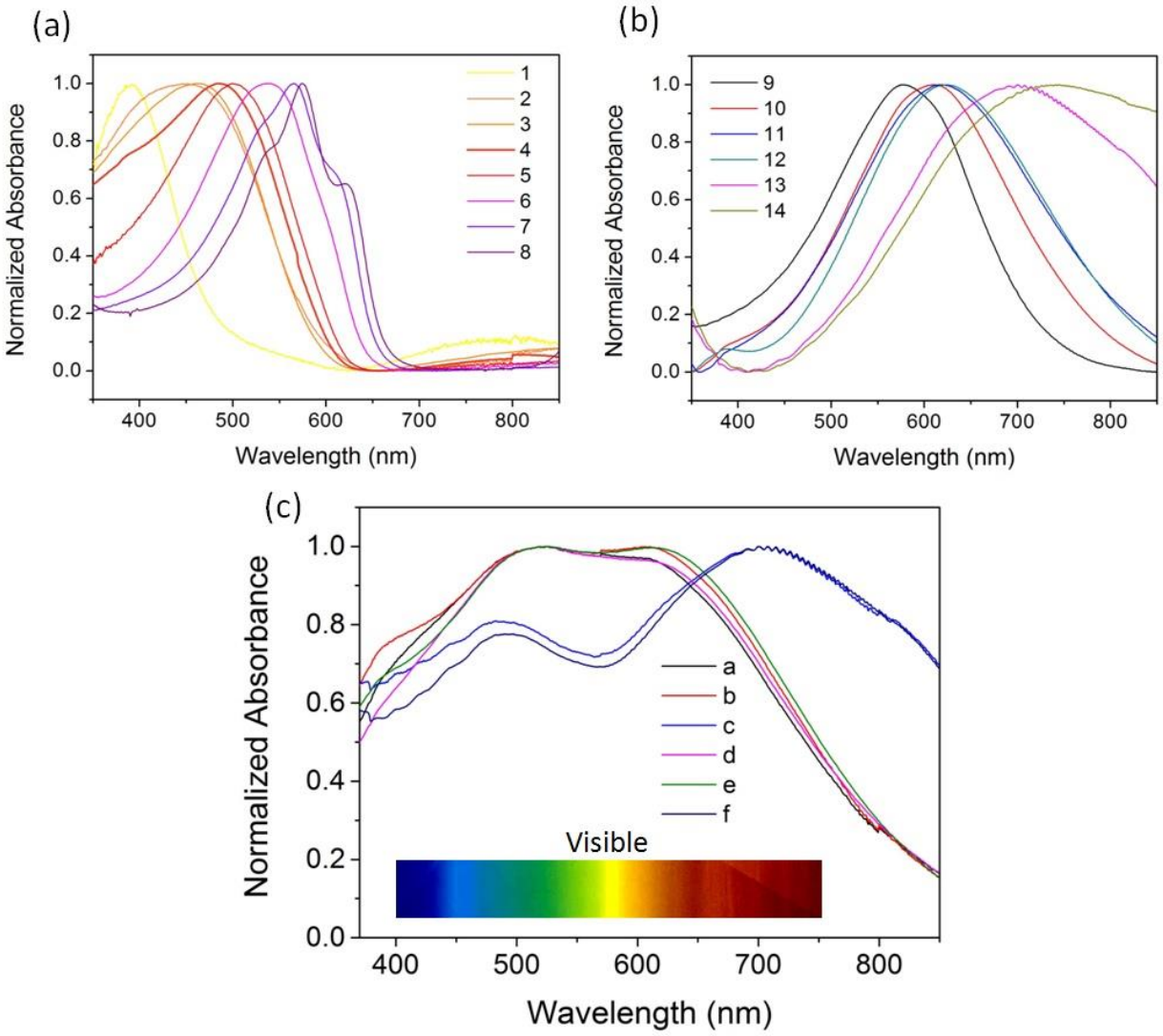

Figure 6.1. (a) Normalized Absorbance of Homopolymers or Copolymers by *in situ* polymerization of monomers at different feed ratios: 1. 100 wt% ProDOT-tBu_2, Abs max= 392 nm; 2. 80 wt% ProDOT-tBu_2 : 20 wt% ProDOT-Me_2 ,Abs max=446 nm; 3. 75% wt% ProDOT-tBu_2: 25% ProDOT-Me_2, Abs max= 460 nm 4. 65% ProDOT-tBu_2 : 35% ProDOT-Me_2, Abs max= 485 nm 5. 60% ProDOT-tBu_2 :40% ProDOT-Me_2, Abs max = 500 nm 6. 40% ProDOT-tBu_2: 60% ProDOT-Me_2, Abs max= 537 nm 7. 25% ProDOT-tBu_2: 75% ProDOT-Me_2 , abs max= 565 nm 8. 100% ProDOT-Me_2, Abs max= 575 nm.

(b) Normalized Absorbance of Copolymers *in situ* polymerization of monomers at different feed ratio: 9. 99 wt% ProDOT-Me_2 : 1 wt% T34bT, Abs max= 580 nm; 10. 98 wt% ProDOT-Me_2 : 2% T34bT, Abs max=608 nm; 11. 97.5% ProDOT-Me_2: 2.5 wt% T34bT, Abs max=618 nm; 12. 97 wt% ProDOT-Me_2 : 3 wt% T34bT, Abs max=626 nm; 13. 94 wt% ProDOT-Me_2 : 6 wt% T34bT, Abs max=700 nm; 14. 90 wt% ProDOT-Me_2 : 10 wt% T34bT, Abs max=745 nm.

(c) Theoretical modeled normalized absorbance spectrum with desired neutrality (<12%) by combing the absorbance spectra of a. Copolymer 2 + 11; b. Copolymer 2 + 12; c. Copolymer 2 + 13; d. Copolymer 3 + 11; d. Copolymer 3 + 12; e. Copolymer 3 + 13 to cover the entire visible region (400 -750 nm).

To color tune for neutrality a series of copolymers were investigated. First a series of copolymers consisting of ProDOT-Me_2 and ProDOT-tBu_2 were studied in solid state devices using the previously described *in situ* procedure.[15] This copolymer system was chosen due to the results yielded in a previous study from our lab involving high-throughput screening that demonstrated the ability to color tune using diffusion in a solid state device that generated a series of copolymers of different feed ratios covering the entire visible spectrum.[6] The gel electrolyte composition for the copolymerization studies consisted of 1g of lithium triflate (LiTRIF), 3g of propylene carbonate (PC), 7g of poly(ethylene glycol) methacrylate (PEG-MA) and 17.5mg of dimethoxyphenylacetophenone (DMPAP) together and was sonicated until fully dissolved. The feed ratios for the monomers that was added to the gel electrolyte composition were adjusted as seen in **Figure 6.1a** to produce 6 copolymers of absorptions between the two homopolymers of ProDOT-tBu_2 and ProDOT-Me_2 with a

λ_{max} of 392 nm and 575 nm, respectively. The goal was to find a copolymer combination that filled the lower wavelength visible spectrum, and also had a broad absorption. The most promising PProDOT-tBu_2-co-PProDOT-Me_2 systems were copolymers 2, 3, and 4 whose λ_{max} were 446 nm, 460 nm, and 485 nm, respectively, and all three systems exhibited broad absorptions. Subsequently, a series of copolymers were explored to cover the higher wavelengths of the visible absorption spectrum to achieve a dual copolymer system that complimentarily covers the entire visible spectrum thus achieving neutrality. ProDOT-Me_2 was again chosen for use in this system due to it's low cost for synthesizing and high contrast, and T34bT was chosen due to its λ_{max} at 850 nm and broad absorption. T34bT when copolymerized with ProDOT-Me_2 theoretically would red shift the λ_{max} of ProDOT-Me_2 and cover the higher wavelengths with a broad absorption. A series of copolymers consisting of ProDOT-Me_2-co-T34bT were studied as shown in **Figure 6.1 b** band the most promising copolymer systems were 10, 11, and 12 whose λ_{max} absorptions were 608 nm, 618 nm, and 626 nm, respectively. The copolymerizations of the ProDOT-Me_2-co-T34bT systems were also performed using the *in situ* procedure similar to the PProDOT-tBu_2-co-PProDOT-Me_2 system, but one modification to the procedure was required, due to T34bT's sensitivity to UV irradiation, to electrochemically convert the electroactive monomers to copolymers in the *liquid state* before UV curing the liquid gel electrolyte to the solid state. Then all forty-eight combinations of homopolymers and copolymers were then combined to perform theoretical absorbance calculations as shown in Figure 1C, and the goal was to combine spectra of the two copolymer systems, PProDOT-tBu_2-co-PProDOT-Me_2 with ProDOT-Me_2-co-T34bT, to determine which combination of the two had the most absorbance between 400 nm and 750 nm. Based

upon Lambert-Beer's law, the absorbance of the high energy copolymer and the absorbance of the low energy copolymer were adjusted by different factors and combined together to achieve the optimal neutrality value (below 12%) after final absorbance normalization. A total of six systems meet the requirement out of the forty-eight 48 different combinations (8 × 6) that are modeled, and they are listed in **Table 6.1**. Upon inspection of the theoretical data in Table 1 system c and system f were not selected due to their higher dark state transmittance compared with the other four systems, which will lead to a lower contrast.

System d exhibits a similar photopic transmittance value to system a, but a superior neutrality, therefore, system d was selected and evaluated in a solid-state device. Also, system b and system e demonstrate the same transmittance and neutrality values but the color coordinates of system b are closer to the reference white point, therefore it was chosen and tested in a solid state device. In total, two neutral systems are reported in this study consisting of copolymer 3 + 11, and copolymer 2 + 12 as supporting neutral system 1 in the supporting information. The data of the solid state devices consisting of copolymers 3 + 11 detailed in this study are closely matched to the theoretical modeled data displayed in **Table 6.1**.

Table 6.1. Theoretical Results of the Copolymer Systems

System		Color coordinate		Photopic transmittance (%)	Neutrality (%)
		x	y		
a	copolymer 2 + 11	0.300	0.290	10.5	11
b	copolymer 2 + 12	0.294	0.290	10.5	8.5
c	copolymer 2 +13	0.300	0.327	17	11
d	copolymer 3 + 11	0.294	0.280	10.5	10
e	copolymer 3 + 12	0.288	0.279	10.5	8.5
f	copolymer 3 + 13	0.296	0.319	18.5	11.5

A series of dual copolymer devices were then investigated to achieve neutrality using the single-lamination procedure, and the variety of copolymers allowed for precise color tuning of the neutral system to achieve the most favorable characteristics for windows and displays. Neutrality was determined using the current window industry specifications. The main system reported in this study is shown in **Fig. 6.2** consisting of PProDOT-tBu_2-co-PProDOT-Me_2 copolymer 3 and ProDOT-Me_2-co-T34bT copolymer 11. The color coordinates for each copolymer system and the actual dual copolymer solid state device is shown in Figure 2A. The copolymer system 3 exhibits an orange dark state (**Fig. 6.2b**) with color coordinates of x = 0.398 and y = 0.376, while copolymer 11 shows a blue color in the dark state with color coordinates of x = 0.311 and y = 0.335. The dual copolymer solid state device has a dark state of x = 0.301 and y = 0.304 with a calculated neutrality of 6%. The photopic contrast of this system was 37%, and was the best compromise of neutrality and photopic contrast of all the systems studied. Also, the dual copolymer devices all exhibited fast switch speeds of < 1 s. The fabrication of the dual

copolymer devices entailed one additional step than the single copolymer devices described previously. The modification was to first drop cast and electrochemically convert ProDOT-Me_2 and T34bT in the liquid state in between two ITO coated substrates. Then the device was disassembled, the electrochromic layer was washed with PC, and then built normally using the previously described *in situ* method with ProDOT-tBu_2 and ProDOT-Me_2 added to the gel electrolyte to form the second copolymer layer.

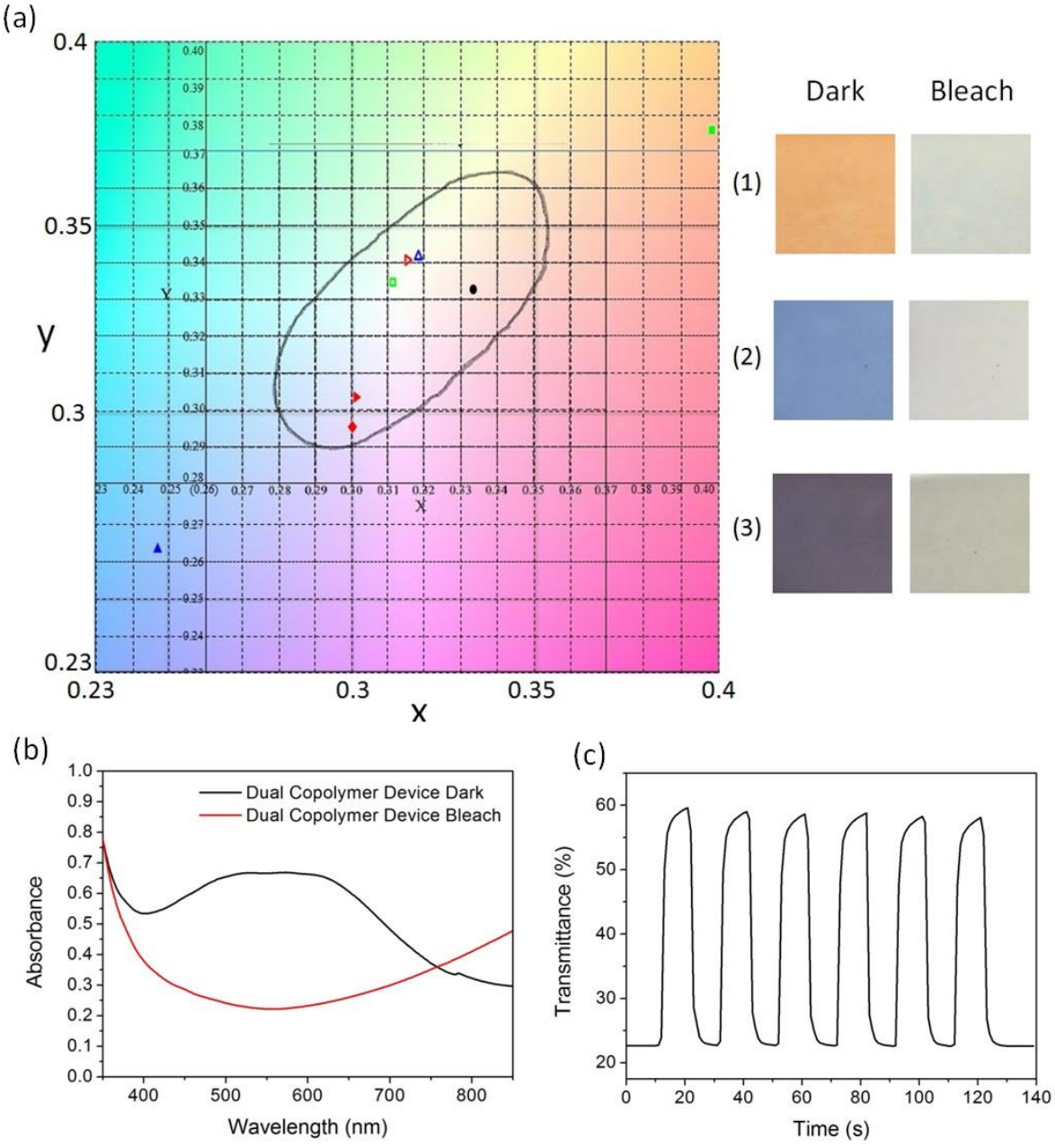

Fig. 6.2. (a). Color coordinates and images of (1). ProDOT-Me_2/ ProDOT-tBu_2 copolymer device: dark state (solid green square on color space) and bleach state (open green square on color space); (2). ProDOT-Me_2/T34bT copolymer device: dark state (solid blue triangle on color space) and bleach state (open blue triangle on color space); (3). Dual layer Copolymer Device: dark state (solid red triangle on color space), theoretical modeled dark state (solid red diamond), and bleach state (open red triangle on color space), Reference white point (solid black circle on color space); Grey circle in color space represents the neutral color region.

(b). UV-Vis absorption spectra of the dual copolymer single electrochromic layer device.

(c). Percent transmittance change at 555 nm for dual copolymer layer device during constant potential stepping between -2 V to +2 V.

To demonstrate the utility of this method for color tuning neutrality, one other system was color tuned by using copolymer 2 (λ_{max} = 446 nm) and copolymer 11 (λ_{max} = 618 nm) which had an extremely flat and broad absorbance spectrum resulting in a neutrality of 2% for the dark state, and as a result, color coordinates of the device dark state also moved closer to the white reference point. However, the device photopic contrast decreased to 31% due to the red shift of copolymer 12's absorbance to the edge of the visible region away from 555 nm. Several other variables can be experimented in the future, for example, shorter polymer conversion time that results in a thinner electrochromic layer increasing the clear state's %T and thus increasing photopic contrast.

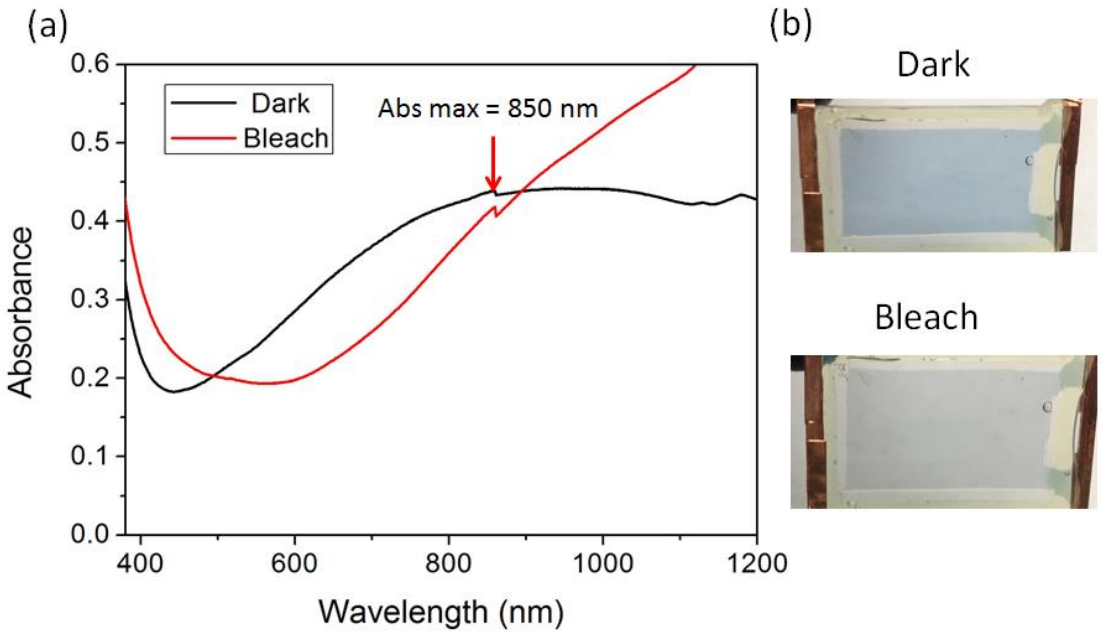

Figure 6.3 (a). Absorbance spectra and (b). Images of dark and bleached states for an *in situ* PT34bT device. The absorbance max is at 850 nm in its dark state.

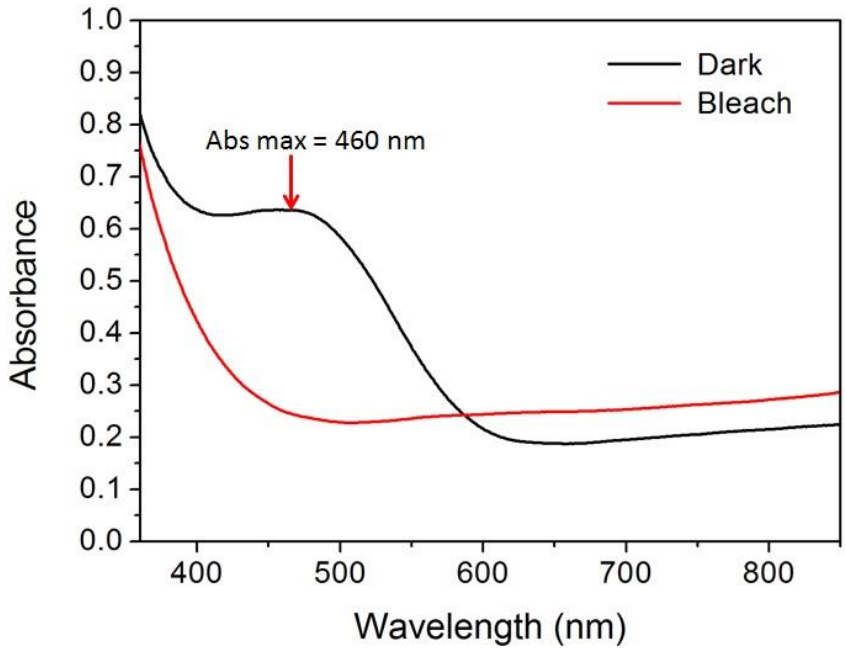

Fig. 6.4. Absorbance spectra of dark and bleach states for the *in situ* ProDOT-Me_2/ProDOT-tBu_2 device (monomer feed ratio: 75 wt% ProDOT-Me_2 : 25 wt% ProDOT-tBu_2) shown in Figure 2 (a). The absorbance max is at 460 nm in its dark state. The

device has the same peak intensity at 460 nm as the control dual copolymer layer device in the main article.

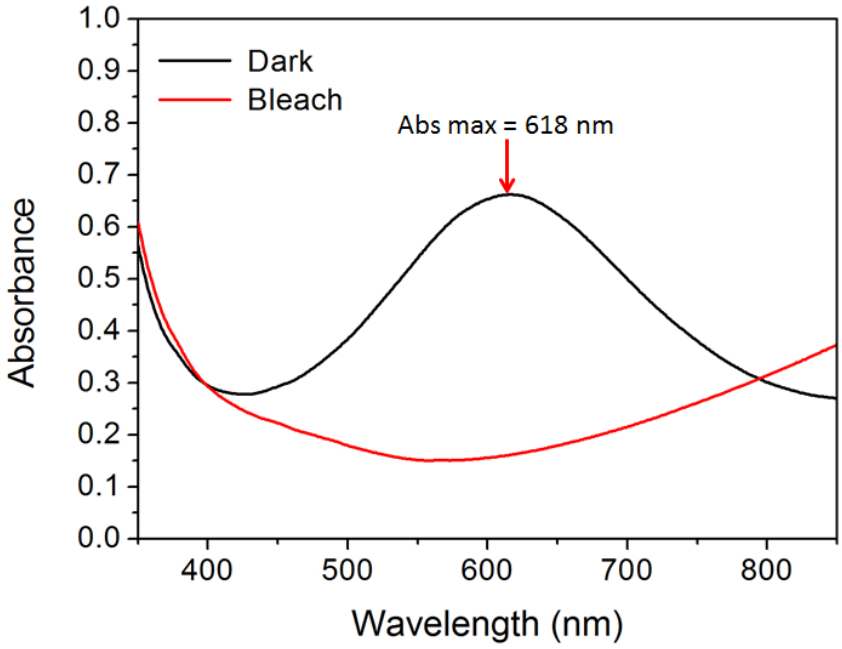

Fig. 6.5. Absorbance spectra of dark and bleached states for the *in situ* PProDOT-Me_2/PT34bT device (monomer feed ratio: 98.5 wt% ProDOT-Me_2 : 1.5 wt% T34bT) shown in Figure 2 (a). The absorbance max is at 618 nm in its dark state.

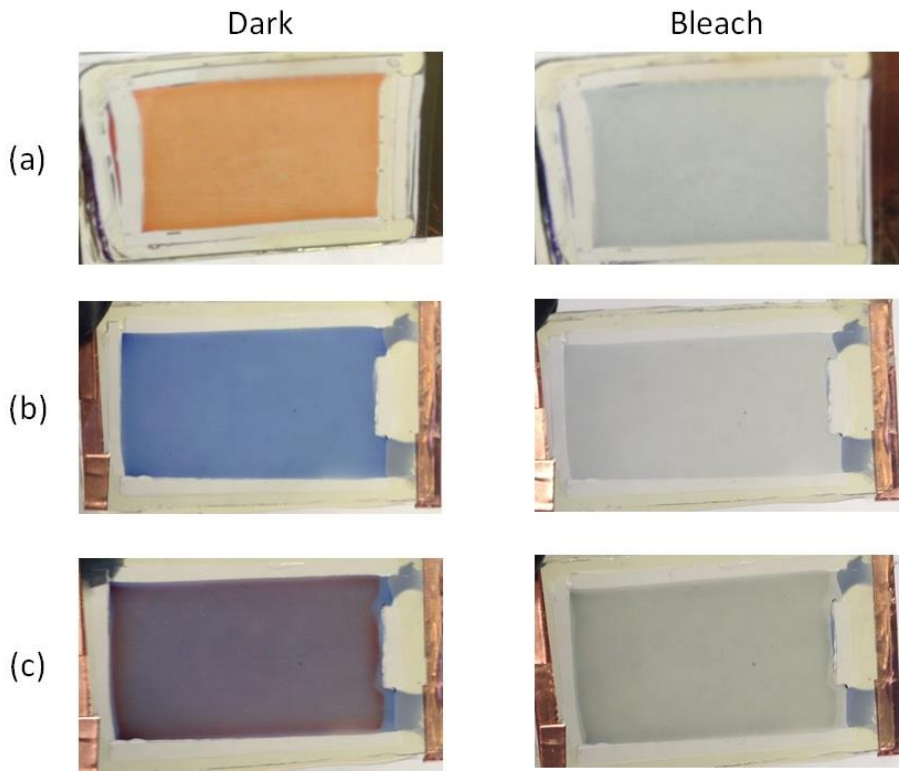

Fig. 6.6. Images of Dark and Bleach states for the small area (2×4 cm^2) devices shown in Figure 2(a): (a) ProDOT-Me_2/ProDOT-tBu_2 device (absorbance spectra corresponds to Figure S2), (b). *in situ* PProDOT-Me_2/PT34bT device (absorbance spectra corresponds to Figure S3) and (c). dual layer copolymer device (absorbance spectra corresponds to Figure 2(b)).

In a second study, another dual copolymer device was fabricated utilizing copolymer 2 and copolymer 12, of which the absorbance max were at 446 nm and 626 nm respectively. The reason to select this two copolymers is because one is more blue shifted and the other one is more red shifted, which, could lead to a wider expansion of the overall absorbance of the final dual copolymer layer device across the entire visible region to achieve better neutrality.

In this system, ProDOT-Me_2/T34bT (monomer feed ratio: 97 wt% ProDOT-Me_2 : 3 wt% T34bT) was converted in liquid state for 40 s, 20 s fewer than the control system in main article and following solid state conversion time of ProDOT-Me2/ProDOT-tBu2 (monomer feed ratio: 80 wt% ProDOT-Me_2 : 20 wt% ProDOT-tBu2) was 30 s, 20 s fewer than that in control system. As a result, two thinner polymer layers were generated, giving less absorbance in both device dark and bleach states. The absorbance spectra and images of the device is shown below in **Fig. 6.7**. Color coordinates, photopic transmittance and neutrality for each state is summarized in **Table 6.2**.

In comparison with the neutral systems mentioned earlier, a low of neutrality of 2% was achieved in the device dark state due to a better balanced absorbance intensity across the entire visible region, and as a result, color coordinates of the device dark state also got closer to the white reference point. However, the device photopic contrast decreased to 31% due to the shift of copolymer absorbance to the end of visible region and the low absorbance in both dark and bleach states.

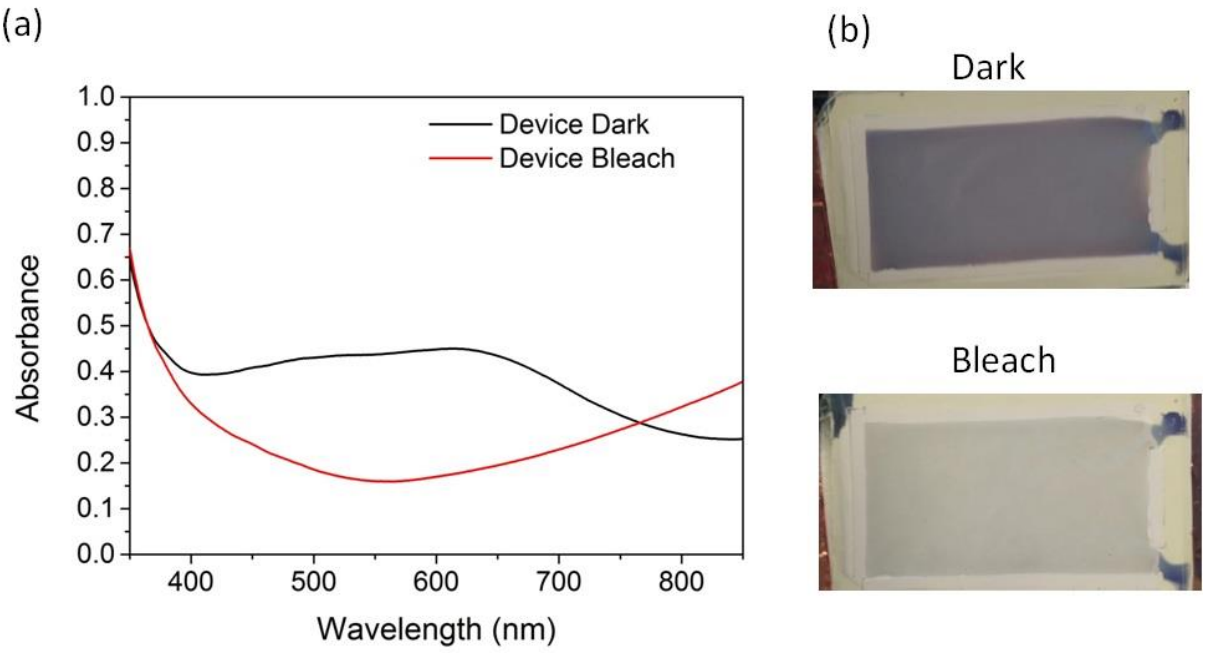

Fig. 6.7. (a). Absorbance spectrum and (b). Images of dark and bleached states for the *in situ* neutral color device utilizing Copolymer 2 and Copolymer 12.

Table 6.2. Color coordinates, photopic transmittance and neutrality for the *in situ* neutral color device utilizing Copolymer 2 and Copolymer 12.

	x	**y**	**Neutrality (%)**	**Photopic transmittance (%)**
Dark	0.303	0.317	2	36.5
Bleach	0.318	0.345	4	67.5
Theoretical modeled Dark	0.302	0.310	3.5	36

The color coordinates (x, y) for the supporting neutral system are shown in **Fig.6.8**.

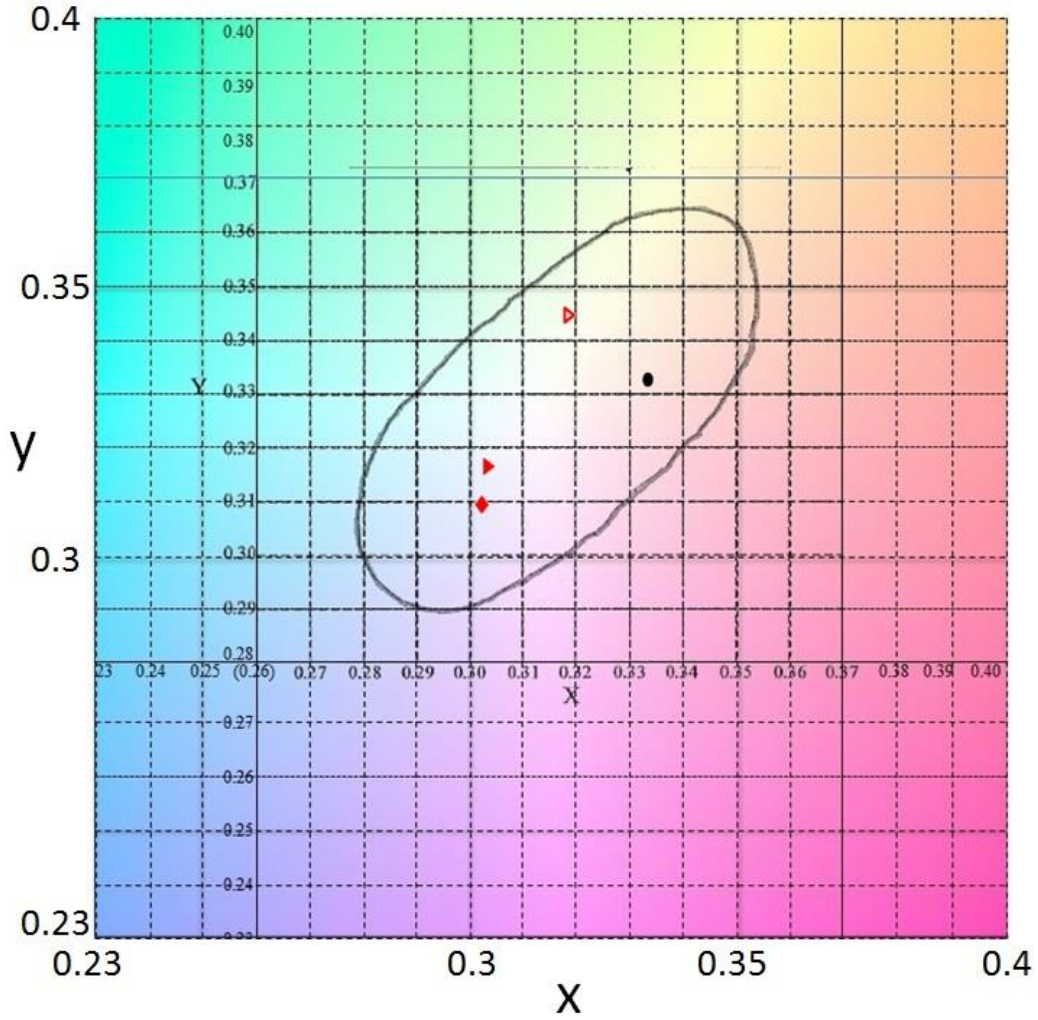

Fig 6.8. Color coordinates for the supporting neutral system (solid red triangle represents dark state and open red triangle represents bleach state); Theoretical modeled dark state (solid red diamond); Reference white point (solid black circle on color space); Grey circle in color space represents the neutral color region.

The dual copolymer system (copolymer 3 + 11) exhibited in **Fig. 6.2** was then used as the electrochrome for neutral colored flexible devices. The flexible device seen in **Fig. 6.9** consists of two ITO coated PET substrates with a modified gel electrolyte differing from the gel electrolyte in the previously described devices with the addition of poly(ethylene glycol) dimethacrylate to the electrolyte composition. This allows the device to flex without cracking of the gel electrolyte that would shorten the lifetime of the device. The flexible PET device displayed similar properties to the rigid glass with a photopic contrast of 32% due to the lower transmissivity substrate. However, the neutrality remained the same at 5% for the dark state, and also exhibited sub second switch speeds.

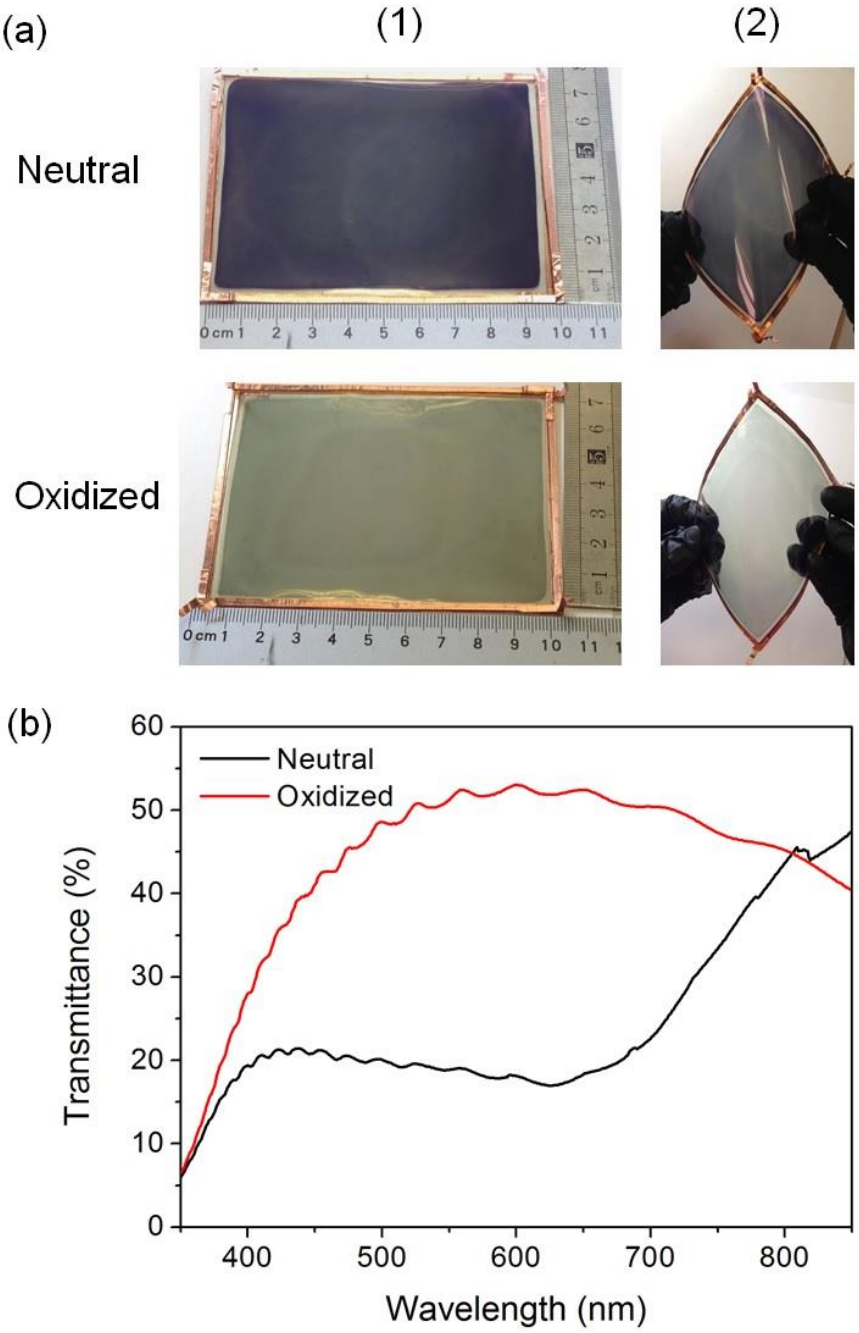

Fig. 6.9. (a). Neutral and oxidized state images of a 75 cm^2 flexible dual copolymer layer device in its (1). non-bent and (2). bent states.

(b). Percent Transmittance of the 75 cm^2 flexible dual copolymer layer device in its neutral and oxidized states

6.4 Conclusion

In summary, the demonstration of color tuning based on determining feed ratios using two distinct complimentary copolymer systems consisting of only 3 monomers in a single electrochromic layer solid state device achieved excellent neutrality (2%). To date most neutral colored electrochromic devices in the literature report single-wavelength contrasts, and this is the highest reported photopic contrast of a neutral colored electrochromic device *ca*. 38%. Also of note, is the use of theoretical calculations to predict absorptions for electrochromic devices that can save time eliminating the fabrication of unwarranted devices. These devices also exhibited color uniformity, low haze, and switch speeds of less than 1 second. In addition, this method was used to fabricate a large area flexible electrochromic device of 75 cm^2 exceeding the size of small displays demonstrating the ability for use in future electrochromic displays and even fabric.

6.5 References

[1] R. J. Mortimer, *Am. Sci.* **2013**, *101*, 38.

[2] A. P. Weidner, U.S. Patent No. 7,450,294, **2008**.

[3] a) C. G. Granqvist, *Sol. Energ. Mater. Sol. C.* **2000**, *60*, 201; b) S. K. Deb, *Sol. Energ. Mat. Sol. C.* **2008**, *92*, 245; c) E. Avendaño, L. Berggren, G. A. Niklasson, C. G. Granqvist, A. Azens, *Thin Solid Films* **2006**, *496*, 30.

[4] P. M. S. Monk, *The Viologens: Physicochemical Properties, Synthesis and Applications of the Salts of 4,4'-Bipyridine*, J. Wiley & Sons, Chichester, **1998**; b) R. Cinnsealach, G. Boschloo, S. N. Rao, D. Fitzmaurice, *Sol. Energ. Mat. Sol. C.* **1998**, *55*, 215; c) X. W. Sun, J. X. Wang, *Nano Lett.* **2008**, *8*, 1884; d) D. G. Kurth, J. P. López, W. Dong, *Chem. Commun.* **2005**, *16*, 2119; e) C. G. Granqvist, *Handbook of Inorganic Electrochromic Materials*, Elsevier, **1995**, 663; f) Y. Ohsedo, I. Imae, Y. Shirota, *J. Poly. Sci. Part B: Polym. Phys.* **2003**, *41*, 2471; g) I. Imae, K. Nawa, Y. Ohsedo, N. Noma, Y. Shirota, *Macromolecules* **1997**, *30*, 380.

[5] P. M. Beaujuge, J. R. Reynolds, *Chem. Rev.* **2010**, *110*, 268.

[6] a) R. H. Bulloch, J. A. Kerszulis, A. L. Dyer, J. R. Reynolds, *ACS Appl. Mater. Interfaces* **2014**, DOI: 10.1021/am500290d; b) G. Sonmez, C. K. F. Shen, Y. Rubin, F. Wudl, *Angew. Chem. Int. Ed.* **2004**, *116*, 1524; c) F. Alhashmi Alamer, M. T. Otley, Y. Ding, G. A. Sotzing, *Adv. Mater.* **2013**, *25*, 6256.

[7] Q. B. Pei, G. Zuccarello, M. Ahlskog, O. Inganas, *Polymer* **1994**, *35*, 1347.

[8] D. M. Welsh, A. Kumar, E. W. Meijer, J. R. Reynolds, *Adv. Mater.* **1999**, *11*, 16.

[9] T. Dey, M. A. Invernale, Y. Ding, Z. Buyukmumcu, G. A. Sotzing, *Macromolecules* **2011**, *44*, 2415.

[10] V. Seshadri, L. Wu, G. A. Sotzing, *Langmuir* **2003**, *19*, 9479.

[11] a) P. M. Beaujuge, S. Ellinger, J. R. Reynolds, *Nat. Mater.* **2008**, *7*, 795; b) P. J. Shi, C. M. Amb, E. P. Knott, E. J. Thompson, D. Y. Liu, J. G. Mei, A. L. Dyer, J. R. Reynolds, *Adv. Mater.* **2010**, *22*, 4949; c) S. V. Vasilyeva, P. M. Beaujuge, S. Wang, J. E. Babiarz, V. W. Ballarotto, J. R. Reynolds, *ACS Appl. Mater. Interfaces*, **2011**, *3*, 1022; d) G. Oktem, A. Balan, D. Baran, L. Toppare, *Chem. Commun.* **2011**, *47*, 3933.

[12] K. R. Lee, G. A. Sotzing, *Chem. Commun.* **2013**, *49*, 5192.

[13] Y. Zhu, M. T. Otley, A. Kumar, M. Li, X. Zhang, C. Asemota, G. A. Sotzing. *Chem. Commun.* **2014**, *50*, 8167.

[14] a) P. Chandrasekhar, B. J. Zay, C. Cai, Y. Chai, D. Lawrence, *J. Appl. Polym. Sci.* **2014**, *131*, 41043. b) M. Icli, M. Pamuk, F. Algi, A. M. Onal, A. Cihaner, *Org. Electron.* **2010**, 11, 1255.

[15] a) Y. Ding, M. A. Invernale, D. M. D. Mamangun, A. Kumar and G. A. Sotzing, *J. Mater. Chem.* **2011**, *21*, 11873; b) M. A. Invernale, Y. Ding, D. M. D. Mamangun, M. S. Yavuz, G. A. Sotzing, *Adv. Mater.* **2010**, *22*, 1379.

[16] M. T. Otley, F. Alhashmi Alamer, Y. Zhu, A. Singhaviranon, X. Zhang, M. Li, A. Kumar, G. A. Sotzing, *ACS Appl. Mater. Interfaces* **2014**, *6*, 1734.

[17] a) A. Kumar, M. T. Otley, F. A. Alamar, Y. Zhu, B. G. Arden, G. A. Sotzing, *J. Mater. Chem. C* **2014**, *2*, 2510; b) Y. Zhu, M. T. Otley, F. Alhashmi Alamer, A. Kumar, X. Zhang, D. M. D. Mamangun, M. Li, B. G. Arden, G. A. Sotzing, *Org. Electron.* **2014**, *15*, 1378.

[18] N. Agarwal, S. P. Mishra, C. H. Hung, A. Kumar, M. Ravikanth, *Bull. Chem. Soc. Jpn.* 2004, **77**, 6, 1173.